

N. Tuning

Lectures Notes on CP violation

February 2020

Table of contents

Introduction	1
1 CP Violation in the Standard Model	3
1.1 Parity transformation	3
1.1.1 The Wu-experiment: ^{60}Co decay	4
1.1.2 Parity violation	5
1.1.3 CPT	7
1.2 C, P and T: Discrete symmetries in Maxwell's equations	8
1.3 C, P and T: Discrete symmetries in QED	9
1.4 CP violation and the Standard Model Lagrangian	12
1.4.1 Yukawa couplings and the Origin of Quark Mixing	12
1.4.2 CP violation	15
2 The Cabibbo-Kobayashi-Maskawa Matrix	17
2.1 Unitarity Triangle(s)	17
2.2 Size of matrix elements	20
2.3 Wolfenstein parameterization	23
2.4 Discussion	26
2.4.1 The Lepton Sector	27
3 Neutral Meson Decays	29
3.1 Neutral Meson Oscillations	29

3.2	The mass and decay matrix	29
3.3	Eigenvalues and -vectors of Mass-decay Matrix	31
3.4	Time evolution	33
3.5	The Amplitude of the Box diagram	35
3.6	Meson Decays	39
3.7	Classification of CP Violating Effects	40
4	CP violation in the B-system	43
4.1	β : the $B^0 \rightarrow J/\psi K_S^0$ decay	44
4.2	β_s : the $B_s^0 \rightarrow J/\psi \phi$ decay	49
4.3	γ : the $B_s^0 \rightarrow D_s^\pm K^\mp$ decay	51
4.4	Direct CP violation: the $B^0 \rightarrow \pi^- K^+$ decay	53
4.5	CP violation in mixing: the $B^0 \rightarrow l^+ \nu X$ decay	54
4.6	Penguin diagram: the $B^0 \rightarrow \phi K_S^0$ decay	55
5	CP violation in the K-system	57
5.1	CP and pions	57
5.2	Description of the K-system	59
5.3	The Cronin-Fitch experiment	60
5.3.1	Regeneration	62
5.4	Master Equations in the Kaon System	63
5.5	CP violation in mixing: ϵ	64
5.6	CP violation in decay: ϵ'	65
5.7	CP violation in interference	67
6	Experimental Aspects and Present Knowledge of Unitarity Triangle	69
6.1	B-meson production	69
6.2	Flavour Tagging	71
6.3	Present Knowledge on Unitarity Triangle	73

6.3.1	Measurement of $\sin 2\beta$	74
6.3.2	Measurement of ϵ_K	74
6.3.3	$ V_{ub}/V_{cb} $	75
6.3.4	Measurement of Δm	75
6.4	Outlook: the LHCb experiment	78
References		80

Introduction

In these lectures we will introduce the subject of CP violation. This subject is often referred to with the more general term “Flavour Physics” since all the interesting stuff concerning CP violation happens in the weak (charged current) interaction when one quark-flavour changes into another quark-flavour, $q \rightarrow Wq'$, even between different families!

The charged current interactions $q \rightarrow Wq'$ form a central element in the Standard Model. Out of the 18 free parameters in the Standard Model, no less than four are related to the coupling constants of the interaction $q \rightarrow Wq'$. In addition, we will see that the origin of these coupling constants is closely related (through the Yukawa couplings) to the masses of the fermions, which form another nine free parameters of the Standard Model. Both the masses of the fermions and the coupling strength of the charged-current quark-couplings form an intriguing, hierarchial, pattern for which some underlying mechanism must exist...

The CP operation changes particles into anti-particles, and changes the coupling constant of $q \rightarrow Wq'$ into its complex conjugate. It turns out that not all processes are invariant under the CP operation and we will show how these complex numbers are determined. In fact, the observation of CP violation allows us to make a convention-free definition of matter, with respect to anti-matter ¹! Maybe not surprising, CP violation is indeed one of the requirements needed to create a universe that is dominated by matter (or by anti-matter for that matter...).

Although CP violation was first discovered in the K -system in 1964, in recent years most experimental and theoretical developments in the field of flavour physics occur in the B -system and as a result the term “ B -physics” is intimately related to flavour physics. The study of B -mesons and their decays is not only interesting for the above mentioned reasons. Many observables in B -physics are dominated by higher order diagrams, and therefore these measurements are extremely sensitive to extra contributions from new, virtual, heavy particles, such as the supersymmetric partners of the Standard Model particles.

¹This could be of importance in a telephone call with aliens, before the first hand-shake. If they ask to meet you, first ask them what the charge of the lepton is to which the neutral kaon preferentially decays. If that is equal to the charge of the orbiting leptons in atoms, you are in business and can safely fix the term...

Very interesting topics such as baryogenesis, sphalerons, the strong CP problem, or neutrino oscillations unfortunately fall beyond the scope of these lectures. These lectures will focus on “normal” CP violation (also known as the Kobayashi Maskawa mechanism, for which these gentlemen were awarded the Nobel Prize in 2008), and its direct connection to the Standard Model, see Fig. 1.

The lectures are organized as follows. We start with the Standard Model Lagrangian and see where the flavour (and even family) changing interactions originate. This leads to the famous CKM-matrix which is discussed in chapter 2. We continue with the description of neutral mesons and their decays in chapter 3. This will be of importance for the discussion of measurements of some important B -decays in chapter 4. The historically important but less instructive K -system is discussed in chapter 5. We conclude with a discussion on experimental aspects and the present status of knowledge of CP violation in the Standard Model.

Most facts in these notes are taken from two excellent books on the topic, *Bigi & Sanda* [1] and *Branco & Da Silva* [2].

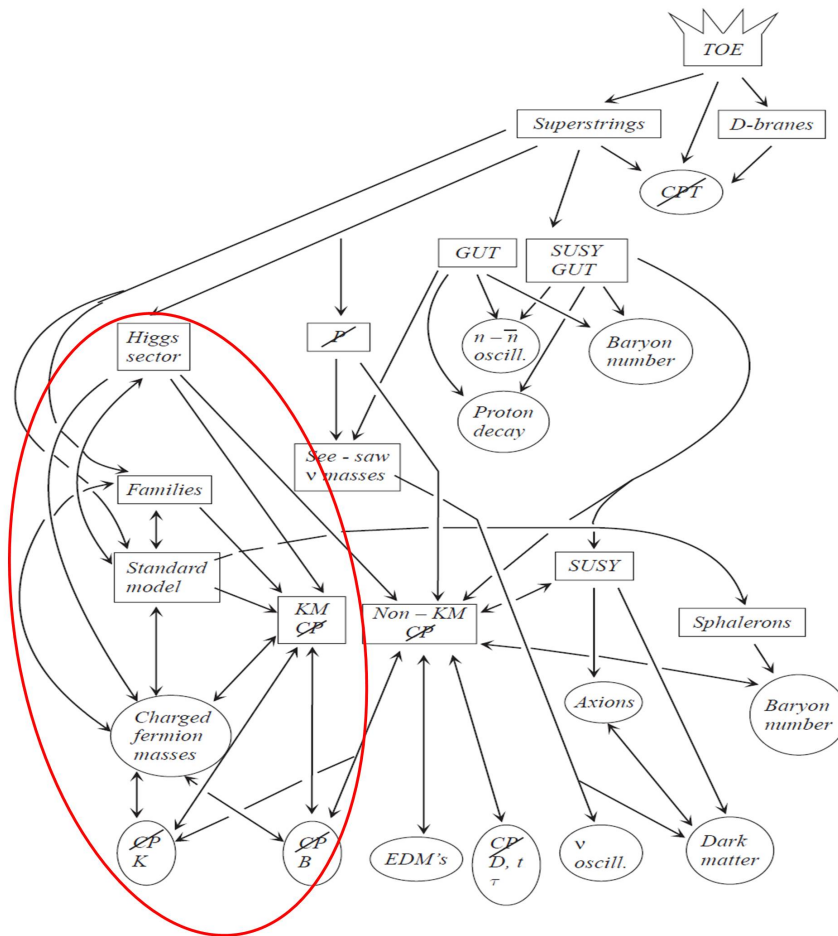


Figure 1: “Nature’s grand tapestry”. [1]

Chapter 1

CP Violation in the Standard Model

1.1 Parity transformation

The parity operator, P , inverts all space coordinates used in the description of a physical process. Consider for instance a scalar wavefunction $\psi(x, y, z, t)$. Performing the parity operation on this wavefunction will transform it to $\psi(-x, -y, -z, t)$, or

$$P\psi(x, y, z, t) = \psi(-x, -y, -z, t)$$

The parity transformation can be viewed as a mirroring with respect to a plane, (for instance $z \rightarrow -z$) followed by a rotation around an axis perpendicular to the plane (the z -axis). As angular momentum is conserved, physics will be invariant under the rotation and so the parity operation tests for invariance to mirroring w.r.t. a plane of arbitrary orientation. Parity conservation or P-symmetry implies that any physical process will proceed identically when viewed in mirror image. This sounds rather natural. After all we would not expect a dice for instance to produce a different distribution of numbers if one swaps the position of the one and the six on the dice.

Up until 1956 the general feeling was that all physical processes would conserve parity. In this year, however, a number of experiments were performed which showed that at least for processes involving the weak interaction this was not the case. For both experiments which will be discussed the properties of the transformation of spin by the parity operation played a crucial role, so let us consider how spin transforms.

Spin like angular momentum transforms as the cross product of a space vector and a momentum vector.

$$\begin{aligned}\vec{L} &= \vec{r} \times \vec{p} \\ P\vec{r} &= -\vec{r} \\ P\vec{p} &= -\vec{p}\end{aligned}$$

and so

$$P\vec{L} = \vec{L}$$

In other words the parity operation leaves the direction of the spin unchanged. If one can thus find a process which produces an asymmetric distribution with respect to the spin direction one proves that P-symmetry is not conserved. Another way of looking at it is by considering helicity which is the projection of the spin of a particle onto its direction of motion,

$$h = \frac{1}{2} \vec{\sigma} \cdot \hat{p}$$

As helicity changes sign under parity transformation ($\vec{p} \rightarrow -\vec{p}$) finding a process which produces a particle with a preferred helicity also proves that P-symmetry is violated.

1.1.1 The Wu-experiment: ^{60}Co decay

The experiment performed by Wu [3] in 1956 took a ^{60}Co source and placed it in a magnetic field. The ^{60}Co nucleus has spin 5 and becomes polarised along the magnetic field lines. The experimental apparatus is shown in Fig. 1.1a. The experimental method

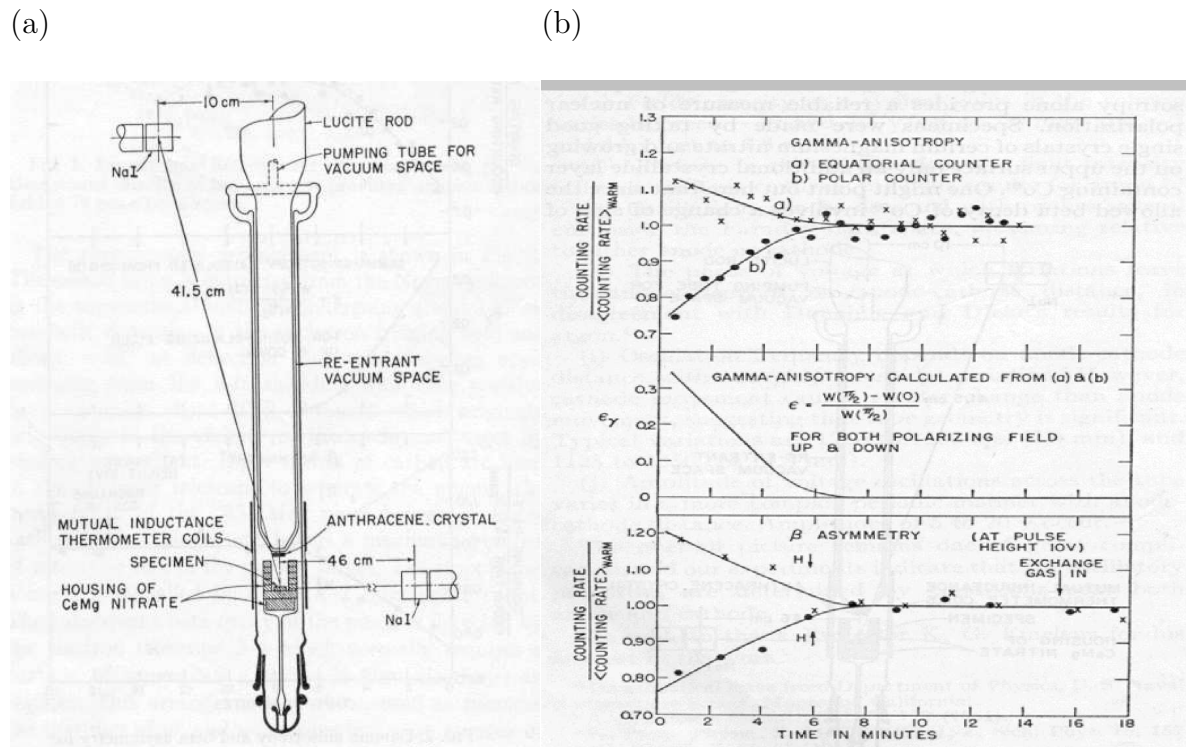


Figure 1.1: (a) The experimental configuration of the Wu experiment. The NaI counters monitor the state of polarisation by measuring the anisotropy of successive γ emissions produced through the polarisation technique. The anthracene crystal measures the β -electrons. (b) The result of the Wu experiment. The top plot shows the rate as a function of time for the two NaI counters, the center shows the degree of polarisation determined from the anisotropy. The lowest plot shows the measured β counting rates for positive and negative magnetic field directions.

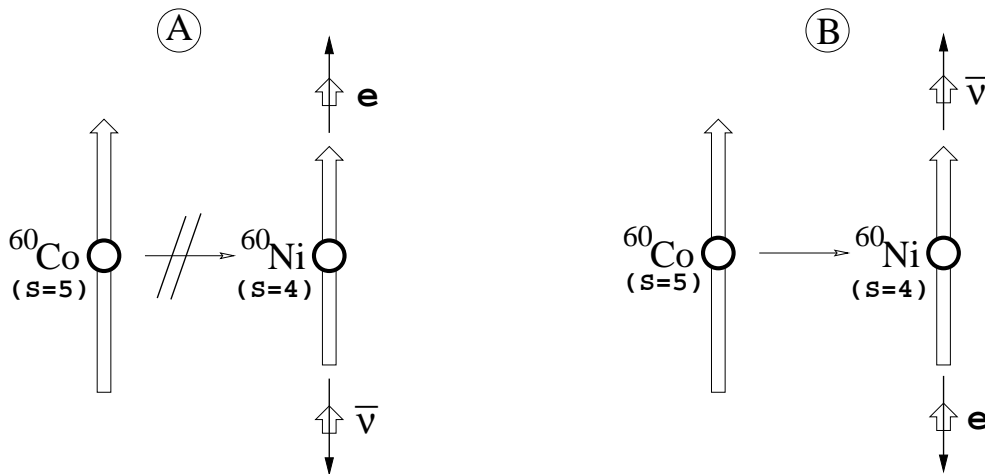


Figure 1.2: The possible transitions of ^{60}Co with spin 5 to ^{60}Ni with spin 4. The open arrows denote the spin. Closed arrows denote the momentum vector. (a) The transition which is forbidden in nature. (b) The allowed transition. The antineutrino is always righthanded.

was then to measure the rate of β -electrons from the decay:



in a small counter placed at small angles with respect to the field lines. By inverting the magnetic field direction and thus the polarisation of the cobalt nucleus, a difference in counting rate could be detected, as shown in Fig. 1.1b. Several control counters were also read out so that the degree of polarisation and the absolute counting rate of the source could be calibrated. The rate asymmetry shown in Fig. 1.1b was convincing evidence for the violation of P-symmetry or parity.

It could be explained by the following argument: The transition from ^{60}Co (spin 5) to ^{60}Ni (spin 4) as shown in Fig. 1.2a apparently does not occur, but the transition shown in Fig. 1.2b does. As the electron was known from other experiments to appear in nature in both helicity states ($\pm 1/2$), the only remaining conclusion was that the anti-neutrino occurred only in one single helicity state, namely $+1/2$.

1.1.2 Parity violation

A more elegant experiment was performed a few weeks later by Lederman [4] which allowed the observation of parity violation in charged pion decay. The experimental setup is shown in Fig. 1.3a. Charged pions of 85 MeV are created in pp collisions and separated

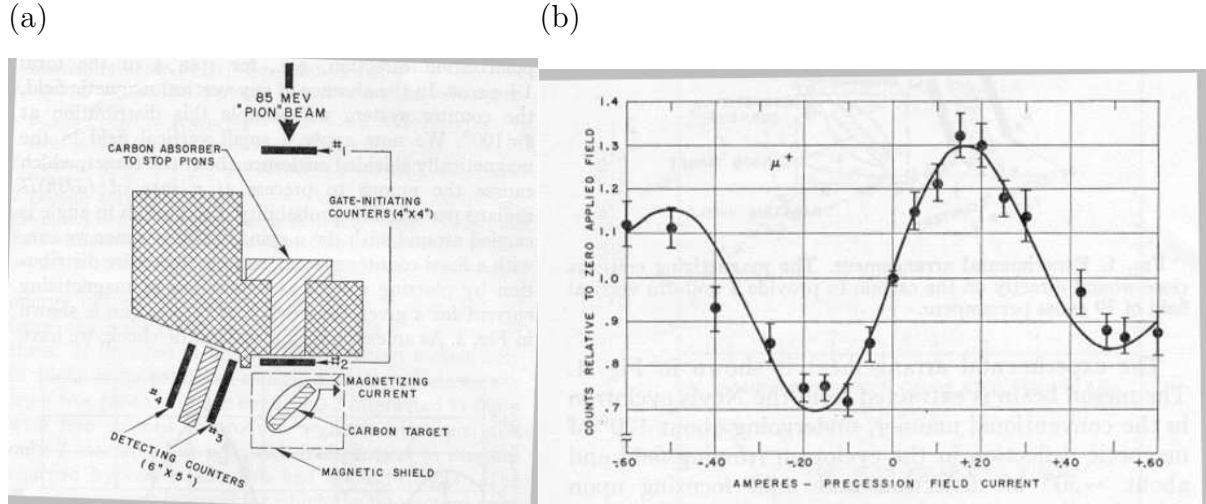


Figure 1.3: (a) The experimental setup of the Lederman experiment. (b) The resulting rate variation as a function of the applied magnetic field.

magnetically according to their charge. They are then allowed to decay according to

$$\pi^+ \rightarrow \mu^+ + \nu_\mu$$

The remaining pions are absorbed. The penetrating muons are stopped in a carbon target which is placed in a magnetic field, perpendicular to their line of flight. The muons will start to precess in the magnetic field and after a while decay. The precession frequency is given by

$$\omega_L = \frac{geB}{2m_\mu} \quad (1.1)$$

with B the magnetic field, e the charge of the muon, m_μ its mass and g the gyromagnetic ratio of the muon which for a spin $1/2$ particle is approximately 2.

A counter placed at fixed angle w.r.t. the original flight direction is gated open with a fixed delay after the entry of the muon into the carbon target. This counter detects the positrons from the decay

$$\mu^+ \rightarrow e^+ + \nu_e + \bar{\nu}_\mu$$

The experiment was repeated for several different settings of the magnetic field and thus different precession frequency. The resulting rate is shown in Fig. 1.3b. A clear oscillation is seen showing that the muons are produced with non-zero polarisation in the pion decay. So also in pion decay parity is not conserved. Again the assumption of a single helicity for the neutrino can explain the result. As an aside the curves also show an asymmetry in the height of the oscillation caused by the violation of parity in the muon decay. Furthermore the wavelength of the oscillation allowed for the first time the measurement of the gyromagnetic moment of the muon, thus confirming the spin $1/2$ nature of the muon.

Let us now take a closer look at the π decay. Fig. 1.4 shows the effect of the parity operation on the decay of a π^+ , which yields an unphysical result. If we now perform

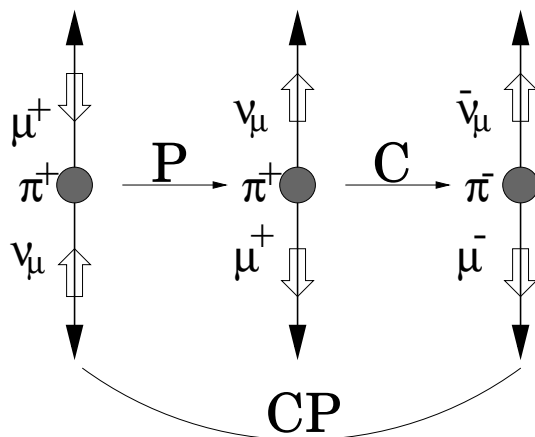


Figure 1.4: The physical π^+ decay is transformed via the parity operation to an unphysical decay, the charge conjugation operation transforms this to a physically allowed situation for π^- decay. The solid arrows denote momentum vectors, the open arrows the spin.

a second operation, that of charge conjugation, C, the final result is again a physically acceptable result. That this is correct could be verified by the Lederman experiment by the use of π^- mesons. So the combined application of the parity operation together with the operation of charge conjugation (or more precisely particle-antiparticle exchange) seems at least to provide a symmetry of nature.

1.1.3 CPT

Sofar we have come across two basic symmetries P and C which both are violated maximally in the weak interaction. The neutrino has only **one** helicity state. A third symmetry which many find an appealing symmetry is that of time reversal, T. Certainly there is a very strong reason for requiring the combination of all three to be a symmetry of nature as it has been proven that any Lorentz invariant local field theory must have the combined CPT symmetry. This is such a basic requirement that it is hard to imagine any theory in particle physics which does not conform to this symmetry. One of the consequences of the CPT symmetry is that particle states i.e. mass eigenstates which are the solution of

$$H\psi - m\psi = 0 \quad (1.2)$$

will have an equivalent antiparticle mass eigenstate with the same mass eigenvalue. The easiest way of conserving the CPT invariance would clearly have been the invariance of physics to all three symmetries separately. As we have seen P-symmetry and C-symmetry are both violated but CP seems for the time being a valid symmetry. The notion of time-reversal invariance is thus closely coupled to that of CP invariance. If CP-invariance is true then T invariance is also true, if CP symmetry is violated then so must timereversal invariance be.

The discrete transformations parity (P), charge conjugation (C) and time reversal (T) will be discussed in more detail in the following sections.

1.2 C, P and T: Discrete symmetries in Maxwell's equations

Consider first how the electric and magnetic fields, currents and charges behave under P, C and T transformation. Under P transformation positions of charges will be exchanged and so the electric field will change sign. Currents will flow in opposite direction so they also will change sign. The magnetic field is proportional to $\vec{j} \times \vec{r}$ and so will conserve its sign:

$$\begin{aligned}\vec{E}(\vec{x}, t) &\xrightarrow{P} -\vec{E}(-\vec{x}, t) \\ \vec{B}(\vec{x}, t) &\xrightarrow{P} \vec{B}(-\vec{x}, t) \\ \vec{j}(\vec{x}, t) &\xrightarrow{P} -\vec{j}(-\vec{x}, t) \\ \nabla &\xrightarrow{P} -\nabla\end{aligned}$$

Under T transformation the charges and positions will remain unchanged, whereas the currents will flow in opposite direction, so we get:

$$\begin{aligned}\vec{E}(\vec{x}, t) &\xrightarrow{T} \vec{E}(\vec{x}, -t) \\ \vec{B}(\vec{x}, t) &\xrightarrow{T} -\vec{B}(\vec{x}, -t) \\ \vec{j}(\vec{x}, t) &\xrightarrow{T} -\vec{j}(\vec{x}, -t) \\ \frac{\partial}{\partial t} &\xrightarrow{T} -\frac{\partial}{\partial t}\end{aligned}$$

and using similar arguments, we get for the C transformation:

$$\begin{aligned}\vec{E}(\vec{x}, t) &\xrightarrow{C} -\vec{E}(\vec{x}, t) \\ \vec{B}(\vec{x}, t) &\xrightarrow{C} -\vec{B}(\vec{x}, t) \\ \vec{j}(\vec{x}, t) &\xrightarrow{C} -\vec{j}(\vec{x}, t) \\ \rho(\vec{x}, t) &\xrightarrow{C} -\rho(\vec{x}, t)\end{aligned}$$

Finally under the combined CPT transformation the charges and currents change sign and electric and magnetic field retain their sign. These properties can be summarised in terms of the scalar potential ϕ and vector potential \vec{A} :

$$\vec{A}(\vec{x}, t) \xrightarrow{P} -\vec{A}(-\vec{x}, t), \quad \vec{A}(\vec{x}, t) \xrightarrow{T} -\vec{A}(\vec{x}, -t), \quad \vec{A}(\vec{x}, t) \xrightarrow{C} -\vec{A}(\vec{x}, t).$$

$$\phi(\vec{x}, t) \xrightarrow{P} \phi(-\vec{x}, t), \quad \phi(\vec{x}, t) \xrightarrow{T} \phi(\vec{x}, -t), \quad \phi(\vec{x}, t) \xrightarrow{C} -\phi(\vec{x}, t).$$

1.3 C, P and T: Discrete symmetries in QED

In this section we will derive expressions for the P, C and T operators. By definition the transformed states $\psi_P(\vec{x}, t)$, $\psi_C(\vec{x}, t)$ and $\psi_T(\vec{x}, t)$ are constructed such that they satisfy the same equation of motions for free fields as $\psi(\vec{x}, t)$. In the derivation of expressions for the P, C and T operators we start from the (correct) assumption that electromagnetic interactions are P, C and T symmetric. In other words, the Dirac equation should also hold for the P, C and T transformed fields. Eventually we will see what CP invariance implies for the weak interactions.

Let us consider the Dirac equation of a particle with charge e in an electro-magnetic field

$$\left(i\gamma^\mu \frac{\partial}{\partial x_\mu} - \gamma^\mu e A_\mu - m \right) \psi(\vec{x}, t) = 0, \quad (1.3)$$

where $\psi(\vec{x}, t)$ is a four component spinor and the matrices γ^μ are given by:

$$\gamma^i = \begin{pmatrix} 0 & \sigma^i \\ -\sigma^i & 0 \end{pmatrix} \text{ for } i = 1, 2, 3; \quad \gamma^0 = \begin{pmatrix} \mathbb{1} & 0 \\ 0 & -\mathbb{1} \end{pmatrix}, \text{ with :}$$

$$\sigma^1 = \begin{pmatrix} 0 & 1 \\ 1 & 0 \end{pmatrix}; \quad \sigma^2 = \begin{pmatrix} 0 & -i \\ i & 0 \end{pmatrix}; \quad \sigma^3 = \begin{pmatrix} 1 & 0 \\ 0 & -1 \end{pmatrix}; \quad \mathbb{1} = \begin{pmatrix} 1 & 0 \\ 0 & 1 \end{pmatrix}.$$

We now write out Eq. (1.3) as

$$\left(\gamma^0 \left[i \frac{\partial}{\partial t} - e\phi(\vec{x}, t) \right] - \gamma^i \left[i \frac{\partial}{\partial x_i} - eA_i(\vec{x}, t) \right] - m \right) \psi(\vec{x}, t) = 0 \quad (1.4)$$

The Dirac equation after parity transformation becomes:

$$\left(\gamma^0 \left[i \frac{\partial}{\partial t} - e\phi(-\vec{x}, t) \right] - \gamma^i \left[i \frac{\partial}{\partial(-x_i)} + eA_i(-\vec{x}, t) \right] - m \right) \psi(-\vec{x}, t) = 0 \quad (1.5)$$

Now, $\psi(-\vec{x}, t)$ is not a solution of the Dirac equation, due to the additional -sign in front of γ_i . Multiplying the Dirac equation (after parity transformation) from the left by γ^0 , we obtain the Dirac equation again:

$$\gamma^0 \left(\gamma^0 \left[i \frac{\partial}{\partial t} - e\phi(-\vec{x}, t) \right] + \gamma^i \left[i \frac{\partial}{\partial x_i} - eA_i(-\vec{x}, t) \right] - m \right) \psi(-\vec{x}, t) = 0$$

and then transport the γ^0 through the equation using the anti-commutation rules $\gamma^0 \gamma^i = -\gamma^i \gamma^0$ for $i = 1, 2, 3$ we get:

$$\left(\gamma^0 \left[i \frac{\partial}{\partial t} - e\phi(-\vec{x}, t) \right] - \gamma^i \left[i \frac{\partial}{\partial x_i} - eA_i(-\vec{x}, t) \right] - m \right) \gamma^0 \psi(-\vec{x}, t) = 0 \quad (1.6)$$

We now see that the spinor $\gamma^0 \psi(-\vec{x}, t)$ obeys the (original) Dirac equation. We come to the conclusion that the original Dirac equation is obeyed by the simultaneous parity

transformation in Lorentz space ($\vec{x} \rightarrow -\vec{x}$) and the transformation in Dirac space of the spinor with γ^0 :

$$\boxed{\psi(\vec{x}, t) \xrightarrow{P} \psi_P(\vec{x}, t) = \gamma^0 \psi(-\vec{x}, t) = P\psi(-\vec{x}, t)}$$

Of course also $e^{i\phi}\gamma^0\psi(-\vec{x}, t)$, with ϕ an arbitrary real phase, would provide a valid solution.

We will now take a look at the charge conjugation and investigate the interaction of a particle of opposite charge with an electro-magnetic field. Starting again from Eq. (1.3) and exchanging $e \rightarrow -e$ we find that the charge conjugate wave-function $\psi_C(\vec{x}, t)$ must satisfy:

$$\left(\gamma^0 \left[i \frac{\partial}{\partial t} + e\phi(\vec{x}, t) \right] - \gamma^i \left[i \frac{\partial}{\partial x_i} + eA_i(\vec{x}, t) \right] - m \right) \psi_C(\vec{x}, t) = 0 \quad (1.7)$$

For our particular representation of the γ matrices we have the following properties: $\gamma^{0*} = \gamma^0$, $\gamma^{1*} = \gamma^1$, $\gamma^{2*} = -\gamma^2$ and $\gamma^{3*} = \gamma^3$. Then taking the complex conjugate of Eq. (1.3) one obtains

$$\begin{aligned} \left(-\gamma^0 \left[i \frac{\partial}{\partial t} + e\phi(\vec{x}, t) \right] + \gamma^1 \left[i \frac{\partial}{\partial x_1} + eA_1(\vec{x}, t) \right] - \gamma^2 \left[i \frac{\partial}{\partial x_2} + eA_2(\vec{x}, t) \right] \right. \\ \left. + \gamma^3 \left[i \frac{\partial}{\partial x_3} + eA_3(\vec{x}, t) \right] - m \right) \psi^*(\vec{x}, t) = 0 \end{aligned} \quad (1.8)$$

Now multiplying from the left with γ^2 and transporting it through the equation we get:

$$\left(\gamma^0 \left[i \frac{\partial}{\partial t} + e\phi(\vec{x}, t) \right] - \gamma^i \left[i \frac{\partial}{\partial x_i} + eA_i(\vec{x}, t) \right] - m \right) \gamma^2 \psi^*(\vec{x}, t) = 0 \quad (1.9)$$

comparing this result with Eq. (1.7) we can readily identify

$$\psi_C(\vec{x}, t) = \gamma^2 \psi^*(\vec{x}, t)$$

Again we can use the arbitrary phase which we now take to be i , causing the combination $i\gamma^2$ to be real:

$$\psi_C(\vec{x}, t) = i\gamma^2 \psi^*(\vec{x}, t).$$

Rewriting this expression using $\bar{\psi}^T \equiv (\psi^\dagger \gamma^0)^T = \gamma^{0T} (\psi^\dagger)^T = \gamma^0 \psi^*$ yields the widely used expression for $\psi_C(\vec{x}, t)$:

$$\boxed{\psi(\vec{x}, t) \xrightarrow{C} \psi_C(\vec{x}, t) = i\gamma^2 \psi^*(\vec{x}, t) = i\gamma^2 \gamma^0 \bar{\psi}^T(\vec{x}, t) = C \bar{\psi}^T(\vec{x}, t)}$$

Similarly, using $C = i\gamma^2 \gamma^0$, we find $C = -C^{-1}$ and $\bar{\psi}(\vec{x}, t) \rightarrow -\psi^T(\vec{x}, t) C^{-1}$.

Finally we take a look at time reversal. We now again start from the complex conjugate equation and now multiply by $\gamma^1 \gamma^3$ we then get

$$\boxed{\psi(\vec{x}, t) \xrightarrow{T} \psi_T(\vec{x}, t) = i\gamma^1 \gamma^3 \psi^*(\vec{x}, -t) = T \psi^*(\vec{x}, -t)}$$

where we again use the arbitrary phase to give the factor i .

For the CP operation we have:

$$CP\psi(\vec{x}, t) = ie^{i\phi}\gamma^2\gamma^0\psi^*(-\vec{x}, t)$$

and for CPT

$$CPT\psi(\vec{x}, t) = e^{i\phi}\gamma^5\psi(-\vec{x}, -t)$$

using $\gamma^5 = i\gamma^0\gamma^1\gamma^2\gamma^3$. Check out the fact that the CP operation transforms an electron into a positron with opposite momentum and opposite helicity.

In summary, we get the following properties of the transformed wave-functions:

Field		P	C
Scalar field	$\phi(\vec{x}, t)$	$\phi(-\vec{x}, t)$	$\phi^\dagger(\vec{x}, t)$
Dirac spinor	$\psi(\vec{x}, t)$	$\gamma^0\psi(-\vec{x}, t)$	$i\gamma^2\gamma^0\bar{\psi}^T(\vec{x}, t)$
	$\bar{\psi}(\vec{x}, t)$	$\bar{\psi}(-\vec{x}, t)\gamma^0$	$-\psi^T(\vec{x}, t)C^{-1}$
Axial vector field	$A_\mu(\vec{x}, t)$	$-A^\mu(-\vec{x}, t)$	$A_\mu^\dagger(\vec{x}, t)$

Table 1.1: C and P transforms of fields. Note that $\mu = 0, 1, 2, 3$ and that $A^k = -A_k$ and $A^0 = A_0$.

Because of Lorentz invariance, spinors typically occur in so-called bilinear forms in the Lagrangian. For example, the bilinear $\bar{\psi}_1\gamma_\mu\psi_2$ transforms under C as follows (using $\gamma^\mu C = -C\gamma^{\mu T}$ and $\gamma^{\mu\dagger}\gamma^0 = \gamma^0\gamma^\mu$) [5]:

$$\bar{\psi}_1\gamma_\mu\psi_2 \xrightarrow{C} -\psi_1^T C^{-1}\gamma_\mu C\bar{\psi}_2^T = \psi_1^T \gamma_\mu^T \bar{\psi}_2^T = -(\bar{\psi}_2\gamma_\mu\psi_1)^T = -\bar{\psi}_2\gamma_\mu\psi_1.$$

The minus-sign at the second step arises from interchanging the (anti-commuting) fermion fields, and the transpose at the last step can be omitted because the entity is a 'one-by-one matrix'.

For completeness the transformation properties of the bi-linear forms are listed below.

	Bilinear	P	C	T	CP	CPT
scalar	$\bar{\psi}_1\psi_2$	$\bar{\psi}_1\psi_2$	$\bar{\psi}_2\psi_1$	$\bar{\psi}_1\psi_2$	$\bar{\psi}_2\psi_1$	$\bar{\psi}_2\psi_1$
pseudo scalar	$\bar{\psi}_1\gamma_5\psi_2$	$-\bar{\psi}_1\gamma_5\psi_2$	$\bar{\psi}_2\gamma_5\psi_1$	$-\bar{\psi}_1\gamma_5\psi_2$	$-\bar{\psi}_2\gamma_5\psi_1$	$\bar{\psi}_2\gamma_5\psi_1$
vector	$\bar{\psi}_1\gamma_\mu\psi_2$	$\bar{\psi}_1\gamma^\mu\psi_2$	$-\bar{\psi}_2\gamma_\mu\psi_1$	$\bar{\psi}_1\gamma^\mu\psi_2$	$-\bar{\psi}_2\gamma^\mu\psi_1$	$-\bar{\psi}_2\gamma_\mu\psi_1$
axial vector	$\bar{\psi}_1\gamma_\mu\gamma_5\psi_2$	$-\bar{\psi}_1\gamma^\mu\gamma_5\psi_2$	$\bar{\psi}_2\gamma_\mu\gamma_5\psi_1$	$\bar{\psi}_1\gamma^\mu\gamma_5\psi_2$	$-\bar{\psi}_2\gamma^\mu\gamma_5\psi_1$	$-\bar{\psi}_2\gamma_\mu\gamma_5\psi_1$
tensor	$\bar{\psi}_1\sigma_{\mu\nu}\psi_2$	$\bar{\psi}_1\sigma^{\mu\nu}\psi_2$	$-\bar{\psi}_2\sigma_{\mu\nu}\psi_1$	$-\bar{\psi}_1\sigma^{\mu\nu}\psi_2$	$-\bar{\psi}_2\sigma^{\mu\nu}\psi_1$	$\bar{\psi}_2\sigma_{\mu\nu}\psi_1$

Table 1.2: C, P transforms of bilinears

1.4 CP violation and the Standard Model Lagrangian

1.4.1 Yukawa couplings and the Origin of Quark Mixing

Let us now have a close look at the Standard Model Lagrangian to see where CP violation originates. The full Standard Model Lagrangian consists of three parts:

$$\mathcal{L}_{SM} = \mathcal{L}_{kinetic} + \mathcal{L}_{Higgs} + \mathcal{L}_{Yukawa}.$$

The kinetic term describes the dynamics of the spinor fields ψ

$$\mathcal{L}_{kinetic} = i\bar{\psi}(\partial^\mu \gamma_\mu)\psi,$$

where $\bar{\psi} \equiv \psi^\dagger \gamma^0$ and the spinor fields ψ are the three fermion generations, each consisting of the following five representations:

$$Q_{Li}^I(3, 2, +1/6), \quad u_{Ri}^I(3, 1, +2/3), \quad d_{Ri}^I(3, 1, -1/3), \quad L_{Li}^I(1, 2, -1/2), \quad l_{Ri}^I(1, 1, -1)$$

This notation [6] means that $Q_{Li}^I(3, 2, +1/6)$ is a $SU(3)_C$ triplet, left-handed $SU(2)_L$ doublet, with hypercharge $Y = 1/6$. The superscript I implies that the fermion fields are expressed in the interaction basis. The subscript i stands for the three generations. Explicitly, $Q_{Li}^I(3, 2, +1/6)$ is a shorthand notation for:

$$Q_{Li}^I(3, 2, +1/6) = \begin{pmatrix} u_g^I, u_r^I, u_b^I \\ d_g^I, d_r^I, d_b^I \end{pmatrix}_i = \begin{pmatrix} u_g^I, u_r^I, u_b^I \\ d_g^I, d_r^I, d_b^I \end{pmatrix}, \begin{pmatrix} c_g^I, c_r^I, c_b^I \\ s_g^I, s_r^I, s_b^I \end{pmatrix}, \begin{pmatrix} t_g^I, t_r^I, t_b^I \\ b_g^I, b_r^I, b_b^I \end{pmatrix}.$$

The interaction terms are obtained by imposing gauge invariance by replacing the partial derivative by the covariant derivative

$$\mathcal{L}_{kinetic} = i\bar{\psi}(D^\mu \gamma_\mu)\psi \quad (1.10)$$

with the covariant derivative defined as

$$D^\mu = \partial^\mu + ig_s G_a^\mu L_a + ig W_b^\mu \sigma_b + ig' B^\mu Y,$$

with L_a the Gell-Mann matrices and σ_b the Pauli matrices. G_a^μ , W_b^μ and B^μ are the eight gluon fields, the three weak interaction bosons and the single hypercharge boson, respectively.

We can now write out the charged current interaction between the (left-handed!) quarks:

$$\begin{aligned} \mathcal{L}_{kinetic,weak}(Q_L) &= i\overline{Q_{Li}^I} \gamma_\mu (\partial^\mu + \frac{i}{2} g W_b^\mu \sigma_b) Q_{Li}^I \\ &= i\overline{(u \ d)_{iL}^I} \gamma_\mu (\partial^\mu + \frac{i}{2} g W_b^\mu \sigma_b) \begin{pmatrix} u \\ d \end{pmatrix}_{iL}^I \\ &= \overline{u_{iL}^I} \gamma_\mu \partial^\mu u_{iL}^I + i\overline{d_{iL}^I} \gamma_\mu \partial^\mu d_{iL}^I - \frac{g}{\sqrt{2}} \overline{u_{iL}^I} \gamma_\mu W^{-\mu} d_{iL}^I - \frac{g}{\sqrt{2}} \overline{d_{iL}^I} \gamma_\mu W^{+\mu} u_{iL}^I + \dots \end{aligned}$$

using $W^+ = \frac{1}{\sqrt{2}}(W_1 - iW_2)$ and $W^- = \frac{1}{\sqrt{2}}(W_1 + iW_2)$.

Next, the W and Z bosons acquire their mass through the mechanism of spontaneous symmetry breaking. For this, the Higgs scalar field and her potential is added to the Lagrangian:

$$\mathcal{L}_{Higgs} = (D_\mu \phi)^\dagger (D^\mu \phi) - \mu^2 \phi^\dagger \phi - \lambda (\phi^\dagger \phi)^2 \quad (1.11)$$

with ϕ an isospin doublet

$$\phi(x) = \begin{pmatrix} \phi^+ \\ \phi^0 \end{pmatrix}.$$

The coupling of the Higgs to the gauge fields follows from the covariant derivative in the kinetic term. However, the interactions between the Higgs and the fermions, the so-called Yukawa couplings, have to be added by hand:

$$\begin{aligned} -\mathcal{L}_{Yukawa} &= Y_{ij} \overline{\psi_{Li}} \phi \psi_{Rj} + h.c. \\ &= Y_{ij}^d \overline{Q_{Li}^I} \phi d_{Rj}^I + Y_{ij}^u \overline{Q_{Li}^I} \tilde{\phi} u_{Rj}^I + Y_{ij}^l \overline{L_{Li}^I} \phi l_{Rj}^I + h.c. \end{aligned} \quad (1.12)$$

with

$$\tilde{\phi} = i\sigma_2 \phi^* = \begin{pmatrix} \overline{\phi^0} \\ -\phi^- \end{pmatrix}.$$

The matrices Y_{ij}^d , Y_{ij}^u and Y_{ij}^l are arbitrary complex matrices that operate in flavour space, giving rise to couplings between different families, or quark mixing, and thus to the field of flavour physics. It is interesting to note how intimately flavour physics is related to the mass of the fermions, see Section 2.4. Since this is the crucial part of flavour physics, we spell out the term $Y_{ij}^d \overline{Q_{Li}^I} \phi d_{Rj}^I$ explicitly:

$$\begin{aligned} Y_{ij}^d \overline{Q_{Li}^I} \phi d_{Rj}^I &= Y_{ij}^d \overline{(u \ d)_L^I} \begin{pmatrix} \phi^+ \\ \phi^0 \end{pmatrix} d_{Rj}^I = \\ &= \begin{pmatrix} Y_{11} \overline{(u \ d)_L^I} \begin{pmatrix} \phi^+ \\ \phi^0 \end{pmatrix} & Y_{12} \overline{(u \ d)_L^I} \begin{pmatrix} \phi^+ \\ \phi^0 \end{pmatrix} & Y_{13} \overline{(u \ d)_L^I} \begin{pmatrix} \phi^+ \\ \phi^0 \end{pmatrix} \\ Y_{21} \overline{(c \ s)_L^I} \begin{pmatrix} \phi^+ \\ \phi^0 \end{pmatrix} & Y_{22} \overline{(c \ s)_L^I} \begin{pmatrix} \phi^+ \\ \phi^0 \end{pmatrix} & Y_{23} \overline{(c \ s)_L^I} \begin{pmatrix} \phi^+ \\ \phi^0 \end{pmatrix} \\ Y_{31} \overline{(t \ b)_L^I} \begin{pmatrix} \phi^+ \\ \phi^0 \end{pmatrix} & Y_{32} \overline{(t \ b)_L^I} \begin{pmatrix} \phi^+ \\ \phi^0 \end{pmatrix} & Y_{33} \overline{(t \ b)_L^I} \begin{pmatrix} \phi^+ \\ \phi^0 \end{pmatrix} \end{pmatrix} \cdot \begin{pmatrix} d_R^I \\ s_R^I \\ b_R^I \end{pmatrix} \end{aligned}$$

After spontaneous symmetry breaking,

$$\phi(x) = \begin{pmatrix} \phi^+ \\ \phi^0 \end{pmatrix} \xrightarrow{sym. \ breaking} \frac{1}{\sqrt{2}} \begin{pmatrix} 0 \\ v + h(x) \end{pmatrix},$$

the following mass terms for the fermion fields arise:

$$\begin{aligned} -\mathcal{L}_{Yukawa}^{quarks} &= Y_{ij}^d \overline{Q_{Li}^I} \phi d_{Rj}^I + Y_{ij}^u \overline{Q_{Li}^I} \tilde{\phi} u_{Rj}^I + h.c. \\ &= Y_{ij}^d \overline{d_{Li}^I} \frac{v}{\sqrt{2}} d_{Rj}^I + Y_{ij}^u \overline{u_{Li}^I} \frac{v}{\sqrt{2}} u_{Rj}^I + h.c. + \text{interaction terms} \\ &= M_{ij}^d \overline{d_{Li}^I} d_{Rj}^I + M_{ij}^u \overline{u_{Li}^I} u_{Rj}^I + h.c. + \text{interaction terms} \end{aligned}$$

The interaction terms of the fermion fields to the Higgs field, $\bar{q}qh(x)$, are omitted.

To obtain proper mass terms, the matrices M^d and M^u should be diagonalized. We do this with unitary matrices V^d as follows:

$$\begin{aligned} M_{diag}^d &= V_L^d M^d V_R^{d\dagger} \\ M_{diag}^u &= V_L^u M^u V_R^{u\dagger} \end{aligned}$$

Using the requirement that the matrices V are unitary ($V_L^{d\dagger} V_L^d = \mathbb{1}$) the Lagrangian can now be expressed as follows:

$$\begin{aligned} -\mathcal{L}_{Yukawa}^{quarks} &= \overline{d_{Li}^I} M_{ij}^d d_{Rj}^I + \overline{u_{Li}^I} M_{ij}^u u_{Rj}^I + h.c. + \dots \\ &= \overline{d_{Li}^I} V_L^{d\dagger} V_L^d M_{ij}^d V_R^{d\dagger} V_R^d d_{Rj}^I + \overline{u_{Li}^I} V_L^{u\dagger} V_L^u M_{ij}^u V_R^{u\dagger} V_R^u u_{Rj}^I + h.c. + \dots \\ &= \overline{d_{Li}^I} (M_{ij}^d)_{diag} d_{Rj}^I + \overline{u_{Li}^I} (M_{ij}^u)_{diag} u_{Rj}^I + h.c. + \dots \end{aligned}$$

where the matrices V are absorbed in the quark states, resulting in the following quark mass eigenstates:

$$\begin{aligned} d_{Li} &= (V_L^d)_{ij} d_{Lj}^I & d_{Ri} &= (V_R^d)_{ij} d_{Rj}^I \\ u_{Li} &= (V_L^u)_{ij} u_{Lj}^I & u_{Ri} &= (V_R^u)_{ij} u_{Rj}^I \end{aligned}$$

Note that we can thus express the quark states as interaction eigenstates d^I , u^I or as quark mass eigenstates d , u .

If we now express the Lagrangian in terms of the quark mass eigenstates d , u instead of the weak interaction eigenstates d^I , u^I , the price to pay is that the quark mixing between families (i.e. the off-diagonal elements) appears in the charged current interaction:

$$\begin{aligned} \mathcal{L}_{kinetic,cc}(Q_L) &= \frac{g}{\sqrt{2}} \overline{u_{iL}^I} \gamma_\mu W^{-\mu} d_{iL}^I + \frac{g}{\sqrt{2}} \overline{d_{iL}^I} \gamma_\mu W^{+\mu} u_{iL}^I + \dots \\ &= \frac{g}{\sqrt{2}} \overline{u_{iL}} (V_L^u V_L^{d\dagger})_{ij} \gamma_\mu W^{-\mu} d_{iL} + \frac{g}{\sqrt{2}} \overline{d_{iL}} (V_L^d V_L^{u\dagger})_{ij} \gamma_\mu W^{+\mu} u_{iL} + \dots \end{aligned}$$

The unitary 3×3 matrix

$$V_{CKM} = (V_L^u V_L^{d\dagger})_{ij} \quad (1.13)$$

is the Cabibbo-Kobayashi-Maskawa (CKM) mixing matrix [7].

By convention, the interaction eigenstates and the mass eigenstates are chosen to be equal for the up-type quarks, whereas the down-type quarks are chosen to be rotated, going from the interaction basis to the mass basis:

$$\begin{aligned} u_i^I &= u_j \\ d_i^I &= V_{CKM} d_j \end{aligned}$$

or explicitly:

$$\begin{pmatrix} d^I \\ s^I \\ b^I \end{pmatrix} = \begin{pmatrix} V_{ud} & V_{us} & V_{ub} \\ V_{cd} & V_{cs} & V_{cb} \\ V_{td} & V_{ts} & V_{tb} \end{pmatrix} \begin{pmatrix} d \\ s \\ b \end{pmatrix} \quad (1.14)$$

The connection between the charged current couplings and the quark masses will be discussed further in Section 2.4.

From the definition of V_{CKM} , see Eq. (1.13), follows that the transition from a down type quark to an up-type quark is described by V_{ud} , whereas the transition from an up type quark to a down-type quark is described by V_{ud}^* :

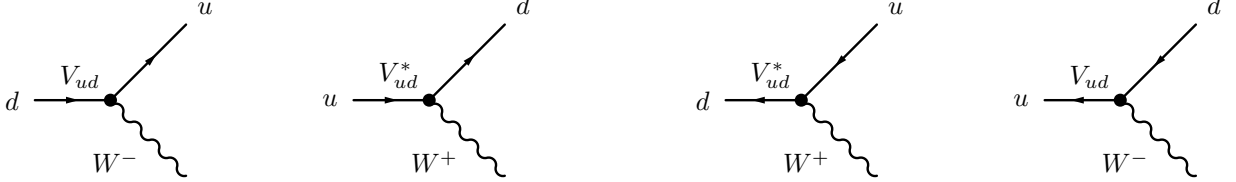


Figure 1.5: *The definition of V_{ij} and V_{ij}^* . Note that if the arrow of time points from left to right, that the two right diagrams represent the situation for anti-quarks.*

1.4.2 CP violation

CP violation shows up in the complex Yukawa couplings. We examine once more the Yukawa part of the Lagrangian:

$$\begin{aligned} -\mathcal{L}_{Yukawa} &= Y_{ij} \overline{\psi_{Li}} \phi \psi_{Rj} + h.c. \\ &= Y_{ij} \overline{\psi_{Li}} \phi \psi_{Rj} + Y_{ij}^* \overline{\psi_{Rj}} \phi^\dagger \psi_{Li} \end{aligned}$$

The CP operation transforms the spinor fields as follows:

$$CP(\overline{\psi_{Li}} \phi \psi_{Rj}) = \overline{\psi_{Rj}} \phi^\dagger \psi_{Li}$$

So, \mathcal{L}_{Yukawa} remains unchanged under the CP operation if $Y_{ij} = Y_{ij}^*$.

Similarly, if we look at the charged current coupling in the basis of quark mass eigenstates,

$$\mathcal{L}_{kinetic,cc}(Q_L) = \frac{g}{\sqrt{2}} \overline{u_{iL}} V_{ij} \gamma_\mu W^{-\mu} d_{iL} + \frac{g}{\sqrt{2}} \overline{d_{iL}} V_{ij}^* \gamma_\mu W^{+\mu} u_{iL} \quad (1.15)$$

and the CP-transformed expression,

$$\mathcal{L}_{kinetic,cc}^{CP}(Q_L) = \frac{g}{\sqrt{2}} \overline{d_{iL}} V_{ij} \gamma_\mu W^{+\mu} u_{iL} + \frac{g}{\sqrt{2}} \overline{u_{iL}} V_{ij}^* \gamma_\mu W^{-\mu} d_{iL} \quad (1.16)$$

then we can conclude that the Lagrangian is unchanged if $V_{ij} = V_{ij}^*$.

The complex nature of the CKM matrix is the origin of CP violation in the Standard Model. In the following chapter the properties of the CKM mixing matrix will be examined in detail.

Chapter 2

The Cabibbo-Kobayashi-Maskawa Matrix

In the previous chapter we saw how the introduction of Yukawa couplings (i.e. the terms where the Higgs couples to the fermions) led to off-diagonal elements in the 3×3 matrix between the different families. By diagonalizing the 3×3 Yukawa matrix, these off-diagonal elements appear in the charged current coupling, in the Cabibbo-Kobayashi-Maskawa-matrix. The CKM-mechanism is the origin of CP violation, and earned Kobayashi and Maskawa the Nobel price in 2008, *“for the discovery of the origin of the broken symmetry which predicts the existence of at least three families of quarks in nature”*.

2.1 Unitarity Triangle(s)

In this section we will discuss the properties of the unitary ¹ CKM matrix V_{CKM} . We start by counting the number of free parameters for the CKM-matrix.

- 1) A general $n \times n$ complex matrix has n^2 complex elements, and thus $2n^2$ real parameters.
- 2) Unitarity ($V^\dagger V = \mathbb{1}$) implies n^2 constraints:
 - n unitary conditions (unity of the diagonal elements);
 - $n^2 - n$ orthogonality relations (vanishing off-diagonal elements).
- 3) The phases of the quarks can be rotated freely: $u_{Li} \rightarrow e^{i\phi_i^u} u_{Li}$ and $d_{Lj} \rightarrow e^{i\phi_j^d} d_{Lj}$. Since the overall phase is irrelevant, $2n - 1$ relative quark phases can be removed.

¹Remember from quantum mechanics the evolution of a wave function, $|\psi(t)\rangle = U(t)|\psi(0)\rangle$. The unitarity condition implies conservation of probability: $\langle\psi(t)|\psi(t)\rangle = \langle\psi(0)|U^\dagger U|\psi(0)\rangle = \langle\psi(0)|\psi(0)\rangle$, provided $U^\dagger U = \mathbb{1}$

Summarizing, the CKM-matrix describing the flavour couplings of n generations of up and down type quarks has $2n^2 - n^2 - (2n - 1) = (n - 1)^2$ free parameters. Subsequently, we can divide these free parameters into Euler angles and phases:

- 4) A general $n \times n$ orthogonal matrix can be constructed from $\frac{1}{2}n(n - 1)$ angles describing the rotations among the n dimensions.
- 5) The remaining free parameters are the phases: $(n - 1)^2 - \frac{1}{2}n(n - 1) = \frac{1}{2}(n - 1)(n - 2)$.

For the Standard Model with three generations we find three Euler angles and one complex phase.

At this point we make a short historical excursion. Before the third family was known, Cabibbo suggested in 1963 the mixing between d and s quarks, by introducing the Cabibbo mixing angle θ_C . This is the only free parameter for a 2×2 unitary matrix, and the mixing matrix is a pure real matrix. To allow for CP violation the mixing matrix has to contain complex elements, satisfying $V_{ij} \neq V_{ij}^*$. This requires at least three families. CP violation was first measured in 1964 by Cronin and Fitch (discussed in more detail in Section 5.3). Subsequently, Kobayashi and Maskawa suggested in 1973 the possibility that the existence of a third family could explain the CP violation within the Standard Model. This happened at the time that not even the second family was completed! The 4th quark, the charm quark was only discovered a year later, in 1974, in the form of the J/ψ resonance. The bottom and the top quark were discovered in 1977 and 1994 respectively. In 2008 Kobayashi and Maskawa were awarded the Nobel prize for the discovery of the origin of the broken symmetry which predicts the existence of at least three families of quarks in nature.

Let us now look at the consequences of the unitarity condition for the CKM-matrix:

$$V^\dagger V = VV^\dagger = \begin{pmatrix} V_{ud} & V_{us} & V_{ub} \\ V_{cd} & V_{cs} & V_{cb} \\ V_{td} & V_{ts} & V_{tb} \end{pmatrix} \begin{pmatrix} V_{ud}^* & V_{cd}^* & V_{td}^* \\ V_{us}^* & V_{cs}^* & V_{ts}^* \\ V_{ub}^* & V_{cb}^* & V_{tb}^* \end{pmatrix} = \begin{pmatrix} 1 & 0 & 0 \\ 0 & 1 & 0 \\ 0 & 0 & 1 \end{pmatrix} \quad (2.1)$$

This leads to the following three unitary relations:

$$\begin{aligned} V_{ud}V_{ud}^* + V_{us}V_{us}^* + V_{ub}V_{ub}^* &= 1 \\ V_{cd}V_{cd}^* + V_{cs}V_{cs}^* + V_{cb}V_{cb}^* &= 1 \\ V_{td}V_{td}^* + V_{ts}V_{ts}^* + V_{tb}V_{tb}^* &= 1 \end{aligned} \quad (2.2)$$

These relations express the so-called *weak universality*, because it shows that the squared sum of the coupling strengths of the u -quark to the d , s and b -quarks is equal to the overall charged coupling of the c -quark (and the t -quark). In addition, we see that this sum adds up to 1, meaning that “there is no probability remaining” to couple to a 4th down-type quark. Obviously, this relation deserves continuous experimental scrutiny.

The remaining relations are known as the orthogonality conditions:

$$\begin{aligned}
V_{ud}V_{cd}^* + V_{us}V_{cs}^* + V_{ub}V_{cb}^* &= 0 \\
V_{ud}V_{td}^* + V_{us}V_{ts}^* + V_{ub}V_{tb}^* &= 0 \\
V_{cd}V_{ud}^* + V_{cs}V_{us}^* + V_{cb}V_{ub}^* &= 0 \\
V_{cd}V_{td}^* + V_{cs}V_{ts}^* + V_{cb}V_{tb}^* &= 0 \\
V_{td}V_{ud}^* + V_{ts}V_{us}^* + V_{tb}V_{ub}^* &= 0 \\
V_{td}V_{cd}^* + V_{ts}V_{cs}^* + V_{tb}V_{cb}^* &= 0
\end{aligned} \tag{2.3}$$

Three of the six equations are simply the complex conjugate version. An additional three interesting equations arise from the unitarity relation $V^\dagger V = \mathbb{1}$:

$$\begin{aligned}
V_{ud}^*V_{us} + V_{cd}^*V_{cs} + V_{td}^*V_{ts} &= 0 \\
V_{ud}^*V_{ub} + V_{cd}^*V_{cb} + V_{td}^*V_{tb} &= 0 \\
V_{us}^*V_{ud} + V_{cs}^*V_{cd} + V_{ts}^*V_{td} &= 0 \\
V_{us}^*V_{ub} + V_{cs}^*V_{cb} + V_{ts}^*V_{tb} &= 0 \\
V_{ub}^*V_{ud} + V_{cb}^*V_{cd} + V_{tb}^*V_{td} &= 0 \\
V_{ub}^*V_{us} + V_{cb}^*V_{cs} + V_{tb}^*V_{ts} &= 0
\end{aligned} \tag{2.4}$$

Equations (2.3-2.4) give relations in which the complex phase is present. As these are sums of three complex numbers that must yield zero they can be viewed as a triangle in the complex plane.

In the literature there are many different parameterizations of the CKM matrix. A convenient representation uses the Euler angles θ_{ij} with i, j denoting the family labels. With the notation $c_{ij} = \cos \theta_{ij}$ and $s_{ij} = \sin \theta_{ij}$ the following parameterization was introduced by Chau and Keung, and has been adopted by the Particle Data Group:

$$\begin{aligned}
V_{CKM} &= \begin{pmatrix} c_{12} & s_{12} & 0 \\ -s_{12} & c_{12} & 0 \\ 0 & 0 & 1 \end{pmatrix} \begin{pmatrix} c_{13} & 0 & s_{13}e^{-i\delta_{13}} \\ 0 & 1 & 0 \\ -s_{13}e^{i\delta_{13}} & 0 & c_{13} \end{pmatrix} \begin{pmatrix} 1 & 0 & 0 \\ 0 & c_{23} & s_{23} \\ 0 & -s_{23} & c_{23} \end{pmatrix} = \\
&\begin{pmatrix} c_{12}c_{13} & s_{12}c_{13} & s_{13}e^{-i\delta_{13}} \\ -s_{12}c_{23} - c_{12}s_{23}s_{13}e^{i\delta_{13}} & c_{12}c_{23} - s_{12}s_{23}s_{13}e^{i\delta_{13}} & s_{23}c_{13} \\ s_{12}s_{23} - c_{12}c_{23}s_{13}e^{i\delta_{13}} & -c_{12}s_{23} - s_{12}c_{23}s_{13}e^{i\delta_{13}} & c_{23}c_{13} \end{pmatrix} \tag{2.5}
\end{aligned}$$

The phase can be made to appear in many elements, and is chosen here to appear in the matrix describing the relation between the 1st and 3rd family.

2.2 Size of matrix elements

We will now briefly discuss the experimental evidence for the size of the matrix elements of the CKM-matrix.

$|V_{ud}|$: is determined from comparing nuclear β -decay rates or neutron decay rates to the μ -decay rate, see Fig. 2.1. In the calculations there are some theoretical uncertainties due to binding energy corrections in nuclei. The best value obtained by averaging many experiments is:

$$|V_{ud}| = 0.97420 \pm 0.00021$$

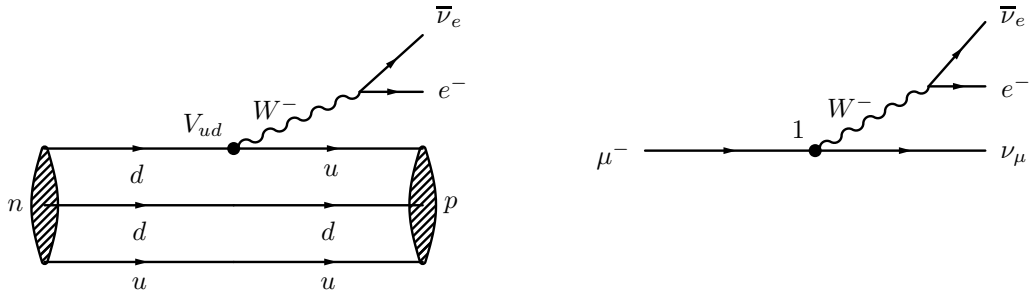


Figure 2.1: Diagrams important for determining V_{ud} .

$|V_{us}|$: is obtained by analysing semi-leptonic K -decays, shown in Fig. 2.2:

$$|V_{us}| = 0.2243 \pm 0.0005$$

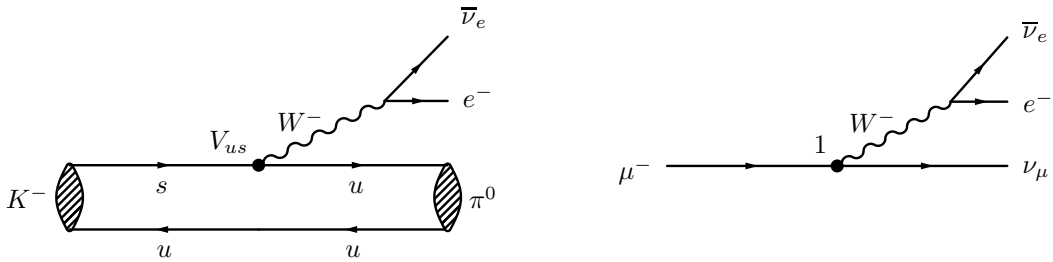
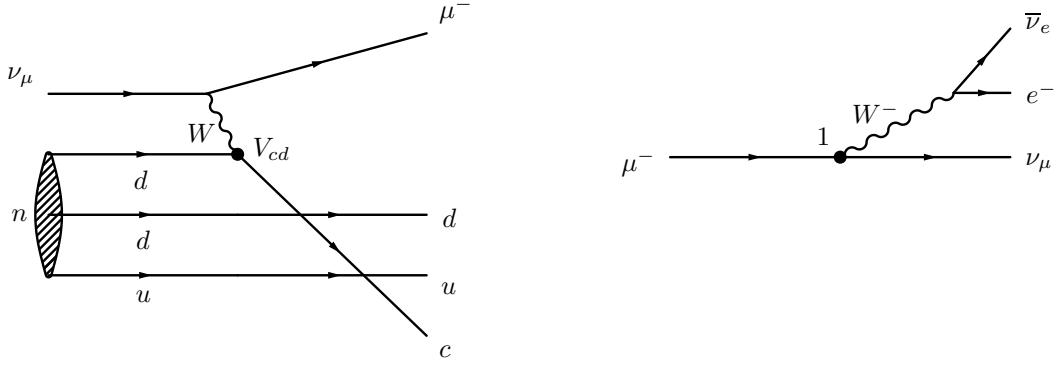


Figure 2.2: Diagrams important for determining V_{us} .

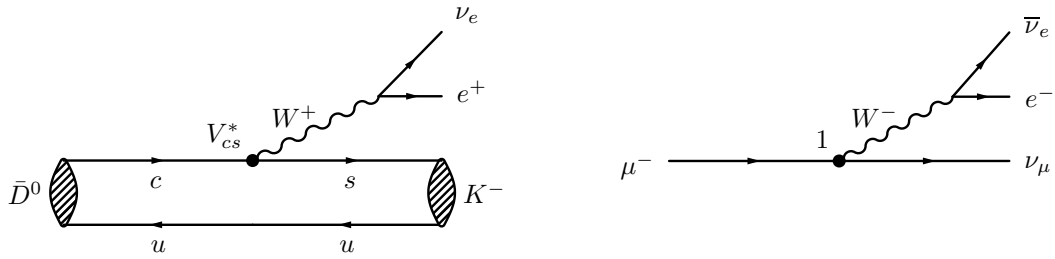
$|V_{cd}|$: was originally obtained by the analysis of neutrino and anti-neutrino induced charm-particle production of the valence d-quark in a neutron (or proton) (see Fig. 2.3). Averaged with measurements on semileptonic charm decays, and also fully leptonic decays like $D^+ \rightarrow \mu^+ \nu$, yields

$$|V_{cd}| = 0.218 \pm 0.004$$

Figure 2.3: Diagrams important for determining V_{cd} .

$|V_{cs}|$: is the matrix element relevant for the dominant decay modes of the charm quark. Here an analogous analysis is performed for semileptonic D -decays, or fully leptonic D_s -decays (see Fig. 2.4). The final result is

$$|V_{cs}| = 0.997 \pm 0.017$$

Figure 2.4: Diagrams important for determining V_{cs} .

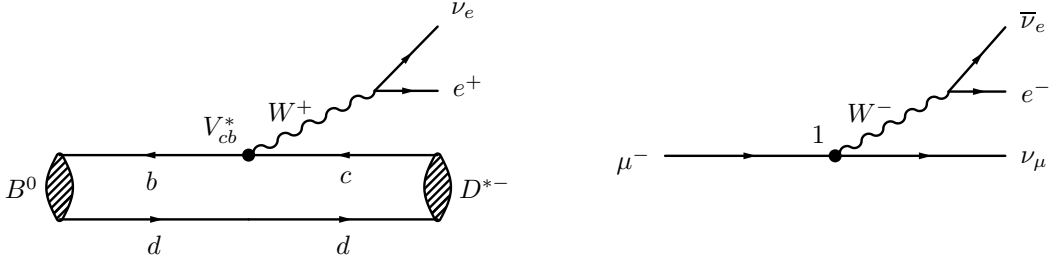
$|V_{cb}|$: is determined from the exclusive $B \rightarrow \bar{D}^{(*)}\mu^+\nu_\mu$ and inclusive $B \rightarrow \bar{D}^{(*)}X\mu^+\nu_\mu$ decays (see Fig. 2.5). A large amount of data is available on these decays both from LEP and from the lower energy e^+e^- experiments BaBar and Belle, giving an average result of

$$|V_{cb}| = 0.0422 \pm 0.0008$$

$|V_{ub}|$: is determined from the semi-leptonic exclusive $B \rightarrow \pi\mu^+\nu_\mu$ and inclusive $B \rightarrow X_u\mu^+\nu_\mu$ decays, similar to the determination of $|V_{cb}|$.

$$|V_{ub}| = 0.00394 \pm 0.00036$$

$|V_{td}|$ and $|V_{ts}|$: These elements cannot be measured from tree-level top-quark decays, and so these elements are probed through loop diagrams such as the box-diagram, as will be

Figure 2.5: *Diagrams important for determining V_{cb} .*

discussed in detail in Section 3.5. Using lattice calculations to take long-distance effects into account, and assuming $|V_{tb}| = 1$, yields:

$$|V_{td}| = 0.0081 \pm 0.0005$$

$$|V_{ts}| = 0.0394 \pm 0.0023$$

$|V_{tb}|$: CDF, D0, ATLAS and CMS measured the ratio of branching ratios $Br(t \rightarrow Wb)/Br(t \rightarrow Wq)$, yielding the following 95% confidence level limit:

$$|V_{tb}| = 1.019 \pm 0.025$$

Taking all the information above, a global fit with Standard Model constraints leads to the following result for the absolute values of the elements:

$$V_{CKM} = \begin{pmatrix} 0.97446 & 0.22452 & 0.00365 \\ 0.22438 & 0.97359 & 0.04214 \\ 0.00896 & 0.04133 & 0.99911 \end{pmatrix} \pm \begin{pmatrix} 0.00010 & 0.00044 & 0.00012 \\ 0.00044 & 0.00011 & 0.00076 \\ 0.00024 & 0.00974 & 0.00003 \end{pmatrix} \quad (2.6)$$

The strength of the charged current couplings seem to exhibit a hierarchy. This pattern motivated Wolfenstein [8] to parametrize the CKM-matrix in powers of the parameter $\lambda \approx \sin \theta_{12} \approx \sqrt{\frac{m_d}{m_s}}$, which is described in the next section.

$$|V_{CKM}| \sim \begin{pmatrix} 1 & \lambda & \lambda^3 \\ \lambda & 1 & \lambda^2 \\ \lambda^3 & \lambda^2 & 1 \end{pmatrix}$$

2.3 Wolfenstein parameterization

Comparing the expressions (2.5) and (2.6) we see that typically the $\sin\theta_{ij}$ are small numbers and that $\sin\theta_{12} \gg \sin\theta_{23} \gg \sin\theta_{13}$. This leads to a very popular *approximate* parameterization of the CKM matrix proposed by Wolfenstein.

$$\sin\theta_{12} = \lambda \quad (2.7)$$

$$\sin\theta_{23} = A\lambda^2 \quad (2.8)$$

$$\sin\theta_{13}e^{-i\delta_{13}} = A\lambda^3(\rho - i\eta) \quad (2.9)$$

where A , ρ and η are numbers of order unity. The CKM matrix then becomes $\mathcal{O}(\lambda^3)$:

$$V_{CKM} = \begin{pmatrix} 1 - \frac{1}{2}\lambda^2 & \lambda & A\lambda^3(\rho - i\eta) \\ -\lambda & 1 - \frac{1}{2}\lambda^2 & A\lambda^2 \\ A\lambda^3(1 - \rho - i\eta) & -A\lambda^2 & 1 \end{pmatrix} + \delta V \quad (2.10)$$

The higher order terms in the Wolfenstein parametrization are of particular importance for the B_s -system, as we will see in chapter 4, because the phase in $|V_{ts}|$ is only apparent at $\mathcal{O}(\lambda^4)$:

$$\delta V = \begin{pmatrix} -\frac{1}{8}\lambda^4 & 0 & 0 \\ \frac{1}{2}A^2\lambda^5(1 - 2(\rho + i\eta)) & -\frac{1}{8}\lambda^4(1 + 4A^2) & 0 \\ \frac{1}{2}A\lambda^5(\rho + i\eta) & \frac{1}{2}A\lambda^4(1 - 2(\rho + i\eta)) & -\frac{1}{2}A^2\lambda^4 \end{pmatrix} + \mathcal{O}(\lambda^6) \quad (2.11)$$

Let us now return to the six orthogonality relations that give rise to the six unitarity triangles. Only two out of the six equations have terms with equal powers in λ .

$$\begin{array}{ccc} V_{ud}V_{ub}^* & + & V_{cd}V_{cb}^* & + & V_{td}V_{tb}^* & = & 0 \\ \mathcal{O}(\lambda^3) & & \mathcal{O}(\lambda^3) & & \mathcal{O}(\lambda^3) & & \end{array} \quad (2.12)$$

$$\begin{array}{ccc} V_{td}V_{ud}^* & + & V_{ts}V_{us}^* & + & V_{tb}V_{ub}^* & = & 0 \\ \mathcal{O}(\lambda^3) & & \mathcal{O}(\lambda^3) & & \mathcal{O}(\lambda^3) & & \end{array} \quad (2.13)$$

These two triangles are relevant for B -decays. The other four equations contain terms with different powers of λ and hence give rise to “squashed” triangles.

The relation shown in Eq. 2.12 is known as *the* unitarity triangle. By dividing the three sides by $|V_{cd}V_{cb}|$ and subsequently rotating the whole triangle (i.e. rephasing all sides, without affecting the relative phases), yields the famous unitarity triangle shown in Fig. 2.6. One side now has unit length and points along the real axis. The apex of the triangle is located by definition at $(\bar{\rho}, \bar{\eta})$ ²:

$$\bar{\rho} + i\bar{\eta} \equiv \frac{V_{ud}V_{ub}^*}{V_{cd}V_{cb}^*}.$$

²Occasionally the generalized parameters $\bar{\rho}$ and $\bar{\eta}$ are defined in the literature as the approximation $\bar{\rho} \equiv \rho(1 - \frac{1}{2}\lambda^2)$ and $\bar{\eta} \equiv \eta(1 - \frac{1}{2}\lambda^2)$ [9].

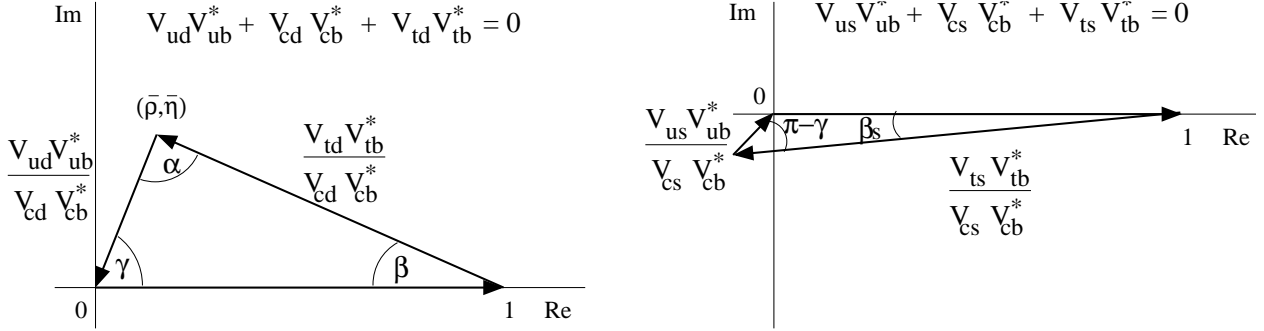


Figure 2.6: (a) “The” unitarity triangle. Shown in the complex plane is the relation $1 + V_{td}V_{tb}^*/V_{cd}V_{cb}^* + V_{ud}V_{ub}^*/V_{cd}V_{cb}^* = 0$. (b) The analogous unitarity triangle for the B_s^0 -system, with the d -quark replaced by the s -quark, $1 + V_{ts}V_{tb}^*/V_{cs}V_{cb}^* + V_{us}V_{ub}^*/V_{cs}V_{cb}^* = 0$.

The parameters $\bar{\rho}$, and $\bar{\eta}$ can be expressed in terms of the Wolfenstein parameters ρ and η as follows:

$$\bar{\rho} = \rho(1 - \frac{1}{2}\lambda^2) + \mathcal{O}(\lambda^4) \quad \bar{\eta} = \eta(1 - \frac{1}{2}\lambda^2) + \mathcal{O}(\lambda^4) \quad (2.14)$$

The angles in “the” unitarity triangle are defined as follows:

$$\alpha \equiv \arg \left[-\frac{V_{td}V_{tb}^*}{V_{ud}V_{ub}^*} \right] \quad \beta \equiv \arg \left[-\frac{V_{cd}V_{cb}^*}{V_{td}V_{tb}^*} \right] \quad \gamma \equiv \arg \left[-\frac{V_{ud}V_{ub}^*}{V_{cd}V_{cb}^*} \right] \quad \beta_s \equiv \arg \left[-\frac{V_{ts}V_{tb}^*}{V_{cs}V_{cb}^*} \right] \quad (2.15)$$

Note that these definitions are convention independent: any phase added to a specific quark cancels out in either the product or the ratio of the CKM-elements. Equivalently, the CKM triangles can be rotated and scaled in the complex plane, without affecting the internal angles of the triangles.

In the Wolfenstein parametrization a phase convention is used such that the elements V_{td} , V_{ub} and V_{ts} have an imaginary component (to order $\mathcal{O}(\lambda^4)$), and $V_{cd}V_{cb}^*$ is real and negative, see Fig. 2.7.

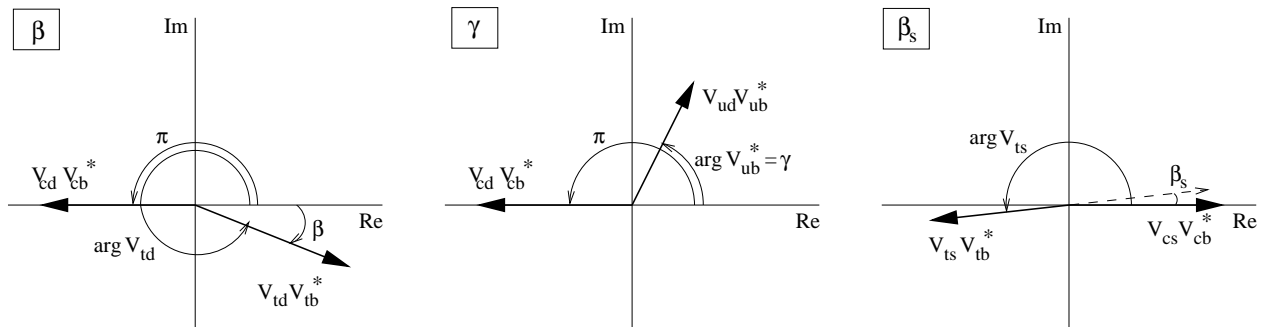


Figure 2.7: The angles β , γ and β_s using the phase convention as given by the Wolfenstein parametrization. (a) β (b) γ (c) β_s .

The expressions for the angles now become:

$$\begin{aligned}\beta &\approx \pi + \arg(V_{cd}V_{cb}^*) - \arg(V_{td}V_{tb}^*) = \pi + \pi - \arg(V_{td}) = -\arg(V_{td}) \\ \gamma &\approx \pi + \arg(V_{ud}V_{ub}^*) - \arg(V_{cd}V_{cb}^*) = \pi - \arg(V_{ub}) - \pi = -\arg(V_{ub}) \\ \beta_s &\approx \pi + \arg(V_{ts}V_{tb}^*) - \arg(V_{cs}V_{cb}^*) = \pi + \arg(V_{ts}) - 0 = \arg(V_{ts}) + \pi\end{aligned}$$

Alternatively, the Wolfenstein phase convention in the CKM-matrix elements can be shown as:

$$V_{CKM, \text{Wolfenstein}} = \begin{pmatrix} |V_{ud}| & |V_{us}| & |V_{ub}|e^{-i\gamma} \\ -|V_{cd}| & |V_{cs}| & |V_{cb}| \\ |V_{td}|e^{-i\beta} & -|V_{ts}|e^{i\beta_s} & |V_{tb}| \end{pmatrix} + \mathcal{O}(\lambda^5) \quad (2.16)$$

As mentioned earlier, CP violation requires $V_{ij} \neq V_{ij}^*$, which is satisfied if the triangle has a finite surface in the complex plane. In fact, it turns out that the surface of all six unitarity triangles have equal surface area.

This quantity denoted as J , also known as the Jarlskog invariant, can be derived in a simple way from the CKM matrix. Remove one column and one row from the CKM matrix and take the product of the diagonal elements with the complex conjugate of the non-diagonal elements. The imaginary part of the product is then equal to J . In total there will be nine possible expressions for J which all give the same result:

$$J = \Im(V_{11}V_{22}V_{12}^*V_{21}^*) = \Im(V_{22}V_{33}V_{23}^*V_{32}^*) = \dots \quad (2.17)$$

In the Wolfenstein parameterization the quantity J becomes

$$J = A^2\lambda^6\eta = 2 \times \text{area} \quad (2.18)$$

In the parameterization of Eq. (2.5) it is

$$J = c_{12}c_{13}^2c_{23}s_{12}s_{13}s_{23}\sin\delta_{13} \quad (2.19)$$

From this form it is clear why this quantity occurs in all CP violation effects. It is zero if any one of the mixing angles is zero. This would reduce the CKM matrix essentially to a 2×2 matrix and allow the removal of the phase. Also if the complex phase would be zero no CP violation is possible. As a final comment the quantity J is just equal to the twice the surface area of the unitarity triangle.

2.4 Discussion

The strong hierarchy in the size of the matrix elements of the quark mixing matrix is intriguing and its origin is not understood. To paraphrase Ikaros Bigi [10]: “*It has to contain a message from nature - albeit in a highly encoded form.*”

We have seen that the origin of the quark mixing matrix lies in the Yukawa couplings between the Higgs field and the quark fields. At the same time, these Yukawa couplings are responsible for the generation of the quark masses, which becomes obvious after diagonalizing the matrix that describes the Yukawa couplings. Also the values of the quark masses show a striking hierarchy, which makes the thought of an underlying connection between the quark masses and the charged current quark couplings fascinating.

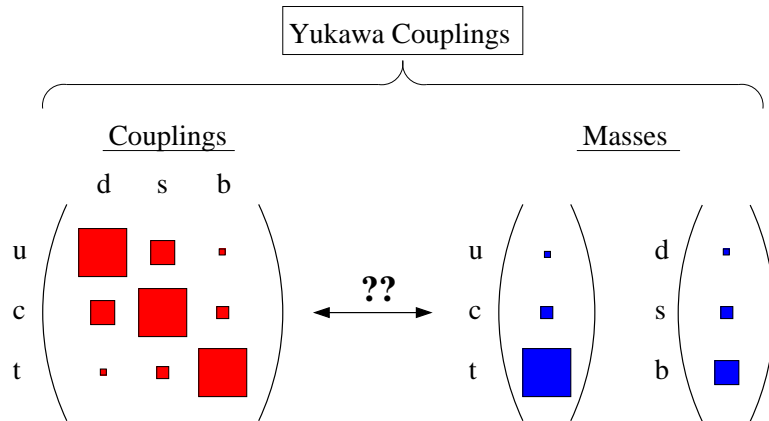


Figure 2.8: *Both the charged current quark couplings and the quark masses originate from the Yukawa couplings and both the couplings and the masses show an intriguing hierarchy. Does this suggest an underlying connection between them?*

We have now set the framework for the incorporation of CP violation in the Standard Model. The question remains of course whether all manifestations of CP violation can be explained. Of course theoretically we can always incorporate new ideas such as supersymmetry or an increase in the number of families to explain any deviations. Experimentally it is now important to verify the Standard Model description. When looking at the unitarity triangle we can see that the length of the sides of the triangle can be extracted from measurable quantities. It is now necessary to investigate whether the angles of the triangle can be measured in an independent way. Disagreement between the angles and the lengths of the side would necessarily signal New Physics. At present many experiments are either running or have been proposed which will be able to give answers to the questions to a greater or lesser extent. In chapter 4 we will proceed to discuss the channels which are considered to be the prime candidates for further investigation of CP violation. Before that, we will introduce the concept of neutral meson oscillations, or mixing, which plays a crucial role in many of the CP-measurements.

2.4.1 The Lepton Sector

We only focussed on the quark couplings, and we will continue to do so in the rest of these notes. Nevertheless it is both enlightening and intriguing to cast some light on the lepton sector.

The discovery of neutrino oscillations [11] implies that neutrinos have non-zero mass, and as a result a similar diagonalization of the Yukawa matrix can be done, compared to the quarks (see Section 1.4.1). The lepton counterpart of the CKM-matrix is called the PMNS-matrix, after Maki, Nakagawa, Sakata and Pontecorvo [12].

The first observation is that the leptons are commonly referred to as the *flavour* eigenstates, in contrast to the *mass* eigenstates that we use for the quarks. For example, we typically picture the W to couple *purely* to a (e, ν_e) pair, whereas the coupling of the W to the quarks we picture as the coupling to a $(u, [d, s, b])$ pair, ie. a mixture of d, s and b quarks. The lepton-equivalent of the down-type mass eigenstates are ν_1, ν_2 and ν_3 .

The second, inspiring, observation is that the magnitude of the elements of the MNSP-matrix show a completely different hierarchy [13]:

$$U_{MNSP} = \begin{pmatrix} U_{e1} & U_{e2} & U_{e3} \\ U_{\mu1} & U_{\mu2} & U_{\mu3} \\ U_{\tau1} & U_{\tau2} & U_{\tau3} \end{pmatrix} \approx \begin{pmatrix} 0.82 & 0.55 & 0.15 \\ 0.37 & 0.57 & 0.70 \\ 0.39 & 0.59 & 0.69 \end{pmatrix}.$$

Interesting numerology appears if we square the matrix elements, revealing the following approximate composition (known as 'tri-bimaximal mixing' [14]):

$$|U_{MNSP}|^2 \approx \begin{pmatrix} \frac{2}{3} & \frac{1}{3} & 0 \\ \frac{1}{6} & \frac{1}{3} & \frac{1}{2} \\ \frac{1}{6} & \frac{1}{3} & \frac{1}{2} \end{pmatrix},$$

or alternatively:

$$U_{MNSP} \approx \begin{pmatrix} \sqrt{\frac{2}{3}} & \sqrt{\frac{1}{3}} & 0 \\ -\sqrt{\frac{1}{3}} & \sqrt{\frac{2}{3}} & 0 \\ 0 & 0 & 1 \end{pmatrix} \begin{pmatrix} 1 & 0 & 0 \\ 0 & 1 & 0 \\ 0 & 0 & 1 \end{pmatrix} \begin{pmatrix} 1 & 0 & 0 \\ 0 & \sqrt{\frac{1}{2}} & \sqrt{\frac{1}{2}} \\ 0 & -\sqrt{\frac{1}{2}} & \sqrt{\frac{1}{2}} \end{pmatrix} = \begin{pmatrix} \sqrt{\frac{2}{3}} & \sqrt{\frac{1}{3}} & 0 \\ -\sqrt{\frac{1}{6}} & \sqrt{\frac{1}{3}} & -\sqrt{\frac{1}{2}} \\ -\sqrt{\frac{1}{6}} & \sqrt{\frac{1}{3}} & \sqrt{\frac{1}{2}} \end{pmatrix}.$$

This comparison should make clear that the hierarchy in the CKM matrix, nor the fact that the matrix is symmetric, is by any means “logical”, or “natural”?!

To date, no experiment has reached the sensitivity to measure complex phases on the MNSP matrix elements, which would indicate CP violation in the lepton sector ³.

³The situation is slightly more complex if the neutrino's are of Majorana nature, ie. if the neutrinos are their own anti-particles. The smallness of the neutrino masses is typically explained with the *see-saw* mechanism, which at the same time predicts a heavy right-handed sterile neutrino at the grand-unification scale.

Chapter 3

Neutral Meson Decays

3.1 Neutral Meson Oscillations

The phenomenon of neutral meson oscillations is important for various reasons. Firstly, in many measurements of CKM-parameters, the oscillations play a crucial role in providing a second transition amplitude from the initial state to a given final state. This second amplitude is needed to determine the relative phase difference between two amplitudes, as described in chapter 4. Secondly, the observation of two K^0 particles with largely varying lifetimes and the resulting discovery of CP violation is of historical importance, see chapter 5, and is described in terms of a superposition of $|K\rangle$ -states and its quantum-mechanical evolution.

The formalism described in this section is valid for all weakly decaying neutral mesons: K^0 , D^0 , B^0 and B_s^0 . We will outline the framework in terms of a generical meson P^0 , which can be substituted at will by K^0 , D^0 , B^0 or B_s^0 . Although we will see that the difference in mass (and thus available phase space for the final state) and coupling strength (CKM-elements) results in dramatically different phenomenology.

3.2 The mass and decay matrix

The states $|P^0\rangle$ and $|\bar{P}^0\rangle$ which are eigenstates of the strong and electromagnetic interactions with common mass m_0 and opposite flavour content. Let us consider an arbitrary superposition of the P^0 and \bar{P}^0 states, which has time-dependent coefficients $a(t)$ and $b(t)$ respectively:

$$\psi(t) = a(t)|P^0\rangle + b(t)|\bar{P}^0\rangle$$

We can write $\psi(t)$ in the subspace of P^0 and \bar{P}^0 as follows

$$\psi(t) = \begin{pmatrix} a(t) \\ b(t) \end{pmatrix}$$

The effective Hamiltonian that governs the time evolution is a sum of the strong, electromagnetic and weak Hamiltonians.

$$H = H_{st} + H_{em} + H_{wk}$$

The wavefunction ψ must then obey

$$i\frac{\partial\psi}{\partial t} = H\psi$$

The Hamiltonian can then, in the (P^0, \bar{P}^0) basis, be written as 2×2 complex matrix:

$$H = M - \frac{i}{2}\Gamma$$

where both M and Γ are Hermitian matrices. M will provide a ‘‘mass’’ term and due to the $-i$, Γ will provide the exponential decay. Note that due to the i , H is not hermitian reflected in the property that the probability to observe either P^0 or \bar{P}^0 is not conserved, but goes down with time:

$$\frac{d}{dt} (|a(t)|^2 + |b(t)|^2) = - (a(t)^*b(t)^*) \begin{pmatrix} \Gamma_{11} & 0 \\ 0 & \Gamma_{22} \end{pmatrix} \begin{pmatrix} a(t) \\ b(t) \end{pmatrix}$$

If the weak part of the Hamiltonian did not exist the P system would be stable and so H would reduce to

$$H \rightarrow M = \begin{pmatrix} m_{P^0} & 0 \\ 0 & m_{\bar{P}^0} \end{pmatrix}$$

where $m_{P^0} = \langle P^0 | H_{st} + H_{em} | P^0 \rangle$ and $m_{\bar{P}^0} = \langle \bar{P}^0 | H_{st} + H_{em} | \bar{P}^0 \rangle$ and the off-diagonal elements are 0 through flavour conservation. With the weak interaction responsible for the decay we get:

$$i\frac{\partial\psi}{\partial t} = H\psi = (M - \frac{i}{2}\Gamma)\psi = \begin{pmatrix} M_{11} - \frac{i}{2}\Gamma_{11} & 0 \\ 0 & M_{22} - \frac{i}{2}\Gamma_{22} \end{pmatrix} \psi$$

If we now allow for the transitions $P^0 \rightarrow \bar{P}^0$, the off-diagonal elements are introduced:

$$i\frac{\partial\psi}{\partial t} = H\psi = (M - \frac{i}{2}\Gamma)\psi = \begin{pmatrix} M_{11} - \frac{i}{2}\Gamma_{11} & M_{12} - \frac{i}{2}\Gamma_{12} \\ M_{21} - \frac{i}{2}\Gamma_{21} & M_{22} - \frac{i}{2}\Gamma_{22} \end{pmatrix} \psi$$

The off-diagonal elements consist of two parts, M_{12} and $\frac{1}{2}\Gamma_{12}$, which describe different ways of the $P^0 \rightarrow \bar{P}^0$ transition. M_{12} quantifies the short-distance contribution from the (calculable) box diagram as will be discussed in Section 3.5. Γ_{12} is a measure of the contribution from the virtual, intermediate, decays to a state f , see Fig. 3.1.

If we now assume that CPT is valid then it follows that $M_{11} = M_{22}$, $M_{21} = M_{12}^*$ and $\Gamma_{11} = \Gamma_{22}$, $\Gamma_{21} = \Gamma_{12}^*$ meaning that mass and total decay width of particle and antiparticle are identical.

$$i\frac{\partial\psi}{\partial t} = H\psi = (M - \frac{i}{2}\Gamma)\psi = \begin{pmatrix} M - \frac{i}{2}\Gamma & M_{12} - \frac{i}{2}\Gamma_{12} \\ M_{12}^* - \frac{i}{2}\Gamma_{12}^* & M - \frac{i}{2}\Gamma \end{pmatrix} \psi \quad (3.1)$$

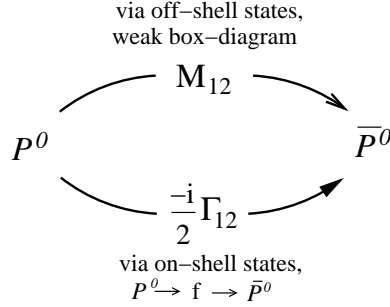


Figure 3.1: The neutral meson oscillation consists of two contributions, namely through off-shell states and on-shell states.

In general there can be a relative phase between Γ_{12} and M_{12} [15]:

$$\phi = \arg\left(-\frac{M_{12}}{\Gamma_{12}}\right) \quad (3.2)$$

which is the relative phase difference between the on-shell (or dispersive) and off-shell (or absorptive) transition. This leads to the relations

$$\Delta m = 2|M_{12}| \quad (3.3)$$

$$\Delta\Gamma = 2|\Gamma_{12}| \cos\phi. \quad (3.4)$$

If T is conserved then it follows that $\Gamma_{12}^*/\Gamma_{12} = M_{12}^*/M_{12}$ so that by introducing a free phase we can make Γ_{12} and M_{12} real.

Under these assumptions we can now find the eigenvalues and eigenvectors of the Hamiltonian. These will describe the masses and decay widths and the P^0, \bar{P}^0 superpositions, that describe the physical particles.

3.3 Eigenvalues and -vectors of Mass-decay Matrix

Given the Schrödinger equation (3.1) we find the eigenvalues of the mass-decay matrix, by solving the determinantal equation [16]:

$$\begin{vmatrix} M - \frac{i}{2}\Gamma - \lambda & M_{12} - \frac{i}{2}\Gamma_{12} \\ M_{12}^* - \frac{i}{2}\Gamma_{12}^* & M - \frac{i}{2}\Gamma - \lambda \end{vmatrix} = 0$$

Using the shorthand notation $F = \sqrt{(M_{12} - \frac{i}{2}\Gamma_{12})(M_{12}^* - \frac{i}{2}\Gamma_{12}^*)}$ we find the eigenvalues $\lambda_{\pm} = M - \frac{i}{2}\Gamma \pm F$. Splitting the real and imaginary part by defining $\lambda_{\pm} = m_{\pm} + \frac{i}{2}\Gamma_{\pm}$ and

$\lambda_+ = m_2 + \frac{i}{2}\Gamma_2$, we obtain:

$$\begin{aligned} m_1 + \frac{i}{2}\Gamma_1 &= M - \Re F - \frac{i}{2}(\Gamma - 2\Im F) \\ m_2 + \frac{i}{2}\Gamma_2 &= M + \Re F - \frac{i}{2}(\Gamma + 2\Im F) \end{aligned}$$

These expressions invite the use of the following notation:

$$\begin{aligned} \Delta m &\equiv m_2 - m_1 = 2\Re F \\ \Delta\Gamma &\equiv \Gamma_1 - \Gamma_2 = 4\Im F \end{aligned}$$

If we express the eigenstates P_1 and P_2 as:

$$\begin{aligned} |P_1\rangle &= p|P^0\rangle - q|\bar{P}^0\rangle \\ |P_2\rangle &= p|P^0\rangle + q|\bar{P}^0\rangle \end{aligned}$$

we find p and q by solving

$$\begin{pmatrix} M - \frac{i}{2}\Gamma & M_{12} - \frac{i}{2}\Gamma_{12} \\ M_{12}^* - \frac{i}{2}\Gamma_{12}^* & M - \frac{i}{2}\Gamma \end{pmatrix} \begin{pmatrix} p \\ q \end{pmatrix} = \lambda_{\pm} \begin{pmatrix} p \\ q \end{pmatrix}$$

yielding:

$$\frac{q}{p} = \pm \sqrt{\frac{M_{12}^* - \frac{i}{2}\Gamma_{12}^*}{M_{12} - \frac{i}{2}\Gamma_{12}}}$$

The state $|P_1\rangle$ is the mass eigenstate with mass m_1 and lifetime Γ_1 . Similarly we obtain the mass m_2 and lifetime Γ_2 for state $|P_2\rangle$. The sign of q/p determines whether $|P_1\rangle$ or $|P_2\rangle$ is heavier. The choice of a positive value of Δm gives:

$$\frac{q}{p} = \sqrt{\frac{M_{12}^* - \frac{i}{2}\Gamma_{12}^*}{M_{12} - \frac{i}{2}\Gamma_{12}}} \quad (3.5)$$

Note that we have *chosen* the sign here, such that $\Delta m > 0$, but that does not imply anything for the sign of $\Delta\Gamma$: experiment has to judge whether $\Delta\Gamma$ is positive or negative, relative to the sign of Δm .

We can also relate q/p to the mixing phase as introduced in Eq.(3.2) [15]:

$$\frac{|\Gamma_{12}|}{|M_{12}|} \sin \phi = \frac{\Delta\Gamma}{\Delta m} \tan \phi = 2 \left(1 - \frac{|q|}{|p|} \right). \quad (3.6)$$

(This will turn out to be the size of a possible CP asymmetry for flavour-specific final states, a_{fs} .)

3.4 Time evolution

We define the two mass eigenstates of the neutral mesons as ¹:

$$\begin{aligned} |P_H\rangle &= p|P^0\rangle + q|\bar{P}^0\rangle \\ |P_L\rangle &= p|P^0\rangle - q|\bar{P}^0\rangle \end{aligned} \quad (3.7)$$

where the subscripts 1 and 2 are replaced by H and L , indicating the heavy and light mass eigenstate, respectively. We can then decompose the P^0 and \bar{P}^0 states as

$$\begin{aligned} |P^0\rangle &= \frac{1}{2p} [|P_H\rangle + |P_L\rangle] \\ |\bar{P}^0\rangle &= \frac{1}{2q} [|P_H\rangle - |P_L\rangle] \end{aligned} \quad (3.8)$$

The states $|P_H\rangle$ and $|P_L\rangle$ are mass eigenstates and from the Schrödinger equation (with diagonal Hamiltonian) the usual time dependent wave functions are obtained:

$$\begin{aligned} |P_H(t)\rangle &= e^{-im_H t - \frac{1}{2}\Gamma_H t} |P_H(0)\rangle \\ |P_L(t)\rangle &= e^{-im_L t - \frac{1}{2}\Gamma_L t} |P_L(0)\rangle \end{aligned} \quad (3.9)$$

By combining Eqs. (3.9), (3.8) and (3.7) we get:

$$\begin{aligned} |P^0(t)\rangle &= \frac{1}{2p} \left\{ e^{-im_H t - \frac{1}{2}\Gamma_H t} |P_H(0)\rangle + e^{-im_L t - \frac{1}{2}\Gamma_L t} |P_L(0)\rangle \right\} \\ &= \frac{1}{2p} \left\{ e^{-im_H t - \frac{1}{2}\Gamma_H t} (p|P^0\rangle + q|\bar{P}^0\rangle) + e^{-im_L t - \frac{1}{2}\Gamma_L t} (p|P^0\rangle - q|\bar{P}^0\rangle) \right\} \\ &= \frac{1}{2} \left(e^{-im_H t - \frac{1}{2}\Gamma_H t} + e^{-im_L t - \frac{1}{2}\Gamma_L t} \right) |P^0\rangle + \frac{q}{2p} \left(e^{-im_H t - \frac{1}{2}\Gamma_H t} - e^{-im_L t - \frac{1}{2}\Gamma_L t} \right) |\bar{P}^0\rangle \\ &= g_+(t)|P^0\rangle + \left(\frac{q}{p} \right) g_-(t)|\bar{P}^0\rangle \end{aligned} \quad (3.10)$$

where we define the functions

$$\begin{aligned} g_+(t) &= \frac{1}{2} \left(e^{-im_H t - \frac{1}{2}\Gamma_H t} + e^{-im_L t - \frac{1}{2}\Gamma_L t} \right) = \frac{1}{2} e^{-iMt} \left(e^{-i\frac{1}{2}\Delta m t - \frac{1}{2}\Gamma_H t} + e^{+i\frac{1}{2}\Delta m t - \frac{1}{2}\Gamma_L t} \right) \\ g_-(t) &= \frac{1}{2} \left(e^{-im_H t - \frac{1}{2}\Gamma_H t} - e^{-im_L t - \frac{1}{2}\Gamma_L t} \right) = \frac{1}{2} e^{-iMt} \left(e^{-i\frac{1}{2}\Delta m t - \frac{1}{2}\Gamma_H t} - e^{+i\frac{1}{2}\Delta m t - \frac{1}{2}\Gamma_L t} \right) \end{aligned}$$

¹There are some subtleties concerning the sign (or phase) convention. Let us assume CP symmetry, $|q/p| = 1$. We can choose $q/p = \pm 1$ and $CP|P^0\rangle = \pm|\bar{P}^0\rangle$. Once the sign of q/p is fixed, see Eq.(3.5), experiment decides if P_H is the state that is (more) even or odd, which fixes $CP|P^0\rangle = \pm|\bar{P}^0\rangle$. In principle this can be different for K^0 , B^0 and B_s^0 . We choose the sign convention $\Delta m_K > 0$ and $CP|K^0\rangle = -|\bar{K}^0\rangle$ such that $CP|K_L\rangle = -|K_L\rangle$ (or $\Delta\Gamma_K = \Gamma_S - \Gamma_L > 0$) according to experiment. This leads to the sign convention in Eq.(3.7), and implies $\Delta m_K = m_L - m_S$. Also in the B -system the heavier mass eigenstate B_H is (more) CP odd, and the CP-even state in the B_s -system can decay to the final state $D_s^+ D_s^-$, and has therefore a slightly shorter lifetime.

where $M = (m_H + m_L)/2$ and $\Delta m = m_H - m_L$. Likewise, we get for the time evolution of the state $|\bar{P}^0\rangle$:

$$|\bar{P}^0(t)\rangle = g_-(t) \left(\frac{p}{q}\right) |P^0\rangle + g_+(t) |\bar{P}^0\rangle \quad (3.11)$$

If we start from a pure sample of $|P^0\rangle$ particles (e.g. produced by the strong interaction) then we can calculate the probability of measuring the state $|\bar{P}^0\rangle$ at time t :

$$|\langle \bar{P}^0 | P^0(t) \rangle|^2 = |g_-(t)|^2 \left| \frac{p}{q} \right|^2$$

with

$$\begin{aligned} |g_{\pm}(t)|^2 &= \frac{1}{4} (e^{-\Gamma_H t} + e^{-\Gamma_L t} \pm e^{-\Gamma t} (e^{-i\Delta m t} + e^{+i\Delta m t})) \\ &= \frac{1}{4} (e^{-\Gamma_H t} + e^{-\Gamma_L t} \pm 2e^{-\Gamma t} \cos \Delta m t) \\ &= \frac{e^{-\Gamma t}}{2} \left(\cosh \frac{1}{2} \Delta \Gamma t \pm \cos \Delta m t \right) \end{aligned} \quad (3.12)$$

where $\Gamma = (\Gamma_L + \Gamma_H)/2$ and $\Delta \Gamma = \Gamma_H - \Gamma_L$. Here we see that Γ fulfills the natural role of decay constant, $\Gamma = 1/\tau$, justifying the choice of $\frac{1}{2}$ in the hamiltonian in Eq. (3.1). The sign of Δm is by definition positive, but the sign of $\Delta \Gamma$ has to be determined experimentally.

3.5 The Amplitude of the Box diagram

The short distance contribution to the $P^0 \leftrightarrow \bar{P}^0$ transitions of neutral meson oscillations is described by Δm and can be represented by a Feynman diagram known as the box diagram, and can be calculated in perturbation theory.

In this section we will calculate the value of Δm by studying this so-called box diagram. We will investigate the process of $K^0 \leftrightarrow \bar{K}^0$ using the CKM matrix. To describe mixing between a K^0 which has strangeness $S = 1$ and a \bar{K}^0 which has $S = -1$ we must introduce an amplitude which creates a $\Delta S = 2$ transition. This must necessarily be a *second order* weak interaction. The transition necessary for mixing is shown in Fig. 3.2. The calculation of the box diagram is quite complicated but we will illustrate some of the features in the calculation of the $K_L^0 - K_S^0$ mass difference.

The mass difference is given by

$$\Delta m = m_{K_L^0} - m_{K_S^0} = \langle K_L^0 | H | K_L^0 \rangle - \langle K_S^0 | H | K_S^0 \rangle \quad (3.13)$$

As we saw in the previous section, the mass eigenstates can be expressed as a linear combination of the flavour eigenstates. The amplitude $\langle K^0 | H | \bar{K}^0 \rangle$ can now be calculated via the box diagram of Fig. 3.2. As an example we use the Feynman rules to derive an expression for the amplitude where both the intermediate quarks are u quarks:

$$\begin{aligned} \mathcal{M}_{uu} = & i \left(\frac{-ig_w}{2\sqrt{2}} \right)^4 (V_{us}^* V_{ud} V_{us} V_{ud}) \\ & \int \frac{d^4 k}{(2\pi)^4} \left(\frac{-ig^{\lambda\sigma} - k^\lambda k^\sigma / m_W^2}{k^2 - m_W^2} \right) \left(\frac{-ig^{\alpha\rho} - k^\alpha k^\rho / m_W^2}{k^2 - m_W^2} \right) \\ & \left[\bar{u}_s \gamma_\lambda (1 - \gamma^5) \frac{\not{k} + m_u}{k^2 - m_u^2} \gamma_\rho (1 - \gamma^5) u_d \right] \left[\bar{v}_s \gamma_\alpha (1 - \gamma^5) \frac{\not{k} + m_u}{k^2 - m_u^2} \gamma_\sigma (1 - \gamma^5) v_d \right] \end{aligned}$$

Here we readily recognise the weak coupling constant to the fourth power, the CKM matrix elements for the vertices, the W propagator terms, the quark and anti-quark spinors and the factors for the intermediate fermion lines.

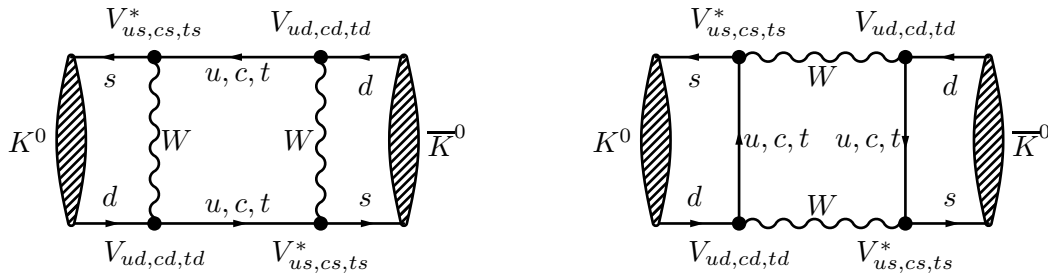


Figure 3.2: Box diagrams responsible for $K^0 \rightarrow \bar{K}^0$ mixing.

Taking the sum of all amplitudes with all possible intermediate quark lines we get an amplitude which is proportional to (assuming $k^2 \ll m_W^2$).

$$\mathcal{M} \propto \int d^4k k_\mu k_\nu \left(\frac{V_{us}^* V_{ud}}{k^2 - m_u^2} + \frac{V_{cs}^* V_{cd}}{k^2 - m_c^2} + \frac{V_{ts}^* V_{td}}{k^2 - m_t^2} \right)^2 \quad (3.14)$$

Which with the aid of the equation $V_{us}^* V_{ud} + V_{cs}^* V_{cd} + V_{ts}^* V_{td} = 0$ we can rewrite as

$$\mathcal{M} \propto \int d^4k k_\mu k_\nu \left(V_{cs}^* V_{cd} \left[\frac{1}{k^2 - m_c^2} - \frac{1}{k^2 - m_u^2} \right] + V_{ts}^* V_{td} \left[\frac{1}{k^2 - m_t^2} - \frac{1}{k^2 - m_u^2} \right] \right)^2$$

This then finally leads to an answer that has three terms [17], one term depending on m_c^2/m_W^2 , one term depending on m_t^2/m_W^2 and and a term which has a complicated dependence on both m_c^2/m_W^2 and m_t^2/m_W^2 . The magnitude of the so-called Inami-Lim factor these three terms is listed in Table 3.1, together with the size of the CKM-elements involved in the box diagram.

This calculation only takes into account the quark level transitions and so the full calculation must take into account the transition from $K^0 \rightarrow d\bar{s}$ and gluonic corrections and colour factors. Because $|V_{td}V_{ts}| \ll |V_{cd}V_{cs}|$ the charm contribution in the loop dominates, and the final answer becomes:

$$\Delta m_K = \frac{G_F^2 m_W^2}{6\pi^2} \eta_{QCD} B_K f_K^2 m_K \left[S_0(m_c^2/m_W^2) |V_{cd}V_{cs}|^2 \right] \quad (3.15)$$

where G_F is the Fermi coupling constant, η_{QCD} is the QCD correction (≈ 0.85), B and f_K^2 is the ‘‘bag-factor’’ and the decay constant, respectively, which describe the effect of the transition from bound to free quarks and V_{ij} are the CKM matrix elements.

In the B -system we have $|V_{td}V_{tb}| \sim |V_{cd}V_{cb}|$, but because $m_t \gg m_c$ now the top contribution in the loop dominates. By replacing the internal charm quark with the top quark, and replacing the strange flavour by the bottom quark we find for the B -system:

$$\Delta m_B = \frac{G_F^2 m_W^2}{6\pi^2} \eta_{QCD} B_B f_B^2 m_B \left[S_0(m_t^2/m_W^2) |V_{td}V_{tb}|^2 \right] \quad (3.16)$$

Internal quarks	Inami-Lim factor	CKM factor		
		K^0	B^0	B_s^0
c, c	$3.5 \cdot 10^{-4}$	λ^2 (2.7 $\cdot 10^{-2}$)	$A^2 \lambda^6$ (7.4 $\cdot 10^{-5}$)	$A^2 \lambda^4$ (1.4 $\cdot 10^{-3}$)
c, t	$3.0 \cdot 10^{-3}$	$A^2 \lambda^6 1 - \rho - i\eta $ (8.8 $\cdot 10^{-6}$)	$A^2 \lambda^6 1 - \rho - i\eta $ (7.3 $\cdot 10^{-5}$)	$A^2 \lambda^4$ (1.5 $\cdot 10^{-3}$)
t, t	2.5	$A^4 \lambda^{10} 1 - \rho - i\eta ^2$ (1.1 $\cdot 10^{-7}$)	$A^2 \lambda^6 1 - \rho - i\eta ^2$ (7.2 $\cdot 10^{-5}$)	$A^2 \lambda^4$ (1.5 $\cdot 10^{-3}$)

Table 3.1: The magnitude of the three terms contributing to the box diagram, expressed separately for the Inami-Lim factors (depending on m_q^2/m_W^2) and for the CKM elements [18]. Clearly, the charm-quark contribution dominates in the K -system, where the CKM-factor compensates for the small Inami-Lim factor. In the B -systems the top-quark contribution dominates.

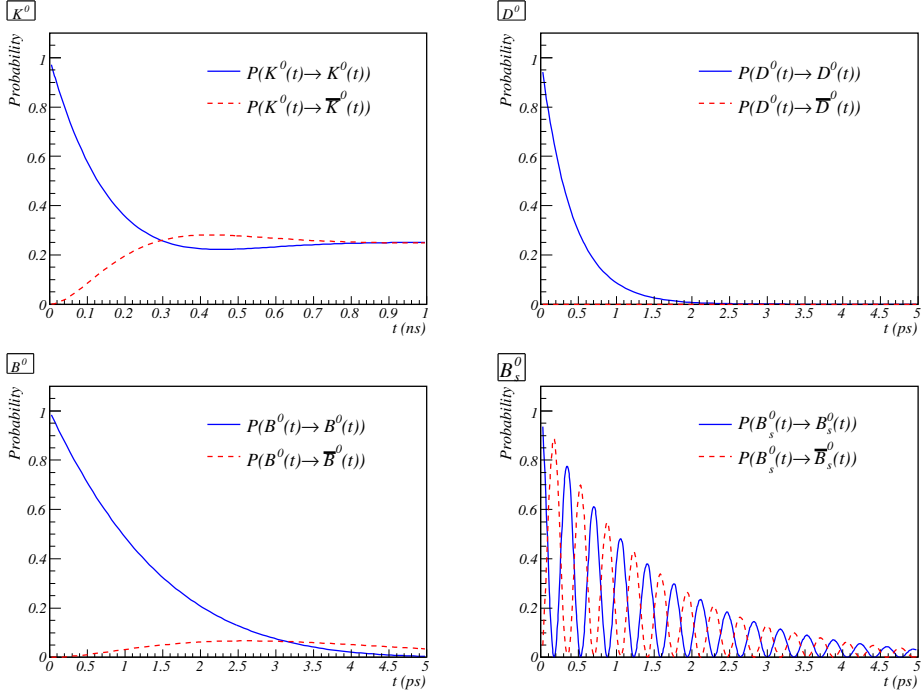


Figure 3.3: If one starts with a pure P^0 -meson beam the probability to observe a P^0 or a \bar{P}^0 -meson at time t is shown, $\text{Prob}(t) = \frac{e^{-\Gamma t}}{2} (\cosh \frac{1}{2} \Delta\Gamma t \pm \cos \Delta m t)$.

At this point we can see how the neutral mesons K^0 , D^0 , B^0 and B_s^0 in reality oscillate and what the differences are. As mentioned earlier, the oscillations consist of two components, M_{12} and $\frac{1}{2}\Gamma_{12}$. As a general rule, all possible quark exchanges contribute to M_{12} , but only actual final states contribute to Γ_{12} [16]. The short-distance, off-shell contribution from M_{12} depends on the size of the CKM-elements at the corners of the box-diagram, and on the mass of the particles in the box. In the case of D^0 -mixing, the mass of the heaviest down-type quark in the box, m_b is not large enough to compensate the suppression of the CKM-elements $|V_{ub}V_{cb}|$. As a result, the light quarks dominate the short-range D^0 -mixing and proceeds proportional to $\sim |V_{us}V_{cs}|^2 m_s^2 \sim \lambda^2 m_s^2$. As a consequence, the mixing parameters are expected to be small, and the D -mesons decay before they have the chance to oscillate.

The oscillation probability of D -mesons is clearly suppressed compared to B^0 -mixing, see Fig. 3.3, which is proportional to $\sim |V_{tb}V_{td}|^2 m_t^2 \sim \lambda^6 m_t^2$. B_s^0 -mixing on the other hand, is more pronounced, see Fig. 3.3d), due to the magnitude of V_{ts} : $\sim |V_{tb}V_{ts}|^2 m_t^2 \sim \lambda^4 m_t^2$. Finally, K^0 -oscillation is dominated by the (light) charm quark in the loop, $\sim |V_{cd}V_{cs}|^2 m_c^2 \sim \lambda^2 m_c^2$. However, the kaons profit from the fact that their lifetime is much higher compared to the B -mesons. Note that the sum of the B^0 and \bar{B}^0 distributions in Fig. 3.3 give a perfect exponential decay, because the mass eigenstates B_H and B_L happen to have equal lifetimes, $\Delta\Gamma = 0$. In contrast, the sum of the K^0 and \bar{K}^0 distributions results in the sum of two exponential distributions, corresponding to the K_S and K_L with short and long lifetime, respectively.

Often the dimensionless variables x and y are used to express the mixing behaviour, expressing the oscillation rate relative to the lifetime:

$$x = \frac{\Delta m}{\Gamma} \qquad y = \frac{\Delta \Gamma}{2\Gamma}$$

The oscillation parameters of the various neutral mesons are summarized in Table 3.2.

	$\tau = 1/\Gamma$	Δm	x	y
K -system	$0.26 \times 10^{-9} \text{ s}^{-1}$	5.29 ns^{-1}	0.477	-1
D -system	$0.41 \times 10^{-12} \text{ s}$	0.0019 ps^{-1}	0.0046	0.0062
B -system	$1.52 \times 10^{-12} \text{ s}$	0.507 ps^{-1}	0.769	0.0005^2
B_s -system	$1.53 \times 10^{-12} \text{ s}$	17.76 ps^{-1}	26.8	0.068^2

Table 3.2: *Oscillation parameters of the various neutral mesons.*

¹Note that the average lifetime Γ is not a very meaningful quantity in the K -system due to the large difference between the lifetimes of the two mass-eigenstates K_s and K_L .

²These numbers are theoretical values, rather than experimental measurements. The transition $T(B_s^0 \rightarrow \bar{D}_s D_s \rightarrow \bar{B}_s^0)$ is the largest contribution and proceeds proportional to $|V_{cb}|^2$. $\Delta\Gamma_{B^0} < \Delta\Gamma_{B_s^0}$ because the transitions $T(B^0 \rightarrow (\bar{D}D), (\pi\pi), (D\pi) \rightarrow \bar{B}^0)$ are all Cabibbo suppressed.

3.6 Meson Decays

In this section we extend the formalism of neutral meson oscillations, and include the subsequent decay of the meson to a final state f . We consider the following four decay amplitudes

$$\begin{aligned} A(f) &= \langle f|T|P^0\rangle & \bar{A}(f) &= \langle f|T|\bar{P}^0\rangle \\ A(\bar{f}) &= \langle \bar{f}|T|P^0\rangle & \bar{A}(\bar{f}) &= \langle \bar{f}|T|\bar{P}^0\rangle \end{aligned}$$

and define the complex parameter λ_f (not be confused with the Wolfenstein parameter λ !):

$$\lambda_f = \frac{q \bar{A}_f}{p A_f}, \quad \bar{\lambda}_f = \frac{1}{\lambda_f}, \quad \lambda_{\bar{f}} = \frac{q \bar{A}_{\bar{f}}}{p A_{\bar{f}}}, \quad \bar{\lambda}_{\bar{f}} = \frac{1}{\lambda_{\bar{f}}} \quad (3.17)$$

The general expression for the time dependent decay rates, $\Gamma_{P^0 \rightarrow f}(t) = |\langle f|T|P^0(t)\rangle|^2$, give us the probability that the state P^0 at $t = 0$ decays to the final state f at time t , and can now be constructed as follows, using Eqs. (3.10) and (3.11):

$$\begin{aligned} \Gamma_{P^0 \rightarrow f}(t) &= |A_f|^2 \left(|g_+(t)|^2 + |\lambda_f|^2 |g_-(t)|^2 + 2\Re[\lambda_f g_+^*(t) g_-(t)] \right) \\ \Gamma_{P^0 \rightarrow \bar{f}}(t) &= |\bar{A}_{\bar{f}}|^2 \left| \frac{q}{p} \right|^2 \left(|g_-(t)|^2 + |\bar{\lambda}_{\bar{f}}|^2 |g_+(t)|^2 + 2\Re[\bar{\lambda}_{\bar{f}} g_+(t) g_-^*(t)] \right) \\ \Gamma_{\bar{P}^0 \rightarrow f}(t) &= |A_f|^2 \left| \frac{p}{q} \right|^2 \left(|g_-(t)|^2 + |\lambda_f|^2 |g_+(t)|^2 + 2\Re[\lambda_f g_+(t) g_-^*(t)] \right) \\ \Gamma_{\bar{P}^0 \rightarrow \bar{f}}(t) &= |\bar{A}_{\bar{f}}|^2 \left(|g_+(t)|^2 + |\bar{\lambda}_{\bar{f}}|^2 |g_-(t)|^2 + 2\Re[\bar{\lambda}_{\bar{f}} g_+^*(t) g_-(t)] \right) \end{aligned} \quad (3.18)$$

with

$$\begin{aligned} |g_{\pm}(t)|^2 &= \frac{e^{-\Gamma t}}{2} \left(\cosh \frac{1}{2} \Delta \Gamma t \pm \cos \Delta m t \right) \\ g_+^*(t) g_-(t) &= \frac{e^{-\Gamma t}}{2} \left(\sinh \frac{1}{2} \Delta \Gamma t + i \sin \Delta m t \right) \\ g_+(t) g_-^*(t) &= \frac{e^{-\Gamma t}}{2} \left(\sinh \frac{1}{2} \Delta \Gamma t - i \sin \Delta m t \right) \end{aligned} \quad (3.19)$$

The terms proportional $|A|^2$ are associated with decays that occurred without oscillation, whereas the terms proportional to $|A|^2 (q/p)^2$ or $|A|^2 (p/q)^2$ are associated with decays following a net oscillation. The third terms, proportional to $\Re g^* g$, are associated to the interference between the two cases.

Combining Eqs. (3.18) and (3.19) results in the following expressions for the decay rates

for neutral mesons, also known as the master equations:

$$\begin{aligned}
\Gamma_{P^0 \rightarrow f}(t) &= |A_f|^2 \frac{e^{-\Gamma t}}{2} \\
&\quad \left((1 + |\lambda_f|^2) \cosh \frac{1}{2} \Delta \Gamma t + 2\Re \lambda_f \sinh \frac{1}{2} \Delta \Gamma t + (1 - |\lambda_f|^2) \cos \Delta m t - 2\Im \lambda_f \sin \Delta m t \right) \\
\Gamma_{\bar{P}^0 \rightarrow f}(t) &= |A_f|^2 \left| \frac{p}{q} \right|^2 \frac{e^{-\Gamma t}}{2} \\
&\quad \left((1 + |\lambda_f|^2) \cosh \frac{1}{2} \Delta \Gamma t + 2\Re \lambda_f \sinh \frac{1}{2} \Delta \Gamma t - (1 - |\lambda_f|^2) \cos \Delta m t + 2\Im \lambda_f \sin \Delta m t \right)
\end{aligned} \tag{3.20}$$

The sinh- and sin-terms are associated to the interference between the decays with and without oscillation. Commonly, the master equations are expressed as:

$$\begin{aligned}
\Gamma_{P^0 \rightarrow f}(t) &= |A_f|^2 (1 + |\lambda_f|^2) \frac{e^{-\Gamma t}}{2} \left(\cosh \frac{1}{2} \Delta \Gamma t + D_f \sinh \frac{1}{2} \Delta \Gamma t + C_f \cos \Delta m t - S_f \sin \Delta m t \right) \\
\Gamma_{\bar{P}^0 \rightarrow f}(t) &= |A_f|^2 \left| \frac{p}{q} \right|^2 (1 + |\lambda_f|^2) \frac{e^{-\Gamma t}}{2} \left(\cosh \frac{1}{2} \Delta \Gamma t + D_f \sinh \frac{1}{2} \Delta \Gamma t - C_f \cos \Delta m t + S_f \sin \Delta m t \right)
\end{aligned} \tag{3.21}$$

with

$$D_f = \frac{2\Re \lambda_f}{1 + |\lambda_f|^2} \quad C_f = \frac{1 - |\lambda_f|^2}{1 + |\lambda_f|^2} \quad S_f = \frac{2\Im \lambda_f}{1 + |\lambda_f|^2}. \tag{3.22}$$

For a given final state f we therefore only have to find the expression for λ_f to fully describe the decay of the (oscillating) mesons. Examples of some final states will be presented in chapter 4.

3.7 Classification of CP Violating Effects

The following classification between the various types of CP violation can be made [6].

- 1) **CP violation in decay.** This type of CP violation occurs when the decay rate of a B to a final state f differs from the decay rate of an anti- B to the CP-conjugated final state \bar{f} :

$$\boxed{\Gamma(P^0 \rightarrow f) \neq \Gamma(\bar{P}^0 \rightarrow \bar{f})}$$

This is obviously satisfied (see Eq. (3.18)) when

$$\left| \frac{\bar{A}_{\bar{f}}}{A_f} \right| \neq 1. \tag{3.23}$$

An example of CP violation in decay for neutral mesons is decay $B^0 \rightarrow K^+ \pi^-$. A sizeable CP-asymmetry has been observed

$$A_{CP} = \frac{\Gamma_{B^0 \rightarrow K^+ \pi^-} - \Gamma_{\bar{B}^0 \rightarrow K^- \pi^+}}{\Gamma_{B^0 \rightarrow K^+ \pi^-} + \Gamma_{\bar{B}^0 \rightarrow K^- \pi^+}} < 0$$

In charged mesons there is no mixing, so this is the only type of CP violation that can occur in charged meson decays.

- 2) **CP violation in mixing.** This implies that the oscillation from meson to anti-meson is different from the oscillation from anti-meson to meson:

$$\boxed{\text{Prob}(P^0 \rightarrow \bar{P}^0) \neq \text{Prob}(\bar{P}^0 \rightarrow P^0)}$$

Experimentally this is searched for in the semi-leptonic decay of both the \bar{B}^0 and the B^0 , coherently produced through $\Upsilon \rightarrow \bar{B}^0 B^0$. The \bar{b} -quark inside the B^0 -meson decays weakly to a positively charged lepton, and vice versa. So, an event with two leptons with equal charge in the final state means that one of the two B -mesons oscillated. So, the asymmetry in the number of two positive and two negative leptons allows us to compare the oscillation rates.

$$A_{CP} = \frac{N_{++} - N_{--}}{N_{++} + N_{--}} = \frac{|p/q|^2 - |q/p|^2}{|p/q|^2 + |q/p|^2}$$

This type is violated if

$$\left| \frac{q}{p} \right| \neq 1. \quad (3.24)$$

In the B^0 - and B_s^0 -system this is not the case, so $|q/p| \approx 1$ both within the experimental accuracy and theoretical expectation, but we will see that this type of CP violation is active in the K -system, see chapter 5 ².

- 3) **CP violation in interference between a decay with and without mixing,** sometimes referred to as CP violation *involving* oscillations. This form of CP violation is measured in decays to a final state that is common for the B^0 and \bar{B}^0 -meson. An interesting category are CP-eigenstates, $f = \bar{f}$ (an example of a non-CP eigenstate are the final states $D_s^\pm K^\mp$ in the B_s^0 -system). CP is violated if the following condition is satisfied:

$$\boxed{\Gamma(P^0(\rightsquigarrow \bar{P}^0) \rightarrow f)(t) \neq \Gamma(\bar{P}^0(\rightsquigarrow P^0) \rightarrow f)(t)}$$

A direct consequence of $f = \bar{f}$ is that there will be two amplitudes that contribute to the transition amplitude from the initial state $|B^0\rangle$ to a final state f , namely $A(B^0 \rightarrow f)$ and $A(B^0 \rightarrow \bar{B}^0 \rightarrow f)$. If we consider the case that $|q/p| = 1$, the following expression is obtained, using Eqs. (3.21):

$$A_{CP}(t) = \frac{\Gamma_{P^0(t) \rightarrow f} - \Gamma_{\bar{P}^0(t) \rightarrow f}}{\Gamma_{P^0(t) \rightarrow f} + \Gamma_{\bar{P}^0(t) \rightarrow f}} = \frac{2C_f \cos \Delta mt - 2S_f \sin \Delta mt}{2 \cosh \frac{1}{2} \Delta \Gamma t + 2D_f \sinh \frac{1}{2} \Delta \Gamma t} \quad (3.25)$$

²Normally expressed in terms of ϵ , for historical reasons: $p = (1 + \epsilon)/\sqrt{2(1 + |\epsilon|^2)}$, $q = (1 - \epsilon)/\sqrt{2(1 + |\epsilon|^2)}$ and thus $q/p = (1 - \epsilon)/(1 + \epsilon)$. The parameters p and q are normalized such that $|p|^2 + |q|^2 = 1$.

This simplifies considerably if the transition is dominated by only one amplitude, i.e. assuming that $|A_f| = |\bar{A}_f|$ (or $|\lambda_f| = 1$), so that $D_f = \Re\lambda_f$, $C_f = 0$ and $S_f = \Im\lambda_f$:

$$A_{CP}(t) = \frac{-\Im\lambda_f \sin \Delta mt}{\cosh \frac{1}{2}\Delta\Gamma t + \Re\lambda_f \sinh \frac{1}{2}\Delta\Gamma t} \quad (3.26)$$

We conclude that CP violation can even occur when both $|q/p| = 1$ and $|A(f)| = |\bar{A}_f|$, namely when the following condition is satisfied:

$$\Im\lambda_f = \Im\left(\frac{q}{p}\frac{\bar{A}_f}{A_f}\right) \neq 0 \quad (3.27)$$

Commonly an alternative classification of **direct** and **indirect** CP violation is made [6]. **Direct** CP violation is defined as $|A(f)| \neq |\bar{A}_f|$. In terms of the above categories, direct CP violation obviously appears in the CP violation in decay. In addition, the term direct CP violation is used for the situation where $C_f \neq 0$, probed by the first term in Eq. (3.25), since $|A(f)| \neq |\bar{A}_f| \rightarrow |\lambda_f| \neq 1 \rightarrow C_f \neq 0$. **Indirect** CP violation is the type of CP violation that involves mixing in any way, either through $|q/p| \neq 1$ or via the second term of Eq. (3.25). Historically this distinction originates from so-called superweak models that predicted CP violation to appear only in mixing diagrams. The discovery of direct CP violation excluded these superweak models.

Finally, we comment on the relative size of CP violation in the interference of mixing and decay in the K and B system. The difference arises from the CKM-factor of the box-diagram. The real part of the CKM-factor in the K -system is given by:

$$(V_{cd}V_{cs}^*)^2 = \lambda^2$$

The imaginary part is proportional to $A^2\lambda^6\eta$. Therefore, we expect for the ratio of the CP violating part to the CP non-violating part of Δm_K to be

$$\frac{\Im\Delta m}{\Re\Delta m} \propto A^2\lambda^4\eta \quad (3.28)$$

In the B system the CKM factor is given by

$$(V_{td}V_{tb}^*)^2 = (1 - \rho - i\eta)^2 A^2\lambda^6$$

from which we can deduce that the ratio of CP violation to CP non-violation in the B system is

$$\frac{\Im\Delta m}{|\Delta m|} \propto \frac{\eta(1 - \rho)}{(1 - \rho)^2 + \eta^2} \quad (3.29)$$

In the B system we then have the strength of CP violation of the same order as CP non-violation, whereas in the K system it is suppressed by a factor of $\lambda^4 \approx 2 \cdot 10^{-3}$.

Chapter 4

CP violation in the B-system

In the previous chapter we have identified where CP violation occurs in the general formalism of meson decays, and classified the various categories. In the coming sections we will investigate a few special decays with which CP violation is measured and the phases of the CKM elements are determined [9].

Remember the Wolfenstein parametrization, Eq. (2.16), since it is so widely used. This parameterization is very convenient to localize weak phase differences in Feynman diagrams:

$$V_{CKM, \text{Wolfenstein}} = \begin{pmatrix} |V_{ud}| & |V_{us}| & |V_{ub}|e^{-i\gamma} \\ -|V_{cd}| & |V_{cs}| & |V_{cb}| \\ |V_{td}|e^{-i\beta} & -|V_{ts}|e^{i\beta_s} & |V_{tb}| \end{pmatrix} + \mathcal{O}(\lambda^5) \quad (4.1)$$

In this chapter we will see how the angles β , β_s and γ can be determined.

At first sight it might be remarkable that complex phases can be observed, because the complex phase in an amplitude $A = |A|e^{i\varphi}$ disappears in the expectation value, $AA^\dagger = |A|^2e^{i(\varphi-\varphi)} = |A|^2$. However, several decay amplitudes $A_i = |A_i|e^{i\varphi_i}$ might contribute to the total amplitude A [19]. Each phase consists of a CP-odd phase ϕ_i originating from complex coupling constants, and a CP-even phase δ_i , typically originating from gluon exchange in the final state (and strong interactions are CP-conserving!). Therefore we have for the CP-conjugated amplitude $\bar{A}_i = |A_i|e^{i(-\phi_i+\delta_i)}$. Now we can calculate the difference in the *magnitude* of the total amplitude $|A(a \rightarrow b)|$ and the CP-conjugate $|\bar{A}(\bar{a} \rightarrow \bar{b})|$:

$$\begin{aligned} |A|^2 = |A_1 + A_2|^2 &= |A_1|^2 + |A_2|^2 + |A_1A_2| \left(e^{i((\phi_1+\delta_1)-(\phi_2+\delta_2))} + e^{i(-(\phi_1+\delta_1)+(\phi_2+\delta_2))} \right) \\ &= |A_1|^2 + |A_2|^2 + 2|A_1A_2| \cos(\Delta\phi + \Delta\delta) \\ |\bar{A}|^2 = |\bar{A}_1 + \bar{A}_2|^2 &= |A_1|^2 + |A_2|^2 + |A_1A_2| \left(e^{i((-\phi_1+\delta_1)-(-\phi_2+\delta_2))} + e^{i(-(-\phi_1+\delta_1)+(-\phi_2+\delta_2))} \right) \\ &= |A_1|^2 + |A_2|^2 + 2|A_1A_2| \cos(-\Delta\phi + \Delta\delta) \end{aligned}$$

An explicit example will be shown in Section 4.1.

4.1 β : the $B^0 \rightarrow J/\psi K_S^0$ decay

In the case of decays into CP eigenstates (i.e. $|\bar{f}\rangle = \text{CP}|f\rangle = \eta_f|f\rangle$, with $\eta_f = \pm 1$) only two independent amplitudes need to be considered: A_f and \bar{A}_f . We define the CP asymmetry as (see Eq. (3.25)):

$$A_{CP}(t) = \frac{\Gamma_{B^0(t) \rightarrow f} - \Gamma_{\bar{B}^0(t) \rightarrow f}}{\Gamma_{B^0(t) \rightarrow f} + \Gamma_{\bar{B}^0(t) \rightarrow f}}$$

Let us now concentrate on specific decays to get an idea where the CKM phase enters the asymmetry measurement. We start with the decay $B^0 \rightarrow J/\psi K_S^0$ [20] and will investigate Eq. (3.26) further.

The first observation is that at the quark level the B^0 decay and the \bar{B}^0 decay have a *different* final state, $B^0 \rightarrow J/\psi K^0$ and $\bar{B}^0 \rightarrow J/\psi \bar{K}^0$. As a result, we need to consider the mass eigenstates in the K system, see Eq. (3.7), to obtain the same final state f for the B^0 and \bar{B}^0 decay: $|K_S^0\rangle = p|K^0\rangle + q|\bar{K}^0\rangle$. (The details of the K -system will be discussed in chapter 5.) Secondly, in the B^0 -system $\Delta\Gamma \approx 0$ (see Table 3.2), so Eq. (3.26) can simply be written as:

$$\boxed{A_{CP}(t) = -\Im\lambda_f \sin(\Delta mt)} \quad (4.2)$$

For a given final state f , the magnitude and phase of λ_f fully describe the decay and oscillation of the B^0 and the \bar{B}^0 -meson. (If the final state is not a CP-eigenstate, we will also need $\lambda_{\bar{f}}$.) Starting from the definition of λ_f we write

$$\lambda_{J/\psi K_S^0} = \left(\frac{q}{p}\right)_{B^0} \left(\eta_{J/\psi K_S^0} \frac{\bar{A}_{J/\psi K_S^0}}{A_{J/\psi K_S^0}}\right) = -\left(\frac{q}{p}\right)_{B^0} \left(\frac{\bar{A}_{J/\psi \bar{K}^0}}{A_{J/\psi K^0}}\right) \left(\frac{p}{q}\right)_{K^0} \quad (4.3)$$

The three parts in this equation correspond to the mixing of the B^0 -meson, $(q/p)_{B^0}$, the decay of the B^0 or \bar{B}^0 , \bar{A}/A , and the mixing of the K^0 -meson, $(q/p)_{K^0}$. These three parts are diagrammatically shown in Fig. 4.1. The factor $\eta_{J/\psi K_S^0}$ accounts for the CP-eigenvalue of the final state. The J/ψ has spin-1 and is CP-even, while K_S has spin-0 and is (almost) CP-even. The B^0 is spin-0, and thus the particles in the final state must have a relative angular momentum $l = 1$. As a result the final state $J/\psi K_S^0$ is CP-odd, $\eta_{J/\psi K_S^0} = -1$ ¹.

The $B^0 \leftrightarrow \bar{B}^0$ mixing is induced by the box diagram shown in Fig. 4.1a). We have seen that the mass matrix element $M_{12} \propto V_{tb}^* V_{td} V_{tb}^* V_{td}$, (see Eq. (3.16)), and that we can neglect the term Γ_{12} , see Table 3.2, and therefore:

$$\left(\frac{q}{p}\right)_{B^0} = \sqrt{\frac{M_{12}^*}{M_{12}}} = \frac{V_{tb}^* V_{td}}{V_{tb} V_{td}^*} \quad (4.4)$$

¹The analogous measurement can be performed with the decay $B^0 \rightarrow J/\psi K_L^0$, with $\eta_{J/\psi K_L^0} = +1$.

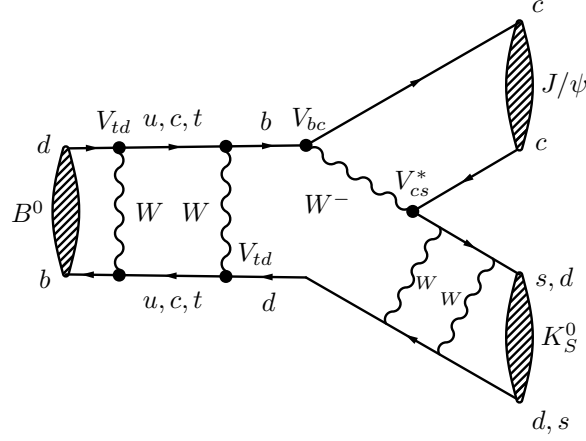


Figure 4.1: The diagrams that enter in the phase of the decay $B^0 \rightarrow J/\psi K_S^0$, B^0 mixing, B^0 decay and, K mixing.

For the ratio of the decay amplitudes we find on inspection of the diagram in Fig. 4.1b) that

$$\left(\frac{\bar{A}}{A}\right) = \frac{V_{cb}V_{cs}^*}{V_{cb}^*V_{cs}}$$

At this point we have however not produced a K_S^0 but either a K^0 or a \bar{K}^0 to finally make a prediction of the CP violation in the decay $B^0 \rightarrow J/\psi K_S^0$ we also have to take into account the $K^0 \leftrightarrow \bar{K}^0$ mixing. This adds a factor in analogy to Eq. (4.4) (see Fig. 4.1c):

$$\left(\frac{p}{q}\right)_K = \sqrt{\frac{M_{12}}{M_{12}^*}} = \frac{V_{cs}V_{cd}^*}{V_{cs}^*V_{cd}}$$

Taking everything together we find for the parameter $\lambda_{J/\psi K_S^0}$:

$$\lambda_{J/\psi K_S^0} = -\left(\frac{V_{tb}^*V_{td}}{V_{tb}V_{td}^*}\right) \left(\frac{V_{cb}V_{cs}^*}{V_{cb}^*V_{cs}}\right) \left(\frac{V_{cs}V_{cd}^*}{V_{cs}^*V_{cd}}\right) = -\frac{V_{tb}^*V_{td}}{V_{tb}V_{td}^*} \frac{V_{cb}V_{cd}^*}{V_{cb}^*V_{cd}} \quad (4.5)$$

and for its imaginary part

$$\Im \lambda_{J/\psi K_S^0} = -\sin \left\{ \arg \left(\frac{V_{tb}^*V_{td}V_{cb}V_{cd}^*}{V_{tb}V_{td}^*V_{cb}^*V_{cd}} \right) \right\} = -\sin \left\{ 2 \arg \left(\frac{V_{cb}V_{cd}^*}{V_{tb}V_{td}^*} \right) \right\} \equiv \sin 2\beta, \quad (4.6)$$

or

$$S_{J/\psi K_S^0} = -\eta_{J/\psi K_S^0} \sin 2\beta, \quad (4.7)$$

where β is defined as in Eq. (2.15). In short we can also write $\lambda_{J/\psi K_S^0} = -e^{-2i\beta}$.

To recapitulate, the CP-asymmetry of the decay $B^0 \rightarrow J/\psi K_S^0$ is given by the imaginary part of $\lambda_{J/\psi K_S^0}$:

$$\boxed{A_{\text{CP}, B^0 \rightarrow J/\psi K_S^0}(t) = -\sin 2\beta \sin(\Delta mt)} \quad (4.8)$$

Using the Wolfenstein parameterization we see that the CKM-element V_{td} is the only component with a non-vanishing imaginary part, leading to Eq. (4.6). We conclude that the CP-asymmetry in the decay $B^0 \rightarrow J/\psi K_S^0$ arises from the phase difference of the amplitudes $B^0 \rightarrow J/\psi K_S^0$ and $B^0 \rightarrow \bar{B}^0 \rightarrow J/\psi K_S^0$. The phase difference arises from the CKM-elements V_{td} (in the Wolfenstein parametrization) originating from the box-diagram that is responsible for the $\bar{B}^0 \leftrightarrow B^0$ oscillations.

The value of $\sin 2\beta$ has been determined very accurately by the BaBar and Belle experiments with the process $e^+e^- \rightarrow \Upsilon \rightarrow B^0\bar{B}^0$. A remarkable feature of this process is that the $B^0\bar{B}^0$ -pair is produced *coherently*, which means that the B^0 -clock only starts ticking when the \bar{B}^0 has decayed. The lifetime of the B^0 -meson is thus expressed as the time difference between the two decays, Δt . The number of decaying B^0 -mesons is determined by requiring that the other B had decayed as a \bar{B}^0 . This number is called the number of *tagged* B^0 -mesons, N_{B^0} . The asymmetry is given by:

$$A_{CP}(\Delta t) = \frac{\Gamma_{B^0(\Delta t) \rightarrow f} - \Gamma_{\bar{B}^0(\Delta t) \rightarrow f}}{\Gamma_{B^0(\Delta t) \rightarrow f} + \Gamma_{\bar{B}^0(\Delta t) \rightarrow f}} = \frac{\Gamma_{\text{tag}=\bar{B}^0} - \Gamma_{\text{tag}=B^0}}{\Gamma_{\text{tag}=\bar{B}^0} + \Gamma_{\text{tag}=B^0}} = \eta_f \sin 2\beta \sin \Delta m \Delta t.$$

After correcting for imperfect tagging, we see that the amplitude of the asymmetry gives the value of $\sin 2\beta$. The present world average is: $\sin 2\beta = 0.68 \pm 0.03$.

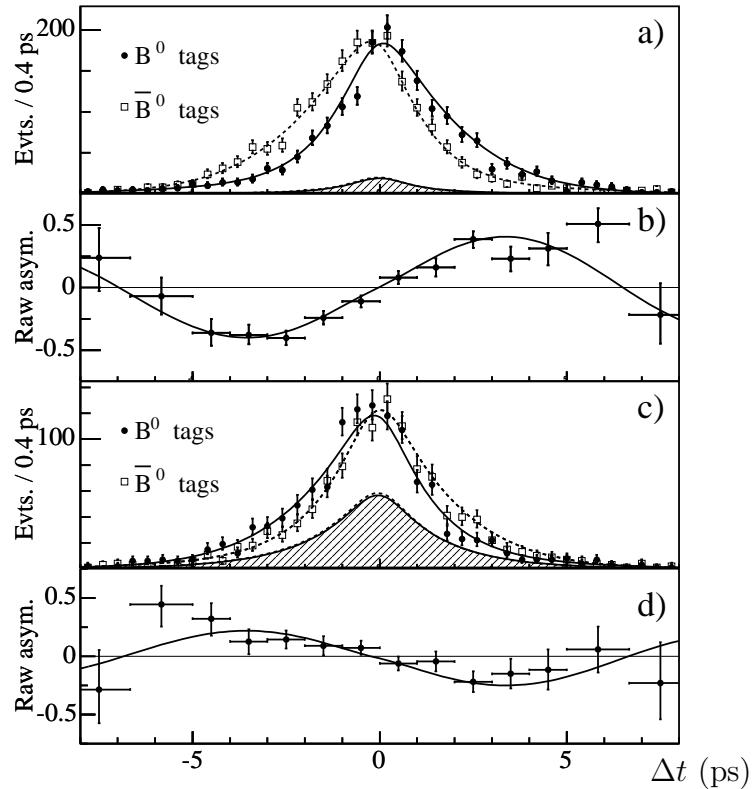


Figure 4.2: Number of $\eta_f = -1$ candidates (mainly $J/\psi K_S^0$) in the signal region with a B^0 tag N_{B^0} and with a \bar{B}^0 tag $N_{\bar{B}^0}$, and b) the raw asymmetry (note the inverted convention here, compared to our notes...) $A_{CP}(t) = (N_{\bar{B}^0} - N_{B^0}) / (N_{\bar{B}^0} + N_{B^0})$, as functions of Δt . Figs. c) and d) are the corresponding plots for the $\eta_f = +1$ mode $J/\psi K_L^0$. The shaded regions represent the estimated background contributions. From [21].

Measuring complex numbers

Before we continue, we can reflect on the principle behind the measurement of the complex phase β . Let us show once more how the complex phase appears as an observable, starting from the $|B^0\rangle$ wave function and the two decay amplitudes. Remember our wave function of the decaying, oscillating neutral meson, Eq. (3.10):

$$|B^0(t)\rangle = g_+(t)|B^0\rangle + \left(\frac{q}{p}\right) g_-(t)|\bar{B}^0\rangle = e^{-iMt - i\frac{1}{2}\Delta\Gamma t} \left(\cos\frac{\Delta mt}{2}|B^0\rangle + i \sin\frac{\Delta mt}{2} \left(\frac{q}{p}\right)|\bar{B}^0\rangle \right)$$

$$|\bar{B}^0(t)\rangle = g_-(t) \left(\frac{p}{q}\right)|B^0\rangle + g_+(t)|\bar{B}^0\rangle = e^{-iMt - i\frac{1}{2}\Delta\Gamma t} \left(i \sin\frac{\Delta mt}{2} \left(\frac{p}{q}\right)|B^0\rangle + \cos\frac{\Delta mt}{2}|\bar{B}^0\rangle \right)$$

again using $\Delta\Gamma \approx 0$ for the B^0 case, see Table 3.2. The factor $\frac{q}{p}$ accounts for the $B^0 \rightarrow \bar{B}^0$ oscillation. We saw that for the B^0 -mesons holds $|\frac{q}{p}| = 1$, more specifically, $\frac{q}{p} = e^{-i2\beta}$. How is this phase factor $e^{-i2\beta}$ measurable, in general? If we would measure the number of B^0 -mesons (i.e. *produced* as a B^0) and compare that to the number of \bar{B}^0 -mesons (i.e. *produced* as a \bar{B}^0) at time $t = \frac{\pi}{2\Delta m}$, then both the unoscillated and the oscillated amplitudes are of equal magnitude, and the CP asymmetry can be written as:

$$A_{CP} \left(t = \frac{\pi}{2\Delta m} \right) = \frac{|1 + ie^{-i2\beta}|^2 - |ie^{+i2\beta} + 1|^2}{|1 + ie^{-i2\beta}|^2 + |ie^{+i2\beta} + 1|^2} = \sin 2\beta \quad (4.9)$$

The situation is schematically shown in Fig. 4.3. The total amplitude of the CP-conjugated situation will have a different magnitude if there are two phases, of which one flips sign under CP transformation!

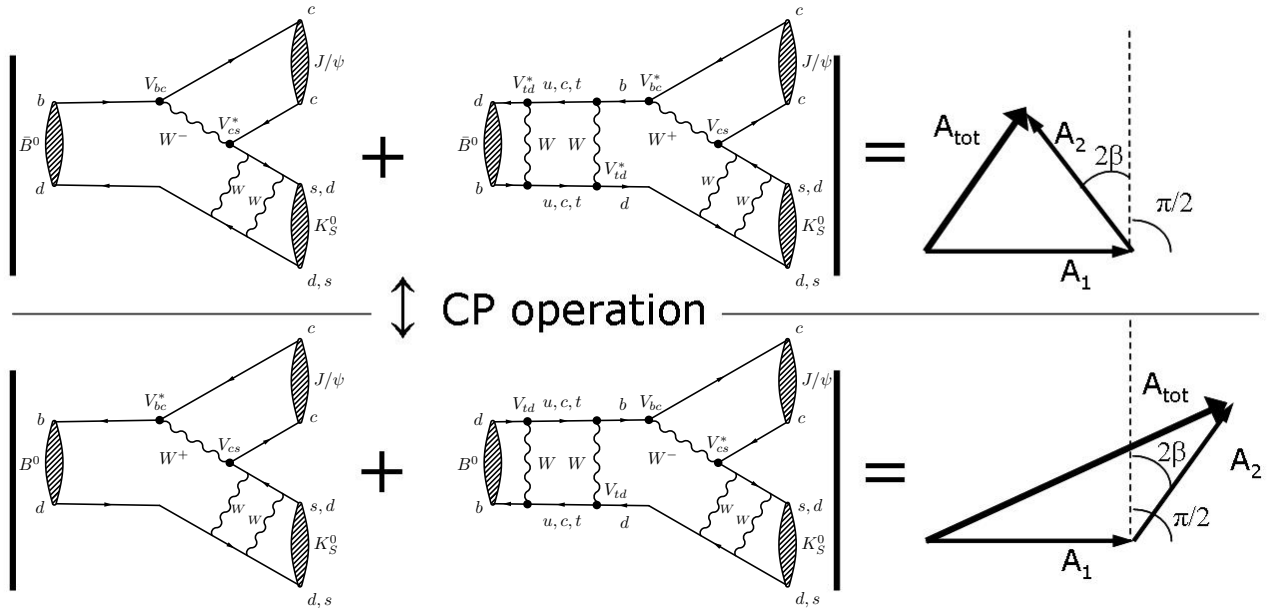


Figure 4.3: Adding two amplitudes results in a A_{tot} with different magnitude under CP.

4.2 β_s : the $B_s^0 \rightarrow J/\psi\phi$ decay

The decay $B_s^0 \rightarrow J/\psi\phi$ is the B_s^0 analogue of the decay $B^0 \rightarrow J/\psi K_S^0$, with the spectator d -quark replaced by an s -quark. However, there are four major differences:

- I **V_{ts} vs V_{td} .** Since the spectator d -quark is replaced by an s -quark, the CKM-element responsible for the CP-asymmetry (in the Wolfenstein parameterization) is now V_{ts} , instead of V_{td} , see Fig. 4.4. In contrast to V_{td} the imaginary part of V_{ts} is no longer of comparable size as the real part, see Eqs. (2.10-2.11), and the predicted CP asymmetry is therefore small, $\arg(V_{ts}) \sim \eta\lambda^2$.
- II **No K -oscillations.** The final state, containing the mesons J/ψ and ϕ , is the same for the B_s^0 and the \bar{B}_s^0 -meson, and hence we do not need the extra K -oscillation step as in the B^0 system.
- III **$\Delta\Gamma \neq 0$.** In contrast to the B^0 case, the B_s^0 -system has non-vanishing $\Delta\Gamma$. This is caused by the existence of a final state common to B_s^0 and \bar{B}_s^0 , with a large branching fraction around 5%, namely the CP-eigenstate $D_s^{\pm(*)}D_s^{\mp(*)}$. Since this is a CP-eigenstate with eigenvalue +1 this decay channel is only accessible for the CP-even eigenstate $B_{s,H}$ and not for $B_{s,L}$. Hence the different lifetime for $B_{s,H}$ and $B_{s,L}$ with a predicted value of $\Delta\Gamma/\Gamma \sim 0.1$. (A similar situation for the B^0 case does not occur, because the branching ratio for $B^0 \rightarrow D^\pm D^\mp$ is Cabibbo suppressed, $A \sim |V_{cd}|$.)
- IV **Vector-vector final state.** The final state now contains two vector-particles with spin-1. As a result the final state is not a pure CP-eigenstate, in contrast to $B^0 \rightarrow J/\psi K_S^0$. The spin of the final state particles J/ψ and ϕ can be pointing parallel,

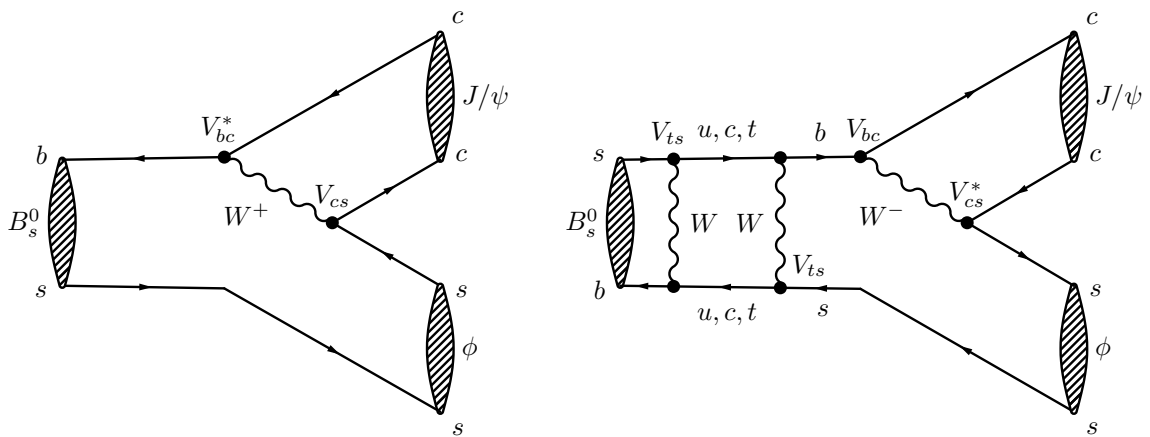


Figure 4.4: The two interfering diagrams of the decay $B_s^0 \rightarrow J/\psi\phi$, with phase difference $2\beta_s$.

orthogonal, or opposite, which need to be compensated by an orbital momentum, of $l = 2, 1$ and 0 , respectively, to obtain the spin of the initial state, $S_{B_s} = 0$. The CP-eigenvalue of the final state now depends on the orbital momentum due to the factor $(-1)^l$ in the total wave function;

$$\text{CP}|J/\psi\phi\rangle_l = (-1)^l|J/\psi\phi\rangle_l$$

The fact that the predicted CP-asymmetry is so small in the Standard Model, makes this decay particularly sensitive to new particles participating in the box-diagram. Any deviation from the Standard Model value would signal New Physics.

The asymmetry for the decay of the B_s^0 -meson to the common final state $J/\psi\phi$ is given by Eq. (3.26):

$$A_{CP}(t) = \frac{\Gamma_{B_s^0(t) \rightarrow J/\psi\phi} - \Gamma_{\bar{B}_s^0(t) \rightarrow J/\psi\phi}}{\Gamma_{B_s^0(t) \rightarrow J/\psi\phi} + \Gamma_{\bar{B}_s^0(t) \rightarrow J/\psi\phi}} = \frac{-\Im\lambda_{J/\psi\phi} \sin \Delta mt}{\cosh \frac{1}{2}\Delta\Gamma t + \Re\lambda_{J/\psi\phi} \sinh \frac{1}{2}\Delta\Gamma t} \quad (4.10)$$

where

$$\lambda_{J/\psi\phi} = \left(\frac{q}{p}\right)_{B_s^0} \left(\eta_{J/\psi\phi} \frac{\bar{A}_{J/\psi\phi}}{A_{J/\psi\phi}}\right) = (-1)^l \left(\frac{V_{tb}^* V_{ts}}{V_{tb} V_{ts}^*}\right) \left(\frac{V_{cb} V_{cs}^*}{V_{cb}^* V_{cs}}\right) \quad (4.11)$$

and

$$\Im\lambda_{J/\psi\phi} = (-1)^l \sin \left\{ 2 \arg \left(\frac{V_{cb} V_{cs}^*}{V_{tb} V_{ts}^*} \right) \right\} \quad (4.12)$$

$$= (-1)^l \sin 2\beta_s \quad (4.13)$$

$$= +\eta_{J/\psi\phi} \sin 2\beta_s \quad (4.14)$$

By comparing Eqs. (4.6) and (4.14) a relative minus sign occurs due to the definition of β and β_s : β is defined with V_{td} in the denominator, whereas β_s has V_{ts} in the numerator, see Eqs. (2.15).

A complication arises from the above mentioned vector-vector final state. The contributions from the terms with different orbital momentum, A_{\parallel} , A_{\perp} and A_0 , for values of the orbital momentum of 2, 1 and 0, respectively, need to be disentangled statistically by examining the angular distributions of the final state particles, $J/\psi \rightarrow \mu^+ \mu^-$ and $\phi \rightarrow K^+ K^-$.

4.3 γ : the $B_s^0 \rightarrow D_s^\pm K^\mp$ decay

CP violation in interference between a decay with and without mixing is most simply realized by considering a final state that is a CP eigenstate. In that case the amplitudes $B \rightarrow f$ and $B \rightarrow \bar{B} \rightarrow f$ occur and interfere. In addition, the formulas simplify because $|A_f| = |\bar{A}_f| = |\bar{A}_{\bar{f}}| = |A_{\bar{f}}|$.

The decay $B_s^0 \rightarrow D_s^\pm K^\mp$ is a final state that is not a CP eigenstate. The interference can however occur when both the B_s^0 and the \bar{B}_s^0 decay to the same final state, albeit with different amplitudes this time. We will first examine the pair $B_s^0 \rightarrow D_s^- K^+$ and $B_s^0 \rightarrow \bar{B}_s^0 \rightarrow D_s^- K^+$ in a similar way as in the previous sections. This is then followed by the pair $B_s^0 \rightarrow D_s^+ K^-$ and $B_s^0 \rightarrow \bar{B}_s^0 \rightarrow D_s^+ K^-$. The information from both pairs allows for the extraction of the angle γ in the unitarity triangle.

By examining Fig. 4.5 we see that the amplitude of the decay $B_s^0 \rightarrow D_s^- K^+$ proceeds proportional to $A_f \sim V_{cb}^* V_{us}$ whereas the decay $\bar{B}_s^0 \rightarrow D_s^- K^+$ proceeds proportional to $\bar{A}_f \sim V_{ub} V_{cs}^*$. At this point we should note three important aspects:

- I Although both the B_s^0 -decay and the \bar{B}_s^0 -decay are equally Cabibbo suppressed, $|A_{D_s^- K^+}| \sim \lambda^3$ and $|\bar{A}_{D_s^- K^+}| \sim \lambda^3$, nevertheless they are not completely equal $|A_{D_s^- K^+}| \neq |\bar{A}_{D_s^- K^+}|$. If we split off the part from the weak couplings, and introduce the hadronic amplitude including effects from the strong interactions in the final state, A_1 and A_2 , we get:

$$\left(\frac{\bar{A}_{D_s^- K^+}}{A_{D_s^- K^+}} \right) = \left(\frac{V_{ub} V_{cs}^*}{V_{cb}^* V_{us}} \right) \left(\frac{A_2}{A_1} \right) \quad (4.15)$$

- II Both amplitudes will not only differ by their *magnitude*, but also by a relative

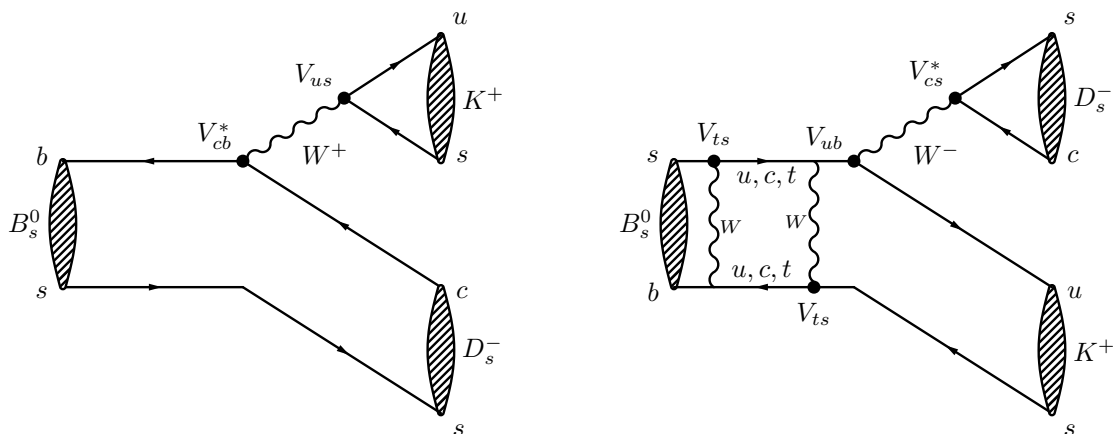


Figure 4.5: The two interfering diagrams of the decay $B_s^0 \rightarrow D_s^- K^+$, with phase difference $-\gamma + 2\beta_s$.

phase γ , originating from V_{ub} , see Eq. (4.1), and therefore

$$\frac{A_{D_s^- K^+}}{\bar{A}_{D_s^- K^+}} = \frac{|A_{D_s^- K^+}|}{|\bar{A}_{D_s^- K^+}|} e^{-i\gamma}. \quad (4.16)$$

III In fact, since the transitions $B_s^0 \rightarrow D_s^- K^+$ and $\bar{B}_s^0 \rightarrow D_s^- K^+$ proceed in a different way, an extra relative phase δ_s needs to be introduced, originating from strong interactions in the final state,

$$\frac{A_{D_s^- K^+}}{\bar{A}_{D_s^- K^+}} = \frac{|A_{D_s^- K^+}|}{|\bar{A}_{D_s^- K^+}|} e^{i(\delta_s - \gamma)}. \quad (4.17)$$

(This complication is exactly the reason why we will need the second pair of decays to the final state $D_s^+ K^-$: to disentangle the two phases γ and δ_s .)

Combining these three points leads to the following expression:

$$\lambda_{D_s^- K^+} = \left(\frac{q}{p}\right)_{B_s^0} \left(\frac{\bar{A}_{D_s^- K^+}}{A_{D_s^- K^+}}\right) = \left|\frac{V_{tb}^* V_{ts}}{V_{tb} V_{ts}^*}\right| \left|\frac{V_{ub} V_{cs}^*}{V_{cb}^* V_{us}}\right| \left|\frac{A_2}{A_1}\right| e^{i(-2\beta_s - \gamma + \delta_s)} \quad (4.18)$$

In a similar way we obtain the expression for the other pair, where the B_s^0 decays to the CP-conjugated final state, $B_s^0 \rightarrow D_s^+ K^-$ and $B_s^0 \rightarrow \bar{B}_s^0 \rightarrow D_s^+ K^-$ (see Fig. 4.6):

$$\lambda_{D_s^+ K^-} = \left(\frac{q}{p}\right)_{B_s^0} \left(\frac{\bar{A}_{D_s^+ K^-}}{A_{D_s^+ K^-}}\right) = \left|\frac{V_{tb}^* V_{ts}}{V_{tb} V_{ts}^*}\right| \left|\frac{V_{us}^* V_{cb}}{V_{cs} V_{ub}^*}\right| \left|\frac{A_1}{A_2}\right| e^{i(-2\beta_s - \gamma - \delta_s)} \quad (4.19)$$

where we used $|A_{D_s^- K^+}| = |\bar{A}_{D_s^+ K^-}| \sim A_1$.

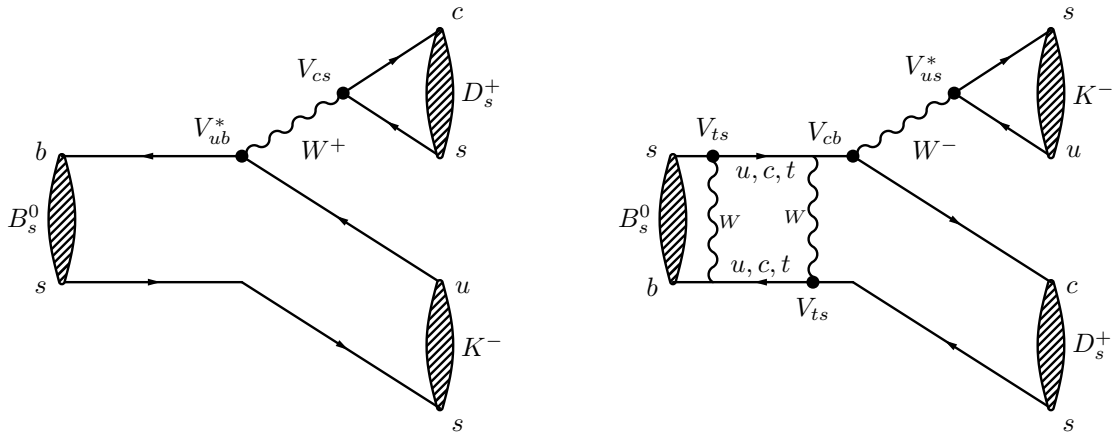


Figure 4.6: (a-b) The two interfering diagrams of the decay $B_s^0 \rightarrow D_s^+ K^-$, with phase difference $-\gamma + 2\beta_s$.

4.4 Direct CP violation: the $B^0 \rightarrow \pi^- K^+$ decay

An example of direct CP violation is given by the decay $B^0 \rightarrow \pi^- K^+$. A CP-asymmetry has been observed in the processes $B^0 \rightarrow \pi^- K^+$ and its CP-conjugate $\bar{B}^0 \rightarrow \pi^+ K^-$, $|A_f| \neq |\bar{A}_f|$ [22]:

$$A_{CP} = \frac{\Gamma_{B^0 \rightarrow \pi^- K^+} - \Gamma_{\bar{B}^0(t) \rightarrow \pi^+ K^-}}{\Gamma_{B^0(t) \rightarrow \pi^- K^+} + \Gamma_{\bar{B}^0(t) \rightarrow \pi^+ K^-}} = -0.083 \pm 0.004 \quad (4.20)$$

As before, a different magnitude of the total amplitude between a decay and its CP-conjugate only appears if the total amplitude $A_{B^0 \rightarrow \pi^- K^+}$ consists of two interfering amplitudes with a phase difference. In addition, as before, this phase difference needs to have two components of which one part is CP-odd and flips sign under the CP-operation, and one part that is CP-even and does not change sign under the CP-operation (often denoted as the strong phase, since this phase often arises from final state gluon exchange).

In the decays described in the previous sections, the second amplitude originated from the possibility that the B -meson oscillated before its decay. That is not possible this time, because the decay $B^0 \rightarrow \bar{B}^0 \rightarrow \pi^+ K^-$ results in a different final state.

The second amplitude is now given by the a so-called penguin-diagram, as shown in Fig. 4.7. These penguin diagrams are notoriously difficult to calculate, and therefore it is difficult to interpret this results in terms of the CKM-angles. However, from Fig. 4.7 it is clear that there is a weak phase difference between the tree ($\sim V_{ub}^* V_{us}$) and penguin amplitude ($\sim V_{tb}^* V_{ts}$), and in general a different strong phase is expected. Intriguingly, no CP-asymmetry has been observed in the analogous decay $B^+ \rightarrow \pi^0 K^+$, where the spectator d -quark is “simply” replaced by a u -quark, $A_{CP} = 0.037 \pm 0.021$ [22].

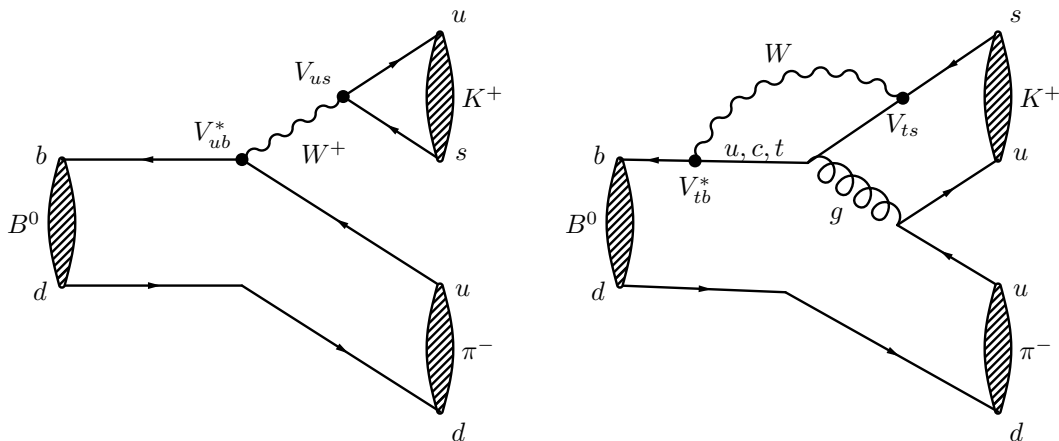


Figure 4.7: (a-b) The two interfering diagrams of the decay $B^0 \rightarrow \pi^- K^+$.

4.5 CP violation in mixing: the $B^0 \rightarrow l^+ \nu X$ decay

In the previous sections we always assumed for the B^0 -mesons that $|q/p| = 1$, originating from calculations of the box diagram responsible for $B^0 \leftrightarrow \bar{B}^0$ oscillations. If $|q/p| \neq 1$ that would mean that the probability to oscillate differ for the B^0 and the \bar{B}^0 :

$$\text{Prob}(B^0 \rightarrow \bar{B}^0) \neq \text{Prob}(\bar{B}^0 \rightarrow B^0)$$

The experimental confirmation has been measured using semi-leptonic decays. A semi-leptonically decaying b -quark proceeds as $b \rightarrow l^- \bar{\nu} X$, whereas the anti- b quark decays as $\bar{b} \rightarrow l^+ \nu X$. The charge of the lepton contains information whether the B -meson decayed as a B^0 (containing a \bar{b} -quark) or whether it oscillated and decayed as a \bar{B}^0 (containing a b -quark). At the B -factories with the BaBar and Belle experiments both a B^0 and a \bar{B}^0 -meson are produced simultaneously through the process $e^+e^- \rightarrow \Upsilon \rightarrow B^0 \bar{B}^0$.

If the probability to oscillate would be larger for the B^0 than for the \bar{B}^0 , then the probability to observe two negatively charged leptons ($B^0 \rightarrow \bar{B}^0 \rightarrow l^- \nu X$ and $\bar{B}^0 \rightarrow l^- \nu X$) would be larger than to observe two positively charged leptons!

$$A_{CP} = \frac{P(\bar{B}^0 \rightarrow B^0) - P(B^0 \rightarrow \bar{B}^0)}{P(\bar{B}^0 \rightarrow B^0) + P(B^0 \rightarrow \bar{B}^0)} = \frac{N^{++} - N^{--}}{N^{++} + N^{--}} = \frac{1 - |q/p|^4}{1 + |q/p|^4}$$

The combined value as measured at the B -factories and LHCb yields [22]:

$$\left| \frac{q}{p} \right|_{B^0} = 1.0010 \pm 0.0008 \quad (4.21)$$

In other words, no CP violation in mixing is observed in the B^0 -system.

The energy at the B -factories is not large enough to produce B_s^0 -mesons. The measurement of $|q/p|$ for the B_s^0 -system has been done at the Tevatron with the D0 and CDF experiments, and at LHCb [22]:

$$\left| \frac{q}{p} \right|_{B_s^0} = 1.0003 \pm 0.0014. \quad (4.22)$$

4.6 Penguin diagram: the $B^0 \rightarrow \phi K_S^0$ decay

Already in the decay $B^0 \rightarrow \pi^- K^+$ we introduced the loop diagram that is known as the penguin diagram, see Section 4.4. On the one hand these diagrams are difficult to calculate, but on the other hand, these loop diagrams are very interesting because new, heavy particles might run around in these loops, affecting the measurements. And because the particles in the loop are virtual, even very heavy particles can contribute.

A particularly interesting example is the decay $B^0 \rightarrow \phi K_S^0$, which caused excitement in recent years. The two interfering diagrams are shown in Fig. 4.8. The situation is completely analogous as for the decay $B^0 \rightarrow J/\psi K_S^0$ from Section 4.1: the $B^0 \rightarrow \bar{B}^0$ oscillation gives rise to the phase difference between the two diagrams ($V_{td} \sim e^{i\beta}$) and the time dependent CP-asymmetry is again given by

$$A_{\text{CP}, B^0 \rightarrow \phi K_S^0}(t) = -\sin 2\beta \sin(\Delta mt)$$

Any difference in the measurement of $\sin 2\beta$ between the decays $B^0 \rightarrow J/\psi K_S^0$ and $B^0 \rightarrow \phi K_S^0$ might be attributed to new particles in the loop adding an extra phase. The value of $\sin 2\beta_{\phi K_S}$ was slightly low compared to the value of $\sin 2\beta_{J/\psi K_S}$ as measured with tree diagrams, which generated considerable debate a few years ago.

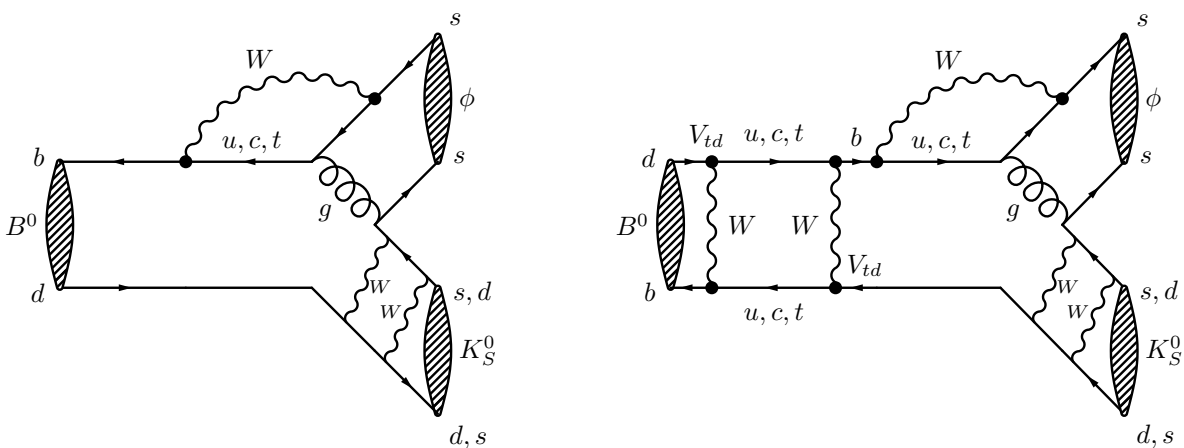


Figure 4.8: The two interfering diagrams of the decay $B^0 \rightarrow \phi K_S^0$, with phase difference 2β .

Chapter 5

CP violation in the K-system

CP violation was first discovered in the kaon system and struck the community with large surprise. CP violation was discovered almost 10 years before the CKM-mechanism was invented, at the time that only the three quarks (u , d and s) were known. We will discuss CP violation in the K -system because of its large historical importance.

The nomenclature used in the K -system has some small differences compared to the B -system, which we will introduce in this chapter. The connection in the K -system between CP violation and our well known Lagrangian and its short range couplings is less straightforward.

5.1 CP and pions

Before we dive into the K -system, we give the CP properties of the pion, which will be relevant when we will discuss the K -decay into pions.

The π^0 is a pseudoscalar meson consisting of a quark and an antiquark. The total wavefunction of the π^0 must be symmetric as it has spin 0. It must however be antisymmetric under the interchange of the spin of quark and anti-quark as these are fermions. Therefore the wave function must also be antisymmetric under interchange of the positions of the quark and antiquark.

$$|\pi^0\rangle = |q \uparrow \bar{q} \downarrow\rangle - |q \downarrow \bar{q} \uparrow\rangle + |\bar{q} \uparrow q \downarrow\rangle - |\bar{q} \downarrow q \uparrow\rangle$$

Performing the parity transformation then yields

$$P|\pi^0\rangle = |\bar{q} \downarrow q \uparrow\rangle - |\bar{q} \uparrow q \downarrow\rangle + |q \downarrow \bar{q} \uparrow\rangle - |q \uparrow \bar{q} \downarrow\rangle = -1 |\pi^0\rangle$$

The π^0 is thus an eigenstate of the Parity operation with eigenvalue -1. One says it has *negative intrinsic parity*.

Performing the C-operation yields (check)

$$C|\pi^0\rangle = |\pi^0\rangle$$

This can also be deduced from the fact that it decays into two photons. As a photon is nothing more than a combination of electric and magnetic fields and the C operation will invert both components (why), so that

$$C|\gamma\rangle = -1 |\gamma\rangle$$

from which it follows that

$$C|\pi^0\rangle = C|\gamma\gamma\rangle = (-1)^2|\gamma\gamma\rangle = |\pi^0\rangle$$

The combined transformation yields:

$$\boxed{CP|\pi^0\rangle = -1 |\pi^0\rangle} \quad (5.1)$$

and so it is a CP eigenstate with eigenvalue -1 or it “has CP=-1” or “is CP-odd”.

The system $|\pi^0\pi^0\rangle$ must be symmetric under interchange of the two particles as they are identical bosons. The CP operation will therefore be merely the product of the CP operation on the two π^0 s separately

$$CP|\pi^0\pi^0\rangle = (-1)^2 |\pi^0\pi^0\rangle = +1 |\pi^0\pi^0\rangle$$

For the $|\pi^+\pi^-\rangle$ system the C operation interchanges π^+ and π^- and the P operation changes them back again so that the full CP operation is equivalent to the identity transformation:

$$CP|\pi^+\pi^-\rangle = \mathbb{1}|\pi^+\pi^-\rangle = +1 |\pi^+\pi^-\rangle$$

All systems of two pions are eigenstates of CP with eigenvalue +1: they are thus “CP-even”.

The $|\pi^0\pi^0\pi^0\rangle$ system is again simple because we are dealing with identical bosons the CP operation is the product of the operation on the three pions separately:

$$CP|\pi^0\pi^0\pi^0\rangle = (-1)^3 |\pi^0\pi^0\pi^0\rangle = -1 |\pi^0\pi^0\pi^0\rangle$$

It is therefore a CP-odd system.

For the $|\pi^+\pi^-\pi^0\rangle$ system the relative angular momenta come into play. Let us consider the situation where the $|\pi^+\pi^-\rangle$ system is produced with angular momentum $L = l$ then if the total angular momentum of the $|\pi^+\pi^-\pi^0\rangle$ system is zero (we are heading for K^0 decay) the relative angular momentum of $\pi^0 \leftrightarrow (\pi^+\pi^-)$ will also be $L = l$. Now performing the CP operation will for the $|\pi^+\pi^-\rangle$ be the identity operation again, performing it on the $|\pi^0\rangle$ will give -1 and for the part of the wavefunction describing the relative angular momentum $L(\pi^0 \leftrightarrow (\pi^+\pi^-)) = l$ one gets $(-1)^l$ (the wave function is proportional to $P_l(\cos\theta)$). So for l even the system is CP-odd, and for l odd the system is CP-even.

Summarizing the results sofar we have:

Pion state	CP eigenvalue	
π^0	-1	
$\pi^+\pi^-$	+1	
$\pi^0\pi^0$	+1	
$\pi^0\pi^0\pi^0$	-1	
$\pi^+\pi^-\pi^0$	-1	$(L_{(\pi^+\pi^-)\leftrightarrow\pi^0} = 0, 2, ..)$
	+1	$(L_{(\pi^+\pi^-)\leftrightarrow\pi^0} = 1, 3, ..)$

So if CP-symmetry holds then a particle will only be able to decay into a two pion system if it is a CP eigenstate with eigenvalue +1.

5.2 Description of the K-system

As was introduced in chapter 3 we express the CP-eigenstates as follows:

$$|K_+^0\rangle = \frac{1}{\sqrt{2}} [|K^0\rangle + |\bar{K}^0\rangle]$$

$$|K_-^0\rangle = \frac{1}{\sqrt{2}} [|K^0\rangle - |\bar{K}^0\rangle]$$

The $|K_+^0\rangle$ and $|K_-^0\rangle$ states have definite CP-eigenvalues

$$CP|K_+^0\rangle = +1 |K_+^0\rangle$$

$$CP|K_-^0\rangle = -1 |K_-^0\rangle$$

If CP is conserved, the state $|K_+^0\rangle$ will only decay into $\pi^+\pi^-$ or $\pi^0\pi^0$ (or with a higher angular momentum to $\pi^+\pi^-\pi^0$) whereas the the state $|K_-^0\rangle$ is strictly forbidden to decay into a two pion final state. Because the mass of the $K_{L/S}^0$ is approximately 497.6 MeV and the mass of a pion is about 139.6 MeV the available phasespace for the two pion decay is almost a factor 1000 larger than that available for the three pion decay. As a result, the lifetime of the CP-odd eigenstate of the K-system is very large, much larger than the lifetime of the CP-even eigenstate. This is the reason that the CP-eigenstates are referred to as the K_S^0 and K_L^0 , where the subscripts stand for short and long, respectively, and not referred to as heavy and light as is done in the B-system ¹.

$$|K_S^0\rangle = \frac{1}{\sqrt{2}} [|K^0\rangle + |\bar{K}^0\rangle]$$

$$|K_L^0\rangle = \frac{1}{\sqrt{2}} [|K^0\rangle - |\bar{K}^0\rangle] \tag{5.2}$$

¹The K_L^0 corresponds to the heavy eigenstate, so could also have been named the K_H ...

5.3 The Cronin-Fitch experiment

Until 1964 all measurements were consistent with the notion of CP-symmetry, even those which involve the weak interaction. In fact CP-symmetry was invoked to explain the large difference in lifetime between the K_L^0 and K_S^0 . The experiment which unexpectedly changed this situation was performed by Christensen, Cronin, Fitch and Turlay [23] in 1964.

The experimental apparatus is shown in Fig. 5.1. It consisted of a Be-target placed in a π^- beam. All particles produced in the interactions, including any K^0 s were allowed to decay in a low pressure He-tank. Decay products were detected in two magnetic spectrometers placed roughly 20 m from the target. The distance of 20 m corresponds to approximately 300 lifetimes for the K_S^0 . All decay products must therefore come from the K_L^0 . All opposite charge combinations of particles, which had a reconstructed decay vertex within the He-volume were analysed and their invariant mass was determined under the assumption that both detected particles were pions. Obviously one expects to observe invariant mass combinations with a mass smaller than the K^0 mass emanating from the $K_L^0 \rightarrow \pi^+\pi^-\pi^0$ decay ($M(\pi^+\pi^-) < M(K_L^0) - M(\pi^0)$). However some background was produced in the experiment from the decays $K_L^0 \rightarrow \pi\mu\nu$ and $K_L^0 \rightarrow \pi e\nu$ where the μ and the e are misidentified as pions (check the mass limit for these decays). Fig. 5.2a) shows the measured spectrum. The figure shows a Montecarlo prediction from all known decays of the K_L^0 (e.g. the peak at about 350 MeV is from the $K_L^0 \rightarrow \pi^+\pi^-\pi^0$ decay. At first

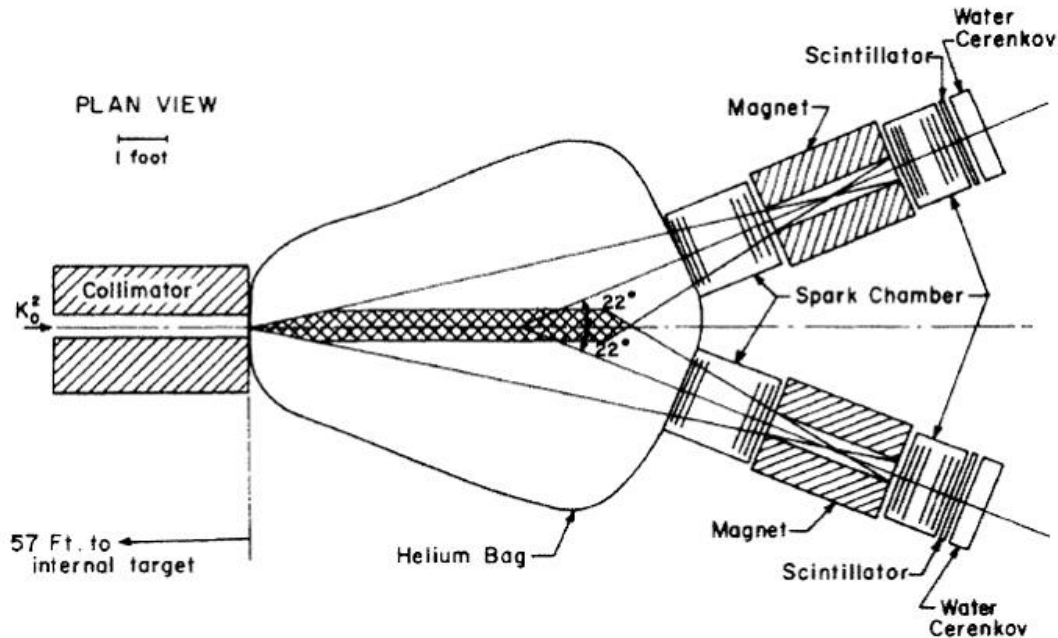


Figure 5.1: *The experimental apparatus with which CP violation was first measured.*

glance there is no real discrepancy between the measurements and the MC prediction. Certainly there is no indication of an excess of events at around 500 MeV. If we however plot the cosine of the angle between the flightpath of the K^0 and the direction of the momentum sum of the two particles for $490 < M(\pi^+\pi^-) < 510$ MeV we start to see an excess appear for $\cos\theta \sim 1$, see Fig. 5.2b). This is of course exactly what one expects for the decay $K_L^0 \rightarrow \pi^+\pi^-$. Fig. 5.2d) shows this in a little more detail. The forward peak is only present for $494 < M(\pi^+\pi^-) < 504$ MeV. Outside this mass interval there is no indication for a forward enhancement. The enhancement contains 49 ± 9 events. This was after many consistency checks finally taken as proof that the decay $K_L^0 \rightarrow \pi^+\pi^-$ occurs in nature. After acceptance correction the experiment gave a branching ratio of:

$$BR(K_L^0 \rightarrow \pi^+\pi^-) = \frac{\Gamma(K_L^0 \rightarrow \pi^+\pi^-)}{\Gamma(K_L^0 \rightarrow \text{all charged decay modes})} = 2.0 \pm 0.4 \times 10^{-3}$$

This result proves then that CP-symmetry is violated in the decay of the K_L^0 , of course

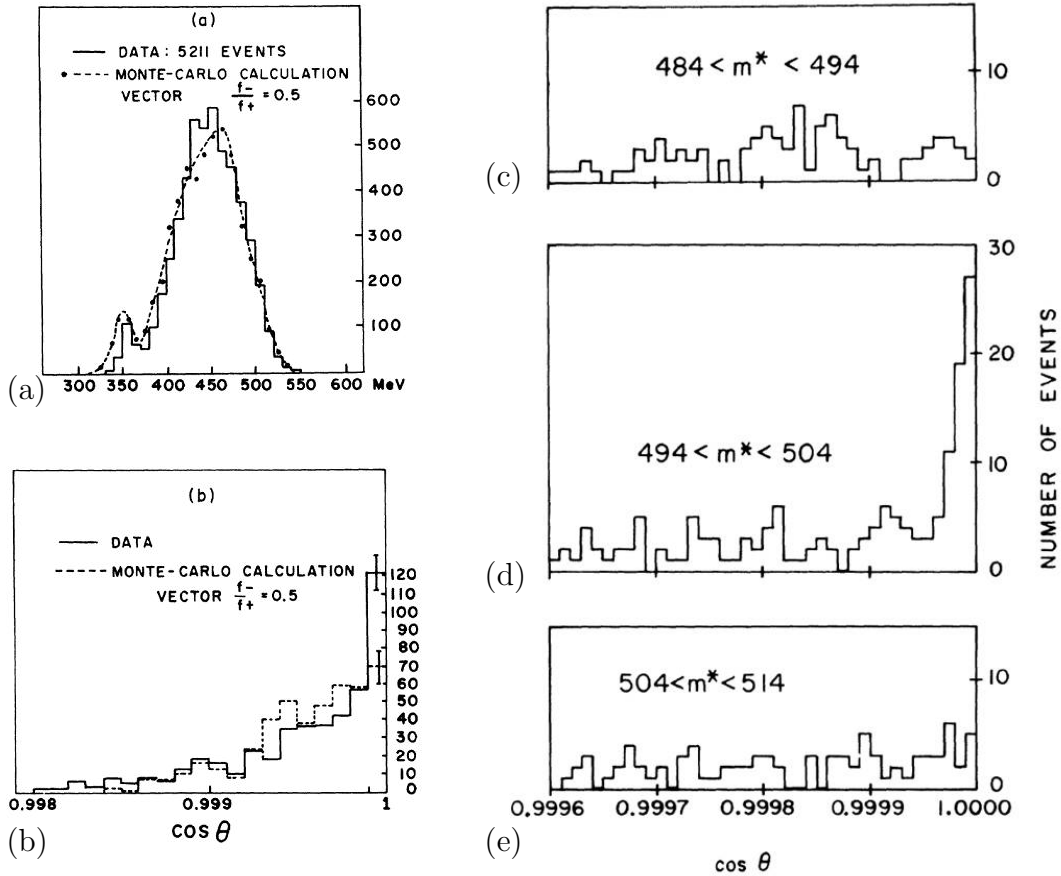


Figure 5.2: (a) The measured two “pion” mass spectrum. (b) The distribution of the cosine of the angle between the summed momentum vector of the two pions and the direction of the K^0 beam. (c-e) The angular distribution for different ranges in the invariant mass.

one has to be careful that the effect seen is indeed the decay of the K_L^0 , as there are some subtle effects that could affect the result.

5.3.1 Regeneration

Here we will discuss the effects of the passage through matter of a state which is a superposition of $|K^0\rangle$ and $|\bar{K}^0\rangle$. In the Hamiltonian we will now also have to take into account the strong interactions of the state with the matter it is passing through. We will neglect any inelastic interactions as these will merely decrease the intensity. We know from experiment that the strong interactions of $|K^0\rangle$ and $|\bar{K}^0\rangle$ are different. The $|\bar{K}^0\rangle$ ($s\bar{d}$) contains an s -quark and can, in its interaction with matter, produce strange baryon resonances, like $\bar{K}^0 + n \rightarrow \Lambda + \pi^0$, whereas the K^0 ($\bar{s}d$) can not. So the total cross section for K^0 scattering will be smaller than for \bar{K}^0 .

Suppose that a pure K_L^0 beam would incident on matter where all \bar{K}^0 would be absorbed, then the outgoing beam would be pure K^0 . Similar to a Stern-Gerlach filter, half of the outgoing kaons would then decay as a K_S^0 and half as K_L^0 , see Eq. 5.2:

$$|K^0\rangle = \frac{1}{\sqrt{2}} [|K_S^0\rangle + |K_L^0\rangle]$$

In principle the effect seen in the Cronin experiment could have been due to regeneration of the K_L^0 beam. If this would be the case then clearly by introducing more material in the path of the K_L^0 beam the effect would increase. The experiment was therefore repeated with liquid hydrogen instead of He in the decay path. The density and so the size of the regeneration then grows by a factor of 1000. The growth of the signal was found to be the equivalent of 10 events. The experiment was also repeated with the He replaced by vacuum. The signal persisted, so that regeneration could be ruled out as the cause.

Finally one has to prove that the particle which decays into the $\pi^+\pi^-$ state is in fact the K_L^0 state. To prove this one determined that there existed interference between the state decaying into $\pi^+\pi^-$ and a regenerated K_S^0 .

The only remaining conclusion was therefore that **CP-symmetry is violated in weak interactions.**

5.4 Master Equations in the Kaon System

In Section 3.7 a classification of the various types of CP violation was made. In the following these various types will be examined in the kaon system. First, let us introduce the quantity η_{+-} by starting from the familiar master equations.

$$\begin{aligned}\Gamma_{K^0 \rightarrow f}(t) &= |A_f|^2 \left(|g_+(t)|^2 + |\lambda_f|^2 |g_-(t)|^2 + 2\Re[\lambda_f g_+^*(t) g_-(t)] \right) \\ \Gamma_{\bar{K}^0 \rightarrow f}(t) &= |A_f|^2 \left| \frac{p}{q} \right|^2 \left(|g_-(t)|^2 + |\lambda_f|^2 |g_+(t)|^2 + 2\Re[\lambda_f g_+(t) g_-^*(t)] \right)\end{aligned}\tag{5.3}$$

with

$$\begin{aligned}|g_{\pm}(t)|^2 &= \frac{1}{4} \left(e^{-\Gamma s t} + e^{-\Gamma L t} \pm e^{-\Gamma t} (e^{-i\Delta m t} + e^{+i\Delta m t}) \right) \\ \lambda_f g_+^*(t) g_-(t) &= \frac{\lambda_f}{4} \left(e^{-\Gamma s t} - e^{-\Gamma L t} + e^{-\Gamma t} (e^{-i\Delta m t} - e^{+i\Delta m t}) \right)\end{aligned}\tag{5.4}$$

yields

$$\begin{aligned}\Gamma_{K^0 \rightarrow f}(t) &= \frac{|A_f|^2}{4} \left(e^{-\Gamma s t} (1 + |\lambda_f|^2 + 2\Re\lambda_f) + e^{-\Gamma L t} (1 + |\lambda_f|^2 - 2\Re\lambda_f) + \right. \\ &\quad \left. e^{-\Gamma t} ((1 - |\lambda_f|^2)(e^{-i\Delta m t} + e^{+i\Delta m t}) + 2\Re(\lambda_f(e^{-i\Delta m t} - e^{+i\Delta m t}))) \right) \\ &= \frac{|A_f|^2}{4} \left(e^{-\Gamma s t} (1 + \lambda_f)(1 + \lambda_f^*) + e^{-\Gamma L t} (1 - \lambda_f)(1 - \lambda_f^*) + \right. \\ &\quad \left. e^{-\Gamma t} ((1 - |\lambda_f|^2)(\cos \Delta m t) + 2\Im(\lambda_f) \sin \Delta m t) \right) \\ &\sim \left(e^{-\Gamma s t} + e^{-\Gamma L t} \frac{(1 - \lambda_f)(1 - \lambda_f^*)}{(1 + \lambda_f)(1 + \lambda_f^*)} + \right. \\ &\quad \left. e^{-\Gamma t} \left(\frac{(1 - |\lambda_f|^2)}{(1 + \lambda_f)(1 + \lambda_f^*)} (2 \cos \Delta m t) - 4 \frac{\Im(\lambda_f)}{(1 + \lambda_f)(1 + \lambda_f^*)} \sin \Delta m t \right) \right)\end{aligned}$$

and finally

$$\begin{aligned}\Gamma_{K^0 \rightarrow f}(t) &= N \left(e^{-\Gamma s t} + e^{-\Gamma L t} |\eta_{+-}|^2 + 2e^{-\Gamma t} |\eta_{+-}| \cos(\Delta m t + \phi_{+-}) \right) \\ \Gamma_{\bar{K}^0 \rightarrow f}(t) &= N \left(e^{-\Gamma s t} + e^{-\Gamma L t} |\eta_{+-}|^2 - 2e^{-\Gamma t} |\eta_{+-}| \cos(\Delta m t + \phi_{+-}) \right)\end{aligned}\tag{5.5}$$

with $\eta_{+-} = \frac{1-\lambda_f}{1+\lambda_f} = |\eta_{+-}| e^{i\phi_{+-}}$.

5.5 CP violation in mixing: ϵ

It is clear that we can no longer identify the K_L^0 with the K_-^0 and the K_S^0 with the K_+^0 , as they are clearly no longer eigenstates of the full Hamiltonian, and therefore we write:

$$\begin{aligned} |K_S^0\rangle &= p|K^0\rangle + q|\bar{K}^0\rangle \\ |K_L^0\rangle &= p|K^0\rangle - q|\bar{K}^0\rangle \end{aligned}$$

Historically, the CP violation was parameterized by introducing an arbitrary complex number ϵ , because the K_S^0 and K_L^0 were *almost* CP-eigenstates:

$$|K_L^0\rangle = \frac{1}{\sqrt{1+|\epsilon|^2}} (|K_-^0\rangle + \epsilon|K_+^0\rangle) \quad (5.6)$$

and

$$|K_S^0\rangle = \frac{1}{\sqrt{1+|\epsilon|^2}} (|K_+^0\rangle - \epsilon|K_-^0\rangle) \quad (5.7)$$

where $p = (1 + \epsilon)/\sqrt{2(1 + |\epsilon|^2)}$, $q = (1 - \epsilon)/\sqrt{2(1 + |\epsilon|^2)}$ and thus $q/p = (1 - \epsilon)/(1 + \epsilon)$. The parameters p and q are normalized such that $|p|^2 + |q|^2 = 1$.

Let us consider the decays $K^0 \rightarrow \pi^+\pi^-$ and $\bar{K}^0 \rightarrow \pi^+\pi^-$ and define the parameter λ_f , as in Eq. (3.17) [2]:

$$\lambda_{\pi^+\pi^-} = \left(\frac{q}{p}\right)_K \frac{\bar{A}_{\pi^+\pi^-}}{A_{\pi^+\pi^-}} \quad (5.8)$$

The amount of CP violation is measured by determining the relative branching ratio of $BR(K_L^0 \rightarrow \pi^+\pi^-)$ over $BR(K_S^0 \rightarrow \pi^+\pi^-)$:

$$\eta_{+-} \equiv \frac{\langle \pi^+\pi^- | T | K_L^0 \rangle}{\langle \pi^+\pi^- | T | K_S^0 \rangle} = \frac{pA_{\pi^+\pi^-} - q\bar{A}_{\pi^+\pi^-}}{pA_{\pi^+\pi^-} + q\bar{A}_{\pi^+\pi^-}} = \frac{1 - \lambda_{\pi^+\pi^-}}{1 + \lambda_{\pi^+\pi^-}}$$

If $\eta_{+-} \neq 0$ then that means $|\lambda_{\pi^+\pi^-}| \neq 1$. In this way we have reduced the CP violation to CP violation in the mixing of the K^0 and \bar{K}^0 , whereas the interaction that describes the decay is still CP-invariant. Only the part of the wavefunction that is CP-even will decay to the CP-even two pion states.

Similarly, for the decay to two neutral pions the parameter η_{00} is introduced. Their measured values are:

$$\begin{aligned} |\eta_{+-}| &= (2.285 \pm 0.019) \times 10^{-3} \\ |\eta_{00}| &= (2.275 \pm 0.019) \times 10^{-3} \end{aligned}$$

The value of ϵ is related to $\epsilon \approx \eta_{+-}$ and $\epsilon \approx \eta_{00}$ (see next section) and amounts to $|\epsilon| = (2.228 \pm 0.011) \times 10^{-3}$ [24], yielding (compare to Eqs. (4.21-4.22)):

$$\left|\frac{q}{p}\right|_{K^0} = \frac{1 - \epsilon}{1 + \epsilon} = 0.995552 \pm 0.000024. \quad (5.9)$$

If this is true this will have consequences for the semi-leptonic decay of the K_L^0 . We rewrite Eq. (5.6) as:

$$\begin{aligned} |K_L^0\rangle &= \frac{1}{\sqrt{1+|\epsilon|^2}} (|K_-^0\rangle + \epsilon|K_+^0\rangle) \\ &= \frac{1}{\sqrt{2(1+|\epsilon|^2)}} [(1+\epsilon)|K^0\rangle - (1-\epsilon)|\bar{K}^0\rangle] \end{aligned}$$

The charge asymmetry in the decay of the K_L^0 will then be

$$\begin{aligned} A_{+-} &= \frac{\Gamma(K_L^0 \rightarrow e^+\pi^-\nu_e) - \Gamma(K_L^0 \rightarrow e^-\pi^+\bar{\nu}_e)}{\Gamma(K_L^0 \rightarrow e^+\pi^-\nu_e) + \Gamma(K_L^0 \rightarrow e^-\pi^+\bar{\nu}_e)} \\ &= \frac{|1+\epsilon|^2 - |1-\epsilon|^2}{|1+\epsilon|^2 + |1-\epsilon|^2} \\ &\sim 2\Re \epsilon \end{aligned} \tag{5.10}$$

If the wavefunction of the K_L^0 is indeed a superposition of the two CP-eigenstates then there will be a difference in the rates. The measured asymmetry [24] is

$$A_{+-} = 3.32 \pm 0.06 \times 10^{-3}$$

confirming the above assumption ($\epsilon = |\epsilon|e^{i\phi_\epsilon}$, with $\phi_\epsilon = 43^\circ$). The size of the effect is consistent with the two pion decay rates.

There is of course still the possibility that the decay of the CP-eigenstates, from which the K_L^0 is built, also violates CP-symmetry: i.e. the $|K_-^0\rangle$ part of the wavefunction decays into $\pi^+\pi^-$ in that case we speak of **direct** CP violation.

5.6 CP violation in decay: ϵ'

If the amount of CP violation would depend on the final state, then that obviously implies that the *decay* contributes to the CP violation. In other words, $\eta_{+-} \neq \eta_{00}$ implies direct CP violation. We will see that this difference is expressed with the parameter ϵ' [2]:

$$\frac{\eta_{00}}{\eta_{+-}} \approx \frac{\epsilon - 2\epsilon'}{\epsilon + \epsilon'} \approx 1 - 3\frac{\epsilon'}{\epsilon}$$

To investigate the possibility of direct CP violation in the K^0 system we consider the transition from the $|K^0\rangle$ state to an eigenstate of the strong interaction and perform the CP transformation:

$$\langle A|H|K^0\rangle \xrightarrow{CP} \langle A|(CP)^{-1}H(CP)|K^0\rangle = \langle A|H|\bar{K}^0\rangle$$

Here we have used the arbitrary phase of the CP-transformation $CP|K^0\rangle = +|\bar{K}^0\rangle$. For one transition amplitude this is always possible. However if a second transition can take

place then this will have to follow the same phase-convention, and so if a transition is found that has a non-zero phase with respect to the first then we will have CP violation.

The two pion system can occur in two distinct eigenstates of the strong interaction, namely $I = 0$ and $I = 2$. So we can decompose the two-pion states emanating from the K_L^0 and K_S^0 decay into the Isospin eigenstates:

$$\begin{aligned} |\pi^+\pi^-\rangle &= \frac{1}{\sqrt{3}} \left(\sqrt{2}|2\pi, I=0\rangle + |2\pi, I=2\rangle \right) \\ |\pi^0\pi^0\rangle &= \frac{1}{\sqrt{3}} \left(|2\pi, I=0\rangle - \sqrt{2}|2\pi, I=2\rangle \right) \end{aligned}$$

We can now define the amplitude for the transitions into the $I = 0$ state as:

$$\langle 2\pi, I=0|T|K^0\rangle = \langle 2\pi, I=0|T|\bar{K}^0\rangle = A_0 e^{i\delta_0}$$

where we have added a phase shift due to the final state strong interactions in the $I = 0$ state, δ_0 . For the $I = 2$ state we will in general then not have a real amplitude:

$$\begin{aligned} \langle 2\pi, I=2|T|K^0\rangle &= A_2 e^{i\delta_2} \\ \langle 2\pi, I=2|T|\bar{K}^0\rangle &= A_2^* e^{i\delta_2} \end{aligned}$$

(δ_2 is the final state strong interaction phaseshift for the $I = 2$ state.) Introducing the following variables:

$$\begin{aligned} F &= e^{i(\delta_2 - \delta_0)} \\ \Delta &= \frac{F \Re A_2}{\sqrt{2} A_0} \\ \epsilon' &= \frac{iF \Im A_2}{\sqrt{2} A_0} \end{aligned}$$

we find for the amplitudes

$$\eta_{+-} = \frac{\langle \pi^+\pi^-|H|K_L^0\rangle}{\langle \pi^+\pi^-|H|K_S^0\rangle} = \epsilon + \epsilon'(1 + \Delta)^{-1}$$

and

$$\eta_{00} = \frac{\langle \pi^0\pi^0|H|K_L^0\rangle}{\langle \pi^0\pi^0|H|K_S^0\rangle} = \epsilon - 2\epsilon'(1 - 2\Delta)^{-1}$$

so that, assuming that $|\Delta| \ll 1$ and $|\epsilon'| \ll 1$ will be small, we find for the rate asymmetry

$$\left| \frac{\eta_{00}}{\eta_{+-}} \right|^2 = \frac{R(K_L^0 \rightarrow \pi^0\pi^0) R(K_S^0 \rightarrow \pi^+\pi^-)}{R(K_S^0 \rightarrow \pi^0\pi^0) R(K_L^0 \rightarrow \pi^+\pi^-)} = 1 - 6\Re \frac{\epsilon'}{\epsilon}$$

So if $\epsilon' \neq 0$ then $\Im A_2 \neq 0$ and so the phase of the transition to the $I = 2$ state is not equal to the phase of the transition to the $I = 0$ state and we will have direct CP violation.

The experimental result is

$$\Re \frac{\epsilon'}{\epsilon} \approx \frac{\epsilon'}{\epsilon} = 1.65 \pm 0.26 \times 10^{-3} \quad (5.11)$$

5.7 CP violation in interference

In Section 3.7 a classification of the various types of CP violation was made. We just saw how CP is violated in the kaon system in decay, and in mixing:

- 1) CP violation in decay: ϵ'
- 2) CP violation in mixing: ϵ
- 3) CP violation in interference between a decay with and without mixing,

The CP violation in the interference between a decay with and without mixing obviously depends on the neutral meson mixing and is therefore time-dependent. Often this is thus referred to as time-dependent CP-asymmetry. Interference occurs when there are two amplitudes for a transition from a given initial state to a given final state. For this to happen, we now need a final state that is a CP eigenstate in order to obtain the two amplitudes $K^0 \rightarrow f_{CP}$ and $\bar{K}^0 \rightarrow \bar{K}^0 \rightarrow f_{CP}$. An example of such a final state is simply $K^0 \rightarrow \pi^+\pi^-$.

The time dependent CP asymmetry of $K^0 \rightarrow \pi^+\pi^-$ and $\bar{K}^0 \rightarrow \pi^+\pi^-$ is shown in Fig 5.3b) and is compared to the time dependent CP asymmetry as measured in the B-system with $B^0 \rightarrow J/\psi K_S$.

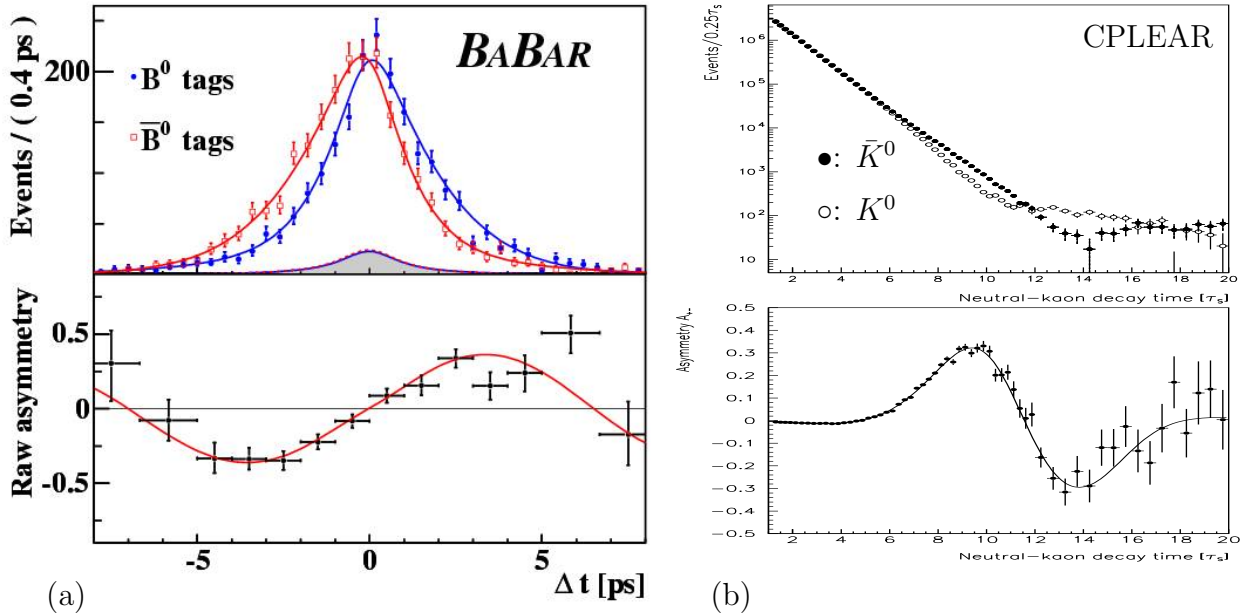


Figure 5.3: Number of $B^0 \rightarrow J/\psi K_S^0$ candidates with a B^0 tag N_{B^0} and with a \bar{B}^0 tag $N_{\bar{B}^0}$, and below the asymmetry $A_{CP}(t) = (N_{B^0} - N_{\bar{B}^0}) / (N_{B^0} + N_{\bar{B}^0})$, as functions of Δt . From [21]. (b) Number of $K^0 \rightarrow \pi^+\pi^-$ candidates. Open circles \circ correspond to kaons that started as K^0 , whereas closed circles \bullet correspond to \bar{K}^0 tags. From [25]

Chapter 6

Experimental Aspects and Present Knowledge of Unitarity Triangle

6.1 B-meson production

In principle b and \bar{b} quarks are always made in pairs, the way they dress up into hadrons is however dependent on the specific production. At present there are three accelerator types, where significant results can be expected for CP violation.

- e^+e^- colliding beam machines at a CM energy of the $\Upsilon(4S)$
- e^+e^- colliding beam machine at a large CM energy (p.e. LEP)
- Hadron colliders such as Tevatron ($p\bar{p}$) or LHC (pp)

e^+e^- colliding beam machines at a CM energy of the $\Upsilon(4S)$

The $\Upsilon(4S)$ resonance is the first $b\bar{b}$ resonance which can decay into “open” b . It decays into $B^0 \bar{B}^0$ or B^+B^- -mesons, see Fig. 6.1. The CM energy (mass of the $\Upsilon(4S)$) is such that only the B -mesons are produced. Most notably the mass of the B_s^0 is such that it can *not* be produced in these collisions. Also additional hadrons (pions and kaons) are kinematically forbidden. In the CM system the B -mesons are produced essentially at rest. This means that the decay-length cannot be measured as the velocity of the meson is to good approximation zero. This means that if a decay-length measurement is to be made one must ensure that the CM system is in motion. For this reason the accelerators at Stanford (BaBar) and KEK (Belle) employ asymmetric beam energies for the e^+ and e^- beams. It has a disadvantage for the machine as one needs two separate accelerators. BaBar for instance has a 3.1 GeV e^+ beam and a 9 GeV e^- beam to produce a CM energy of 10.56 GeV. The CM system thus has a $\beta\gamma = 0.56$ so that the mean decay length

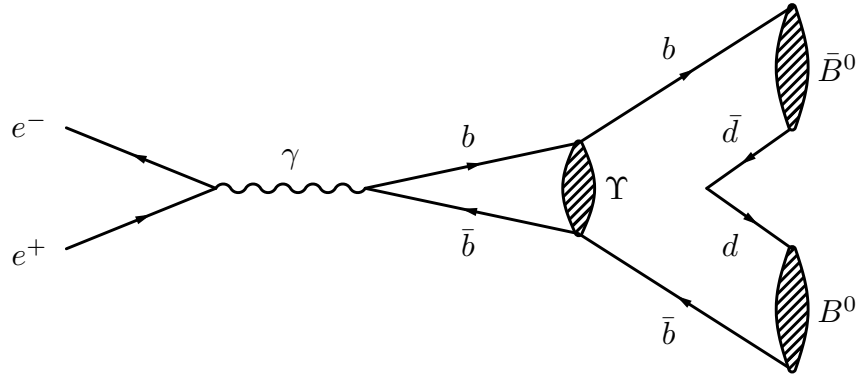


Figure 6.1: $B^0 \bar{B}^0$ production via $\Upsilon(4S)$ decay.

of a B -meson ($\tau = 1.5$ ps) produced at rest in the CM system is $\beta\gamma c\tau \approx 250 \mu\text{m}$. There is also a disadvantage for the analysis as the actual *production vertex* is not known, so that all CP asymmetries must be rewritten in terms of the *difference* of the lifetimes of the two B -mesons.

Hadron colliders such as Tevatron ($p\bar{p}$) or LHC (pp)

The production mechanism for b and \bar{b} quarks is the same in both $p\bar{p}$ and pp collisions. They are formed when a gluon from the proton fuses with a gluon of the (anti-)proton (see Fig. 6.2). From measurements in deep-inelastic scattering we know that the gluon

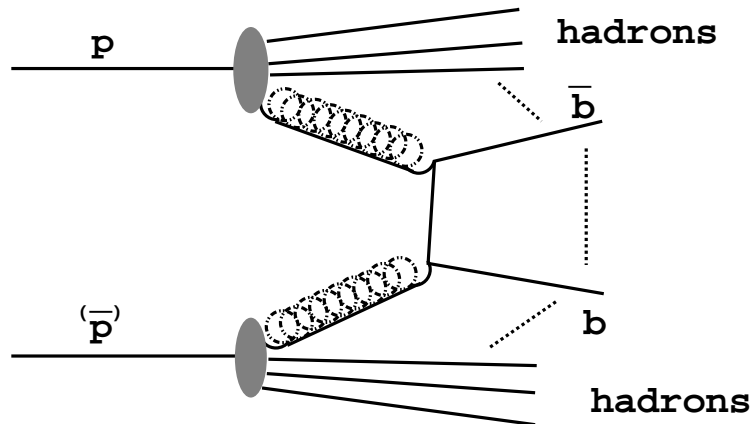


Figure 6.2: $B \bar{B}$ production in high energy hadron machines through gluon-gluon fusion

density in the (anti-)proton is largest at very small fractional momentum (x). In fact the gluon density behaves approximately as

$$g(x) \propto x^{-3/2}$$

This means that to produce a mass $M(\approx 2m_b) = \sqrt{x_1 x_2 s}$, where s is the centre-of-mass energy squared, the most probable situation is that either x_1 or x_2 is very small (and the other large). The b and the \bar{b} are thus produced in the same hemisphere at small angles to the beam and at quite high momentum. The momenta are in the range of 30 to 100 GeV giving a mean decay distance of $\beta\gamma c\tau \approx 3 - 10$ mm. In addition to the B -mesons *many* other particles are produced. A similar mixture of B -meson flavours occurs as in high energy e^+e^- collisions.

At these machines the interaction rate of events with no b quarks is so high that a selection must be performed in order not to be swamped by unwanted events. In fact at the LHC the production rate of b quark containing events is so high that a large fraction have to be filtered away because they do not contain interesting decays. This question is obviously a very subtle one and is too involved for the present lecture.

6.2 Flavour Tagging

As we saw in chapter 4 many measurements depend on the knowledge whether the B -meson oscillated or not. In order to determine whether the B -meson was produced as a B or a \bar{B} , the flavour at production needs to be *tagged*. In principle tagging is simple. All one has to do is identify the flavour of the B meson *accompanying* the one decaying into a CP eigenstate. There are several methods which are or will be used.

- Complete reconstruction of the decay of a charged B -meson. This is the gold plated tagging method. It suffers however from efficiencies and branching ratios. Typically the decay in which one is interested has a branching ratio of less than 10^{-3} . Combining this with a similar branching ratio for the tagging decay gives too small a fraction of events. At the Υ this method is anyway excluded.
- Determination of the charge of the secondary vertex of the accompanying B -meson. Also not usable at the Υ .
- Semi-leptonic decay of the accompanying B -meson. The b -quark will decay into a negatively charged lepton whereas the \bar{b} -quark decays into a positively charged lepton. If these semi-leptonic decays are of charged B -mesons detection of the lepton will provide an unambiguous tag. If however the accompanying B -meson is neutral then the tag only indicates the flavour at the time of the accompanying B -meson's decay and it can have oscillated. It is interesting to calculate that the time integrated CP asymmetry actually becomes zero at the Υ if only the difference in lifetimes and the semi-leptonic tagging are used. In the high energy e^+e^- and hadron machines this method works, be it with some tagging inefficiency. This inefficiency has to be measured using other channels (p.e. double semi-leptonic decays) or estimated from Monte Carlo. This method also suffers from misidentification due to semi-leptonic charm decay in the decay of the accompanying B -meson. The lepton from this decay

has the opposite charge to the one from the original b decay and so will further wash out the tagging information.

- Other methods include reconstruction of charm particles (the charge of the kaon in the decay provides an unambiguous tag, apart from $B^0 \leftrightarrow \bar{B}^0$ oscillations) and charge of the total opposite jet (at high energy e^+e^-)

6.3 Present Knowledge on Unitarity Triangle

At present there are several measurements which constrain the CKM unitarity triangle. Combining all these measurements in a global fit is a stringent test of the internal consistency of the Standard Model. The two best known groups that perform these global fits are *CKMfitter* [26] and *UTfit* [27].

In this section we will present the input to the fit, of which the following four measurements provide the strongest constraints:

- I **$\sin 2\beta$** The measurement of $\sin 2\beta$ constrains one of the three angles of the triangle.
- II **ϵ_K** The measurement of ϵ_K provides a constraint that follows a hyperbola in the (ρ, η) plane.
- III **$|V_{ub}|$** The measurement of $|V_{ub}/V_{cb}|$ constrains one side of the triangle as it is proportional to $\sqrt{\rho^2 + \eta^2}$.
- IV **Δm** The measurements of Δm_d and Δm_s for the B^0 and B_s^0 systems constrain another side, as it is proportional to $((1 - \rho)^2 + \eta^2)$.

The first two measurements are direct proofs of CP violation, in the B and K -system respectively. The last two measurements however, provide strong constraints in the $\bar{\rho}, \bar{\eta}$ -plane, but are no signs of CP violation on their own, since they allow for vanishing imaginary part of the CKM elements, $\bar{\eta} = 0$, see Fig. 6.3.

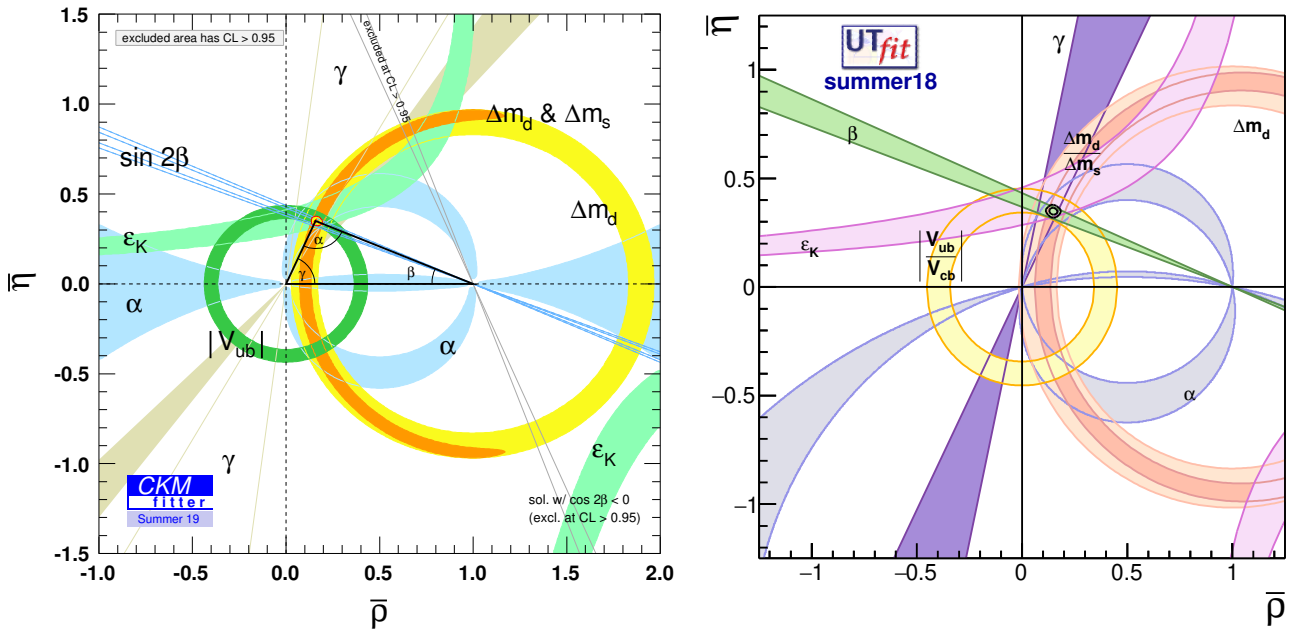


Figure 6.3: Global fits to the unitarity triangle, by (a) *CKMfitter* [26] and (b) *UTfit* [27].

6.3.1 Measurement of $\sin 2\beta$

The determination of the angle β as measured at the B factories with the BaBar and Belle experiments, has been extensively discussed in Section 4.1, which resulted in the present world average when combined with the value from LHCb [28]:

$$\sin 2\beta = 0.70 \pm 0.02$$

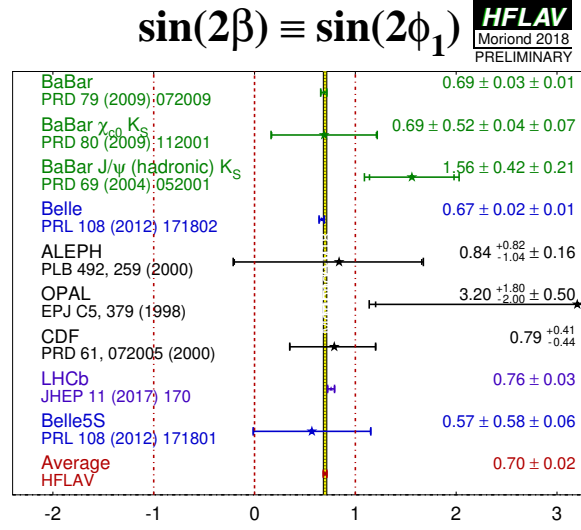


Figure 6.4: Average value of the measurement of $\sin 2\beta$.

6.3.2 Measurement of ϵ_K

The measurement of $|\epsilon_K| = (2.228 \pm 0.011) \times 10^{-3}$ provides a constraint on the position of the apex of the universality triangle in the $(\bar{\rho}, \bar{\eta})$ plane. The value of $|\epsilon_K|$ is a measure of the CP violation in K -mixing, and is thus related to the imaginary part of the box diagram contribution that is responsible for the short range mixing of $K^0 \leftrightarrow \bar{K}^0$: $\epsilon \sim \Im M_{12} / \Delta m_K$. Using the box diagram to calculate $|\epsilon_K|$, see Eq. (3.15), one arrives at the following form [29]:

$$\begin{aligned} |\epsilon_K| &= \frac{G_F^2 m_W^2}{12\sqrt{2}\pi^2} \frac{m_K f_K^2 B_K}{\Delta m_K} \Im [\eta_c S(x_c) (V_{cs}^* V_{cd})^2 + \eta_t S(x_t) (V_{ts}^* V_{td})^2 + 2\eta_{ct} S(x_c, x_t) (V_{cs}^* V_{cd} V_{ts}^* V_{td})] \\ &= \frac{G_F^2 m_W^2}{12\sqrt{2}\pi^2} \frac{m_K f_K^2 B_K}{\Delta m_K} [\eta_c S(x_c) 2\Re(V_{cs}^* V_{cd}) \Im(V_{cs}^* V_{cd}) + \eta_t S(x_t) 2\Re(V_{ts}^* V_{td}) \Im(V_{ts}^* V_{td}) - \\ &\quad \eta_{ct} S(x_c, x_t) \Re(V_{cs}^* V_{cd}) \Im(V_{cs}^* V_{cd})] \end{aligned}$$

here again the functions $S(x_q)$ have been derived by Inami and Lim [17] and quantify the loop contributions from quark q , depending on $x_q = m_q^2/m_W^2$. The η_q include the

NLO QCD corrections for each function. The factors $f_K^2 B_K$ again parameterize the non-perturbative strong corrections. The value of f_K is well known from measurements of charged K decay, so that the most uncertain value is that of the bag-factor B_K . The third term is evaluated as follows: $(V_{cs}^* V_{cd} V_{ts}^* V_{td}) \equiv (\lambda_c \lambda_t) = (\Re \lambda_c + i \Im \lambda_c)(\Re \lambda_t + i \Im \lambda_t)$. Using $\Im \lambda_c \approx -\Im \lambda_t$ and $\Re \lambda_t \ll \Re \lambda_c$, we then find $\Im(V_{cs}^* V_{cd} V_{ts}^* V_{td}) \approx -\Re(V_{cs}^* V_{cd}) \Im(V_{cs}^* V_{cd})$.

Using the Wolfenstein parameterization we find [2]:

$$\begin{aligned} |\epsilon_K| &= \frac{G_F^2 m_W^2}{12\sqrt{2}\pi^2} \frac{m_K f_K^2 B_K}{\Delta m_K} A^2 \lambda^6 \eta [\eta_c S(x_c) - \eta_t S(x_t) A^2 \lambda^4 (1 - \rho) - \eta_{ct} S(x_c, x_t)] \\ &\approx 10^4 A^2 \lambda^6 \eta [\eta_c S(x_c) - \eta_t S(x_t) A^2 \lambda^4 (1 - \rho) - \eta_{ct} S(x_c, x_t)]. \end{aligned}$$

With $|V_{cb}| = A\lambda^2$ and $|V_{us}| = \lambda$ and the evaluation of the Inami-Lim functions $S(x_c) \approx 2.4 \times 10^{-4}$, $S(x_t) \approx 2.6$ and $S(x_c, x_t) = 2.2 \times 10^{-3}$ [30] we can rewrite as:

$$\begin{aligned} |\epsilon_K| &\approx 10^4 \eta |V_{cb}|^2 |V_{us}|^2 [2.4 \times 10^{-4} + 2.6 |V_{cb}|^2 (1 - \rho) - 2.2 \times 10^{-3}] \\ &\approx 10^{-3} \eta [(1 - \rho)] \end{aligned} \tag{6.1}$$

which becomes a hyperbolic band in the $(\bar{\rho}, \bar{\eta})$ plane, given in Fig. 6.3.

6.3.3 $|V_{ub}/V_{cb}|$

The ratio $|V_{ub}/V_{cb}|$ provides a strong constraint on the unitarity triangle. The present measurement is given by

$$|V_{ub}| = (3.94 \pm 0.36) \times 10^{-3}$$

In the Standard Model in the Wolfenstein parameterization this quantity is given by

$$|V_{ub}/V_{cb}| = \frac{\lambda}{1 - \frac{\lambda}{2}} \sqrt{(\bar{\rho}^2 + \bar{\eta}^2)}$$

where $\bar{\rho} = (1 - \lambda^2/2)\rho$ and $\bar{\eta} = (1 - \lambda^2/2)\eta$. This constraint is shown in Fig. 6.3 by the circular band with its origin at (0,0) in the $(\bar{\rho}, \bar{\eta})$ plane. This band is a strong constraint in the $(\bar{\rho}, \bar{\eta})$ plane, but it is on its own not a measurement of CP violation: a solution with the apex of the unitarity triangle at $\bar{\eta} = 0$ would be perfectly consistent with this constraint.

6.3.4 Measurement of Δm

The mass difference Δm of the two mass-eigenstates of a neutral meson system results in an oscillatory behaviour between the meson and anti-meson, $B^0 \leftrightarrow \bar{B}^0$, as explained in chapter 3.

The oscillations of neutral B -mesons were first observed at the PETRA collider at DESY with the ARGUS experiment in 1987 [31]. The oscillations were more rapid than expected at that time, because the mass of the top quark was not expected to be that heavy. In fact, fortunately it turned out that the B^0 -meson has a fair chance to oscillate before she decays. As a consequence of the determination of Δm_d , a lower limit on the top quark mass could be set, $m_t > 40 \text{ GeV}$ ¹

The mass difference Δm_d has been very accurately determined by the B factories.

These decays can, as with semi-leptonic decays, only proceed from the B^0 or \bar{B}^0 part of the wavefunction. In this case the tagging is done using muons detected in the opposite hemisphere to the particle under study. A clear oscillation is seen and the extracted mass difference is obtained

$$\Delta m_d = (0.5065 \pm 0.0019)\text{ps}^{-1}$$

In the Standard Model the calculation of the box-diagram yields the following expression for this mass difference, see Eq. (3.16):

$$\Delta m_d = \frac{G_F^2}{6\pi^2} m_W^2 \eta_C S(x_t) A^2 \lambda^6 [(1 - \bar{\rho})^2 + \bar{\eta}^2] m_{B_d} f_{B_d}^2 B_{B_d}$$

where $S(x_t)$ is again the Inami-Lim function [17], $x_t = m_t^2/m_W^2$, m_t and m_W are the top quark and W masses, $\eta_c = 0.55 \pm 0.01$ is the NLO QCD correction to the box-diagram amplitude and the most uncertain factor $f_{B_d}^2 B_{B_d}$ parameterizes the non-perturbative strong corrections. Using the best estimates of all the parameters this translates into a limiting region in the $(\bar{\rho}, \bar{\eta})$ plane. It is shown as the circular shaded band centered around $(1, 0)$ in Fig. 6.3.

Recently the CDF and D0 experiments at the $p\bar{p}$ collider Tevatron at Fermilab have measured the mass difference in the B_s^0 system:

$$\Delta m_s = (17.757 \pm 0.021)\text{ps}^{-1}$$

The ratio $\Delta m_d/\Delta m_s$ will allow a determination of this radius which is theoretically less uncertain, as this quantity is given by:

$$\frac{\Delta m_d}{\Delta m_s} = \frac{m_{B_d} f_{B_d}^2 B_{B_d}}{m_{B_s} f_{B_s}^2 B_{B_s}} \lambda^2 [(1 - \bar{\rho})^2 + \bar{\eta}^2]$$

Here almost all corrections have cancelled and the ratio of the non-perturbative factors is much better under control, hence the narrow circular band inside the circle coming from Δm_d alone, see Fig. 6.3.

¹This happened at the time that the TOPAZ e^+e^- -collider in Japan was about to become operational with the aim to discover the top quark up to a mass of about 40 GeV...

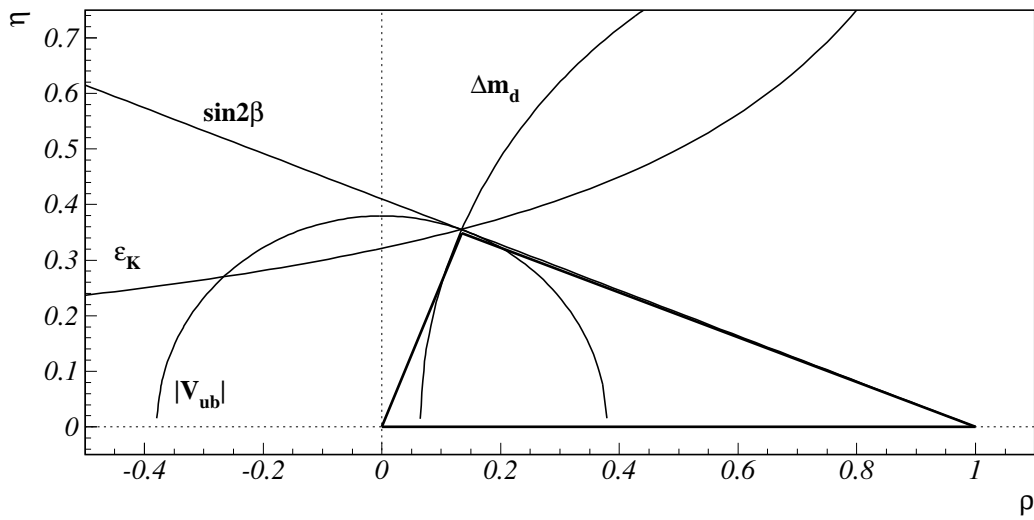


Figure 6.5: Sketch of the four measurements ϵ_K , $|V_{ub}|$, Δm_d and $\sin 2\beta$ in the (ρ, η) plane. In the Standard Model, all four curves should be consistent with one value of (ρ, η) .

6.4 Outlook: the LHCb experiment

The B-factories at the SLAC (USA) and KEK (Japan) with the BaBar and Belle experiments have been extremely successful in measuring CP violation in the B^0 system, resulting in a very accurate determination of the angle β . However, the uncertainty on the angle γ is still large. The angle β_s has not been measured at all yet, although some claims of new physics have been made [32, 33], based on the measurements at the CDF and D0 experiments with the Tevatron collider at Fermilab, Chicago. The B_s^0 system is to date very poorly constrained, and might hide interesting new physics effects in the $b \leftrightarrow s$ transition.

The LHCb detector aims at determining γ and β_s at unprecedented precision. Two prime examples are given in Sections 4.3 and 4.2 where γ and β_s are extracted from the decays $B_s^0 \rightarrow D_s^\pm K^\mp$ and $B_s^0 \rightarrow J/\psi\phi$, respectively. The B-factories run at the $\Upsilon(4S)$ resonance which does not provide enough energy to produce B_s^0 -mesons. On the other hand, B_s^0 -mesons are produced at the $p\bar{p}$ collider at Fermilab. But a relatively low $b\bar{b}$ cross section of $50\mu\text{b}$ at the center-of-mass energy of 2 TeV and a modest yearly collected luminosity of $\sim 1\text{fb}^{-1}$ only yields $\sim 3,000 B_s^0 \rightarrow J/\psi\phi$ events in the period from 2002-2008.

The LHCb experiment operates at the LHC collider running at a center-of-mass energy of 7(8) TeV in 2011 (2012) (with a $b\bar{b}$ cross section of $230\mu\text{b}$) and a yearly luminosity of 2fb^{-1} . In 2015-2018 the LHC operated at 13 TeV, and as a result, the LHCb experiment collected about 100,000 $B_s^0 \rightarrow J/\psi\phi$ events per year. Not only due to the large amount of collected B_s^0 -mesons, but also due to the optimized (forward) detector design, see Fig. 6.6, an accuracy of $\sigma_{\phi_s} = 0.03$ was reached in 2018, combined with results from ATLAS and CMS. The optimized detector design also comprises particle identification

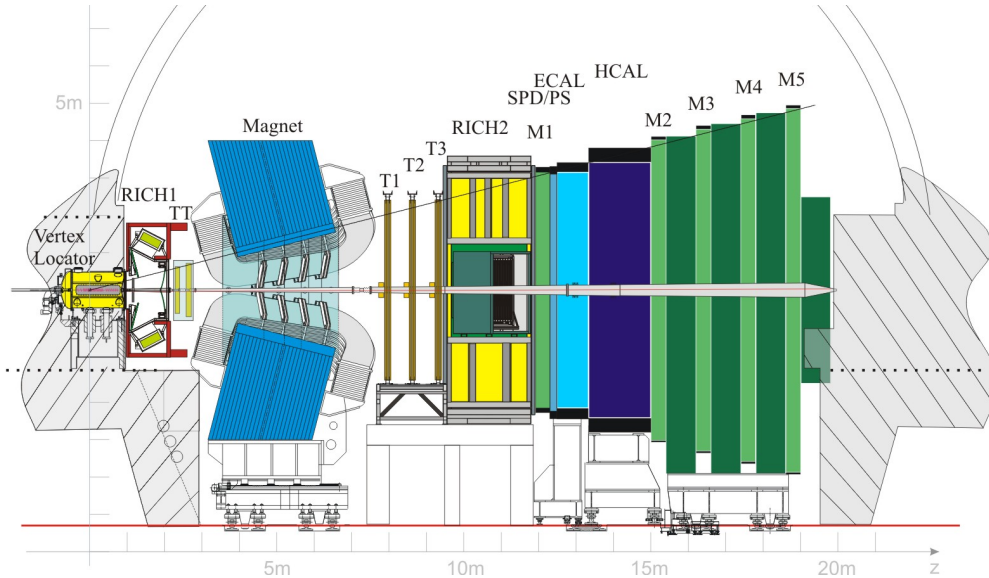


Figure 6.6: Schematic view of the LHCb detector.

(to distinguish kaons from pions) and an efficient hadron trigger, which places LHCb in a special situation compared to the other LHC experiments ATLAS and CMS. Due to these two features, LHCb collected 6000 $B_s^0 \rightarrow D_s^\pm K^\mp$ events in 2011 and 2012, with which γ was determined with $\sigma_\gamma = 20^\circ$, showing the feasibility of this analysis with high precision.

These new precision measurements will scrutinize the Standard Model and her CKM-mechanism. Together with the determination of angular distributions and branching ratios of rare decays such as $B^0 \rightarrow K^* \mu^+ \mu^-$ and $B_s^0 \rightarrow \mu^+ \mu^-$ the measurements at LHCb might reveal new particles inside virtual loops, complementary to the possible direct production of new particles at ATLAS and CMS.

References

- [1] I.I. Bigi and A.I. Sanda, *CP Violation*. Cambridge University Press, Cambridge, (England), 2000.
- [2] G.C. Branco, L. Lavoura and J.P. Silva, *CP Violation*. Clarendon Press, Oxford, (England), 1999.
- [3] C.S. Wu et al., *Experimental test of parity conservation in beta decay*. Phys. Rev. **105**, 1413 (1957).
- [4] R.L.Garwin et al., *Observations of the failure of conservation of parity and charge conjugation in meson decays: The magnetic moment of the free muon*. Phys. Rev. **105**, 1415 (1957).
- [5] C.Jarlskog (editor), *CP Violation*, 1989, available on [http://books.google.com/books?id=U5TC5DSW0mIC&vq=cp violation&pg=PR1](http://books.google.com/books?id=U5TC5DSW0mIC&vq=cp+violation&pg=PR1). Published by World Scientific.
- [6] Y. Nir, *CP violation in meson decays*. Preprint hep-ph/0510413, 2005.
- [7] M.Kobayashi and K.Maskawa, *CP violation in the renormalizable theory of weak interaction*. Prog. Theor. Phys. **49**, 652 (1973).
- [8] L. Wolfenstein, *Parametrization of the kobayashi-maskawa matrix*. Phys. Rev. Lett. **51**, 1945 (1983).
- [9] R. Fleischer, *Flavour physics and CP violation: Expecting the LHC*. Preprint arXiv:0802.2882, 2008.
- [10] I.Y. Bigi, *Flavour dynamics & CP violation in the standard model: A crucial past and an essential future*. Preprint hep-ph/0701273, 2007.
- [11] Fukuda, Y. and others, *Evidence for oscillation of atmospheric neutrinos*. Phys.Rev.Lett. **81**, 1562 (1998), hep-ex/9807003.
- [12] Maki, Ziro and Nakagawa, Masami and Sakata, Shoichi, *Remarks on the unified model of elementary particles*. Prog.Theor.Phys. **28**, 870 (1962).

-
- [13] I. Esteban, M. C. Gonzalez-Garcia, M. Maltoni, I. Martinez-Soler and Th. Schwetz, *Updated fit to three neutrino mixing: exploring the accelerator-reactor complementarity*. JHEP **01**, 087 (2017).
- [14] Harrison, P.F. and Perkins, D.H. and Scott, W.G., *Tri-bimaximal mixing and the neutrino oscillation data*. Phys.Lett. **B530**, 167 (2002), hep-ph/0202074.
- [15] Lenz, A. and others, *Anatomy of New Physics in B-Bbar mixing*. Phys. Rev. **D83**, 036004 (2011), 1008.1593.
- [16] W.E. Burcham and M. Jobes, *Nuclear and Particle Physics*. Longman House, Essex, (England), 1995.
- [17] T. Inami and C. S. Lim, *Effects of superheavy quarks and leptons in low-energy weak processes $K_L \rightarrow \mu^+ \nu_\mu$, $K_L \rightarrow \mu^- \bar{\nu}_\mu$, $K^+ \rightarrow \pi^+ \nu \bar{\nu}$ and $K^0 \leftrightarrow \bar{K}^0$* . Prog. Theor. Phys. **65**, 297 (1981).
- [18] C. Gay, *B mixing*. Ann. Rev. Nucl. Part. Sci. **50**, 577 (2000).
- [19] M. Baak, *Measurement of CKM-angle γ with charmed B^0 meson decays*. Ph.D. Thesis, Free University Amsterdam, 2007.
- [20] I.Y. Bigi and A.I. Sanda, *Notes on the observability of CP violations in B decays*. Nucl. Phys. **B193**, 85 (1981).
- [21] BaBar Coll., Aubert et al., *Improved measurement of CP asymmetries in $B^0 \rightarrow (c\bar{c})K^{0*}$ decays*. Phys. Rev. Lett. **94**, 161803 (2005).
- [22] Amhis, Yasmine Sara and others, *Averages of b-hadron, c-hadron, and τ -lepton properties as of 2018* (2019), 1909.12524.
- [23] J.H. Christenson et al., *Evidence for the 2π decay of the K_2^0 meson*. Phys. Rev. Lett. **13**, 138 (1964).
- [24] Particle Data Group, C. Amsler et al., *Review of particle physics*. Phys. Lett. **B667**, 1 (2008).
- [25] CPLEAR Coll., A. Angelopoulos, *A determination of the cp violation parameter η_{+-} from the decay of strangeness-tagged neutral kaons*.
- [26] CKMfitter Coll., J. Charles et al., *CP violation and the CKM matrix: Assessing the impact of the asymmetric B factories*. Eur. Phys. J. **C41**, 1 (2005).
- [27] UTfit Coll., M. Bona et al., *The unitarity triangle fit in the standard model and hadronic parameters from lattice QCD: A reappraisal after the measurements of Δm_s and $BR(B \rightarrow \tau \nu)$* . JHEP **0610**, 81 (2006).
- [28] Heavy Flavor Averaging Group (HFAG), E. Barberio, et al., *Averages of b-hadron and c-hadron properties at the end of 2007*. Preprint arXiv:0808.1297v3, 2008.

-
- [29] G. Buchalla, A.J. Buras and M.E. Lautenbacher, *Weak decays beyond leading logarithms*. Rev. Mod. Phys. **68**, 1125 (1996).
- [30] G. Colin, *B mixing*. Ann. Rev. Nucl. Part. Sci. **50**, 577 (2000).
- [31] ARGUS Coll., H. Albrecht et al., *Observation of B^0 - anti- B^0 mixing*. Phys. Rev. Lett. **B192**, 245 (1987).
- [32] UTfit Coll., M. Bona et al., *First evidence of new physics in $b \leftrightarrow s$ transitions*. Preprint arXiv:0803.0659, 2008.
- [33] L. Silvestrini, *First evidence of new physics in B_s mixing and its implications*. Nucl. Phys. Proc. Suppl. **185**, 41 (2008).

Acknowledgments

Special thanks to Tristan du Pree, Serena Oggero, Daan van Eijk, Jeroen van Leerdam, Kristof De Bruyn, Meike de With, Rob Knegjens and Lera Lukashenko for spotting mistakes in these lecture notes, and for suggesting many improvements!